AD-A116 126 AIRESEARCH MFG CO OF CALIFORNIA TORRANCE F/G 20/3
ELECTROMECHANICAL ACTUATION DEVELOPMENT PROGRAM (EADP). POWER C--ETC(U)
SEP 81 S ROWE, D BAILEY, R BELANUS F33615-80-C-3620
UNCLASSIFIED 81-18106 AFWAL-TR-81-3106 NL

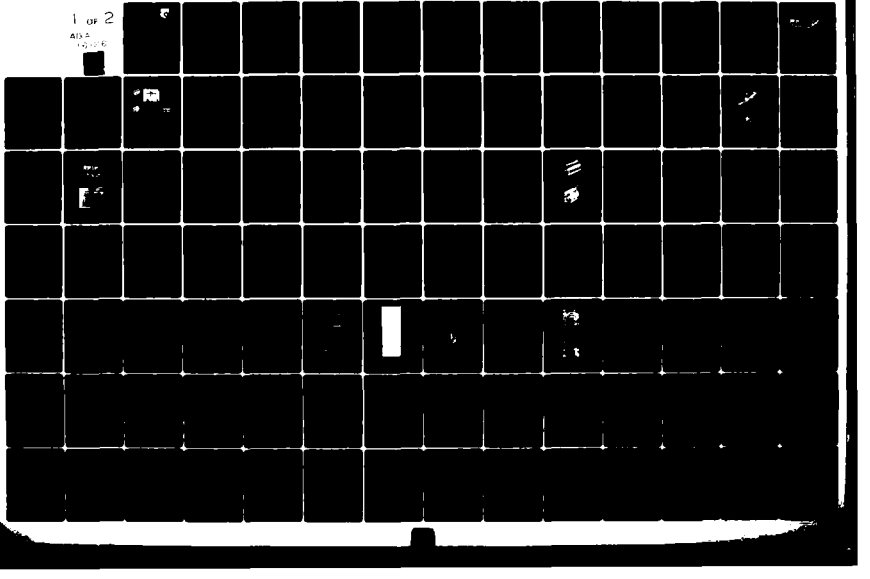

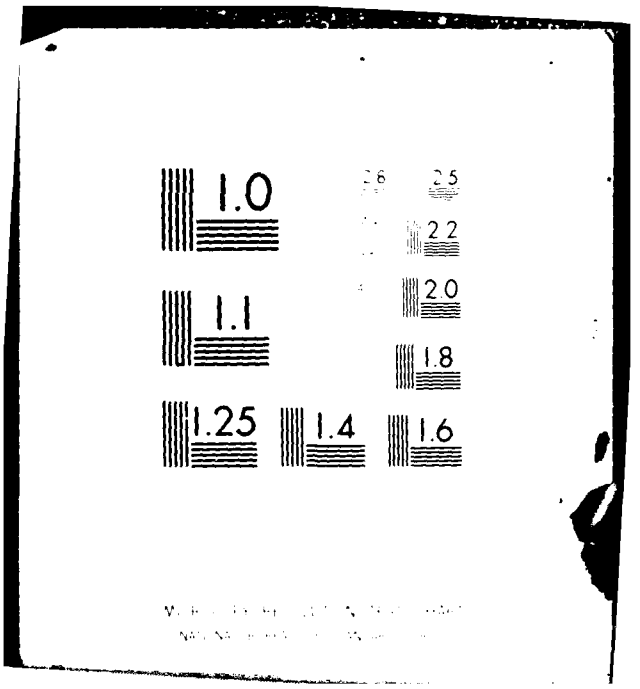
1.0
1.1
1.25
1.4
1.6
1.8
2.0
2.2
2.5

(2)

AFWAL-TR-81-3106

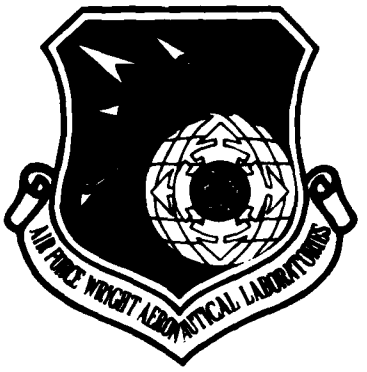

ELECTROMECHANICAL ACTUATION DEVELOPMENT PROGRAM (EADP)

Power Control Development

AiResearch Manufacturing Company
2525 W. 190th Street
Torrance, California 90509

September 1981

Final Report

Prepared for
FLIGHT DYNAMICS LABORATORY
Air Force Wright Aeronautical Laboratories
Air Force Systems Command
Wright-Patterson Air Force Base, Ohio 45433

NOTICE

When Government drawings, specifications, or other data are used for any purpose other than in connection with a definitely related Government procurement operation, the United States Government thereby incurs no responsibility nor any obligation whatsoever; and the fact that the government may have formulated, furnished, or in any way supplied the said drawings, specifications, or other data, is not to be regarded by implication or otherwise as in any manner licensing the holder or any other person or corporation, or conveying any rights or permission to manufacture use, or sell any patented invention that may in any way be related thereto.

This report has been reviewed by the Office of Public Affairs (ASD/PA) and is releasable to the National Technical Information Service (NTIS). At NTIS, it will be available to the general public, including foreign nations.

This technical report has been reviewed and is approved for publication.

Duane P. Rubertus

DUANE P. RUBERTUS
Technical Group Manager
Control Techniques Group

Evard H. Flinn

EVARD H. FLINN, Chief
Control Systems Development Branch
Flight Control Division

FOR THE COMMANDER

Ernest F. Moore

ERNEST F. MOORE
Colonel, USAF
Chief, Flight Control Division

"If your address has changed, if you wish to be removed from our mailing list, or if the addressee is no longer employed by your organization please notify AFWAL/FIGL, *W-PAFB, OH 45433 to help us maintain a current mailing list".*

Copies of this report should not be returned unless return is required by security considerations, contractual obligations, or notice on a specific document.

AIR FORCE/56780/19 April 1982 — 200

Unclassified

SECURITY CLASSIFICATION OF THIS PAGE (When Data Entered)

REPORT DOCUMENTATION PAGE

READ INSTRUCTIONS BEFORE COMPLETING FORM

1. REPORT NUMBER: AFWAL-TR-81-3106	2. GOVT ACCESSION NO.: AD A116126
3. RECIPIENT'S CATALOG NUMBER:	
4. TITLE (and Subtitle): ELECTROMECHANICAL ACTUATION DEVELOPMENT PROGRAM (EADP) Power Controller Development	5. TYPE OF REPORT & PERIOD COVERED: FINAL REPORT 7/80 to 9/81
	6. PERFORMING ORG. REPORT NUMBER: 81-18106
7. AUTHOR(s): STEPHEN ROWE, DAVID BAILEY, ROBERT BELANUS	8. CONTRACT OR GRANT NUMBER(s): F33615-80-C-3620
9. PERFORMING ORGANIZATION NAME AND ADDRESS: AiResearch Manufacturing Company, A Division of The Garrett Corporation, 2525 W. 190th St., Torrance, California 90509	10. PROGRAM ELEMENT, PROJECT, TASK AREA & WORK UNIT NUMBERS: Project 2403, Task 240302 Work Unit 24030273
11. CONTROLLING OFFICE NAME AND ADDRESS: Flight Dynamics Laboratory (AFWAL/FIGL) Air Force Wright Aeronautical Laboratories Wright-Patterson Air Force Base, Ohio 45433	12. REPORT DATE: September 1981
	13. NUMBER OF PAGES: 146
14. MONITORING AGENCY NAME & ADDRESS(if different from Controlling Office)	15. SECURITY CLASS (of this report): Unclassified
	15a. DECLASSIFICATION/DOWNGRADING SCHEDULE

16. DISTRIBUTION STATEMENT (of this Report)

Approved for public release; distribution unlimited.

17. DISTRIBUTION STATEMENT (of the abstract entered in Block 20, if different from Report)

18. SUPPLEMENTARY NOTES

19. KEY WORDS (Continue on reverse side if necessary and identify by block number)

Power-by-wire	Rare earth samarium
Fly-by-wire	Brushless dc motor
270-vdc high power control	Permanent magnet rotor
Pulse width modulation	Cobalt magnets

20. ABSTRACT (Continue on reverse side if necessary and identify by block number)

Electromechanical actuation of primary flight control surfaces has been demonstrated by the development of an integrated rotary hingeline dual-redundant actuation unit. Improved system bandwidth was demonstrated after employing improved sensors and electronic controls.

DD FORM 1 JAN 73 1473 EDITION OF 1 NOV 65 IS OBSOLETE

Unclassified

SECURITY CLASSIFICATION OF THIS PAGE (When Data Entered)

PREFACE

This report was prepared by AiResearch Manufacturing Company, a division of The Garrett Corporation, for the Air Force Flight Dynamics Laboratory, Air Force Wright Aeronautical Laboratories (AFSC), Wright-Patterson AFB, Ohio, in accordance with Air Force Contract No. F33615-80-C-3620. Submittal of this report is intended to satisfy all data requirements of the subject program. Mr. Dan Bird served as the Air Force program monitor, and Mr. Bob Belanus functioned as the AiResearch program manager. Mr. Stephen Rowe was the principal author of this report.

The purpose of this program was to modify and test an existing advanced-technology flight control actuation system. Specifically, the forward control, feedback loops, and feedback sensors were analyzed, modified, and tested. Testing addressed frequency response, transient response, and system stability.

Testing verified the desirability of the new control mechanization. Actuation system performance approached theoretical limits and matched predicted performance.

Mr. Dan Bird is thanked for his constructive comments during the course of the subject program.

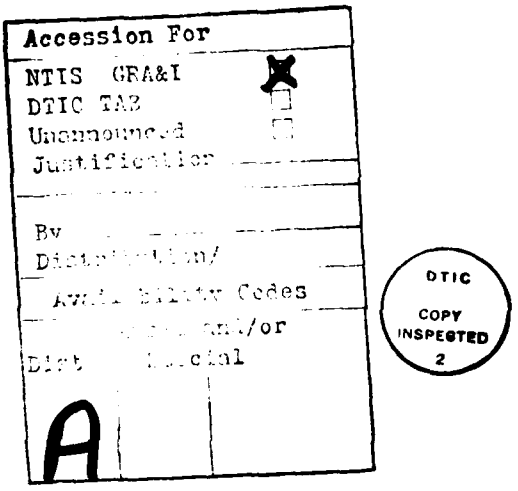

CONTENTS

ILLUSTRATIONS

ILLUSTRATIONS (Continued)

ILLUSTRATIONS (Continued)

ILLUSTRATIONS (Continued)

ILLUSTRATIONS (Continued)

TABLES

1. PROGRAM SUMMARY

This report is submitted by AiResearch Manufacturing Company, a division of The Garrett Corporation, to the Air Force Flight Dynamics Laboratory (AFFDL), Air Force Wright Aeronautical Laboratories (AFWAL) (AFSC), Wright-Patterson AFB, Ohio, in accordance with Air Force Contract No. F33615-80-C-3620. Submittal of this report is intended to satisfy all data requirements of the subject contract.

An existing advanced technology electromechanical actuation system (EMAS) was modified for improved control and performance during the program. Specifically, the forward control, feedback loops, and feedback sensors were analyzed, modified, and tested. Testing addressed frequency response, transient response, and system stability.

General conclusions of the program were that the modifications to the EMAS provided adequate stability and control, and greatly improved performance over that of the baseline system.

1.1 INTRODUCTION

The subject program was pursued for the purpose of advancing EMAS applications to primary flight control systems. The advantages of EMAS (and electrically powered aircraft subsystems) have been well documented during the past decade (References 1 through 10).* This particular program is an extension of two previous programs using much of the same actuation system hardware (see References 11 and 12).

This report is intended to satisfy all data requirements of the program contract. Inclusive within the report are a program summary, a brief synopsis of program history (previous and current), summaries of EMAS modifications and testing, and supporting appendices.

1.2 OBJECTIVES

Objectives were specified in the program contract for the existing EMAS (see Figure 1). The principal objective was to improve the control, stability, and performance characteristics of the existing EMAS.

Due to the objectives specified above, particular emphasis was placed on the EMAS servo loop and inverter control and on the EMAS sensors. Analysis and hardware modification were restricted to the forward control, feedback loops, and feedback sensors (see Figure 2). The actuator itself was not modified.

*All references are included in Section 5.

Figure 1. Existing EMAS Hardware

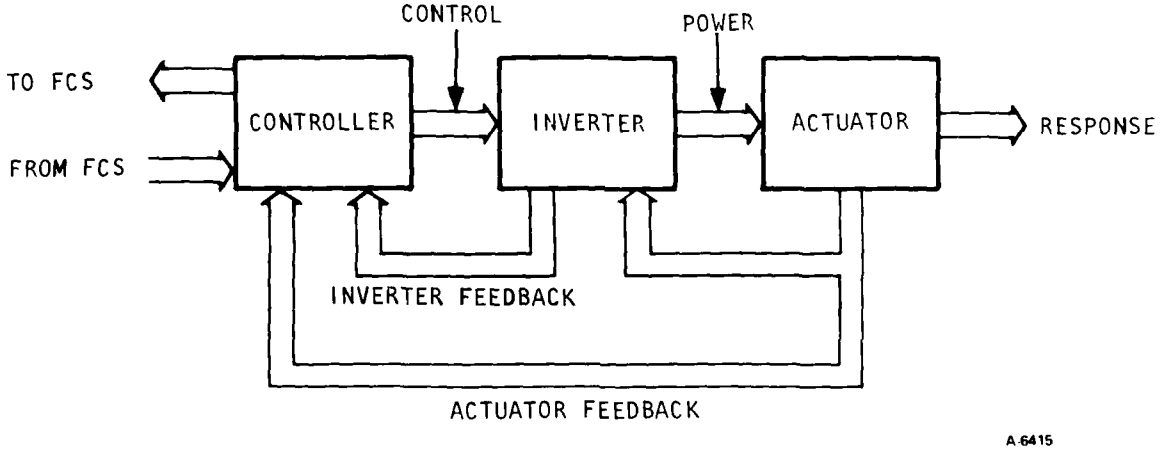

Figure 2. Conceptual EMAS Block Diagram

1.3 RESULTS

As a result of the modeling and simulation work, the control mechanization for the EMAS servo loops and inverter was modified. These modifications required the fabrication of new controller/inverter control circuitry. The revised EMAS block diagram is shown in Figure 3, and the modified hardware is shown in Figure 4.

Specific modifications to the EMAS were:

(a) Implementation of a unique four-quadrant inverter/motor control

(b) Addition of a current minor loop

(c) Addition of rate feedback

(d) Use of an ac synchro with zero-crossing detection for rotor position sensing

(e) Use of a linear, ac tachometer for motor rate feedback

(f) Addition of a cross-channel offset-error compensator

These modifications are discussed in Section 3.

After modifying the EMAS, performance testing was performed; this is described in Section 4. Performance data for the unmodified and modified EMAS are given in Table 1. Significant improvements were demonstrated for system controllability, stability, and performance.

1.4 CONCLUSIONS

The data summarized above were reviewed and conclusions were drawn. The conclusions that were developed were categorized as addressing control, stability, or performance, and are described in more detail in the following text. All test data are presented in Appendix B.

1.4.1 Control

The control approach developed during the present program was found to be successful. Both the inverter and actuator controls offer significant advantages over previously addressed approaches (see References 11 and 12).

The implementation of a four-quadrant motor controller allows linear operation in all four motor voltage - current quadrants (see Figure 5). The principal benefit of this operation is that it allows the actuator to more closely approach idealized transient response. The step response trajectories of Figure 5 illustrate this; e.g., a four-quadrant drive may have little or no overshoot. Additionally, linear control avoids switching of discrete inverter and controller modes, which can introduce discontinuities.

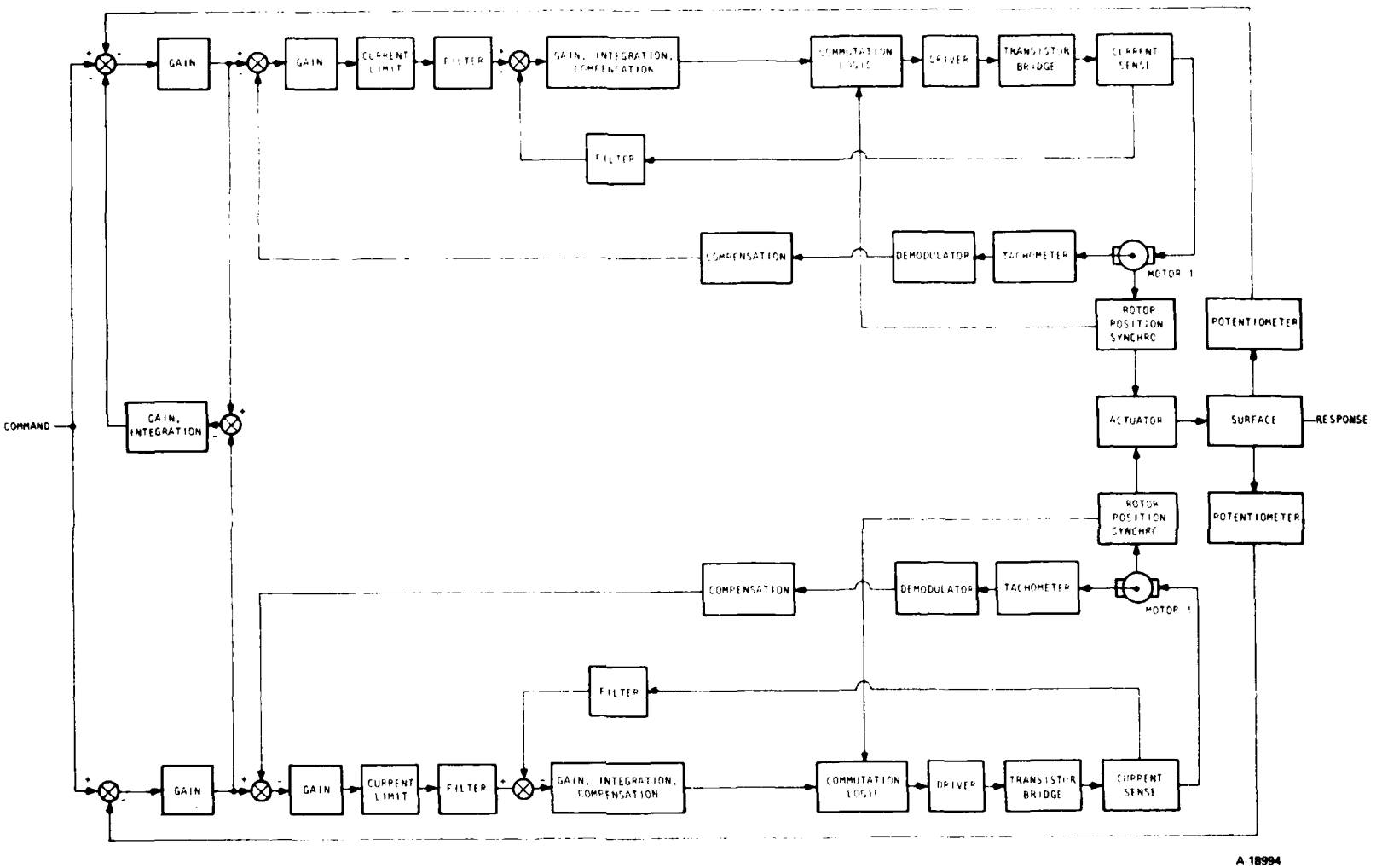

Figure 3. Modified EMAS Block Diagram

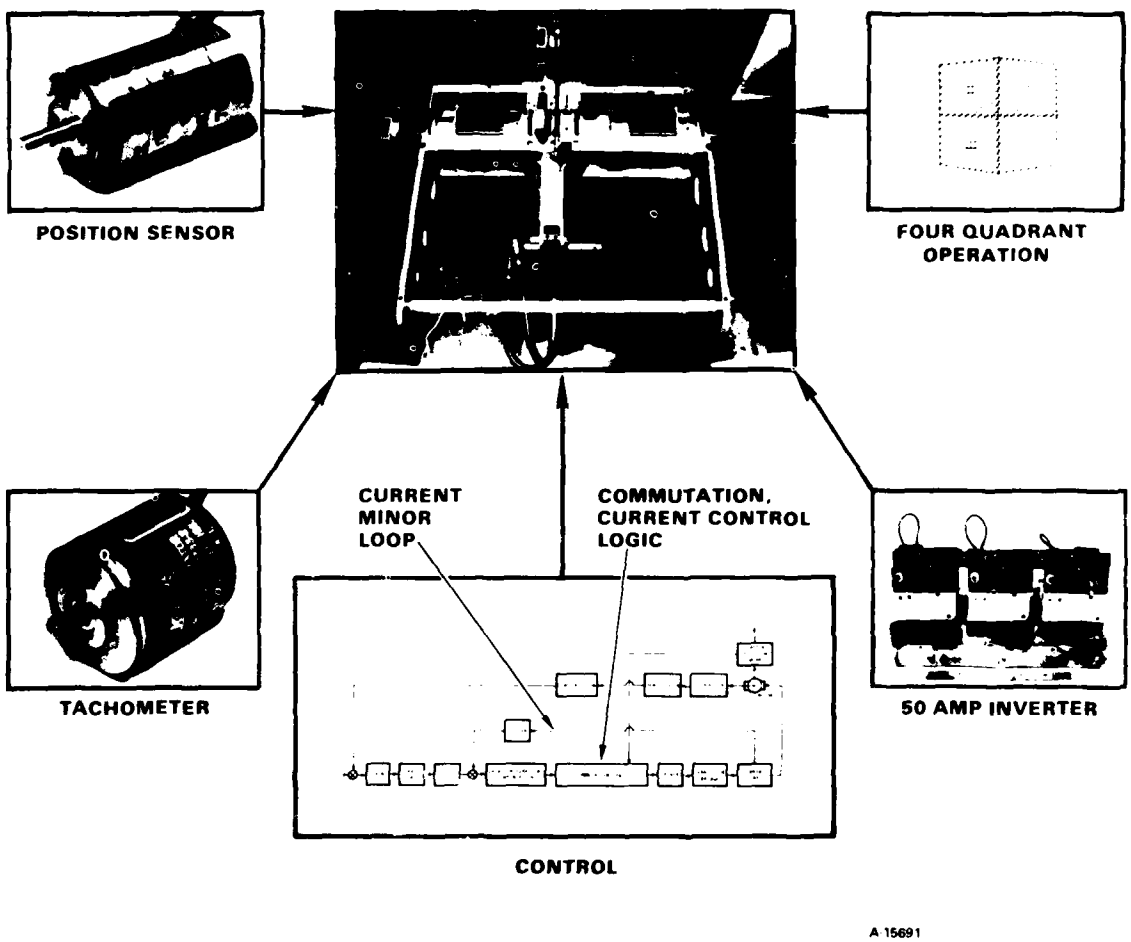

Figure 4. Modified EMAS

Table 1

MODIFIED/UNMODIFIED EMAS PERFORMANCE SUMMARY

Parameter	Modified	Unmodified
Frequency Response		
Frequency	13 Hz	8 Hz
Gain	0 db	-3 db
Phase	-135°	-60°
Amplitude	±1°	±1°
Transient Response		
5° step rise time*	0.05 sec	0.06 sec
10° step rise time*	0.10 sec	0.12 sec
No-Load Rate	95 dps	80 dps
Stall Load**	70,400 in.-lb	70,400 in.-lb

*90 percent of steady state
**Not tested, verified with motor and gearbox data

Note that the two-quadrant drive of Figure 5 would require additional control logic to function as a servo control.

1.4.2 Stability

EMAS stability was found to be acceptable, based on step and frequency response data. Figures 6 and 7 show typical step and frequency response plots, respectively.

All step responses illustrated a single overshoot and undershoot, with rapid decay. There was no indication of any significant limit cycling at steady-state.

Frequency response plots indicated a considerable degree of peaking in the frequency range of 7 to 13 Hz. The maximum amplitude ratio observed was +4.5 db at ±1° input with an inertial load of 8.04 in.-lb-sec^2. Corresponding gain and phase margins for this case were approximately 2 db and 40°, respectively.

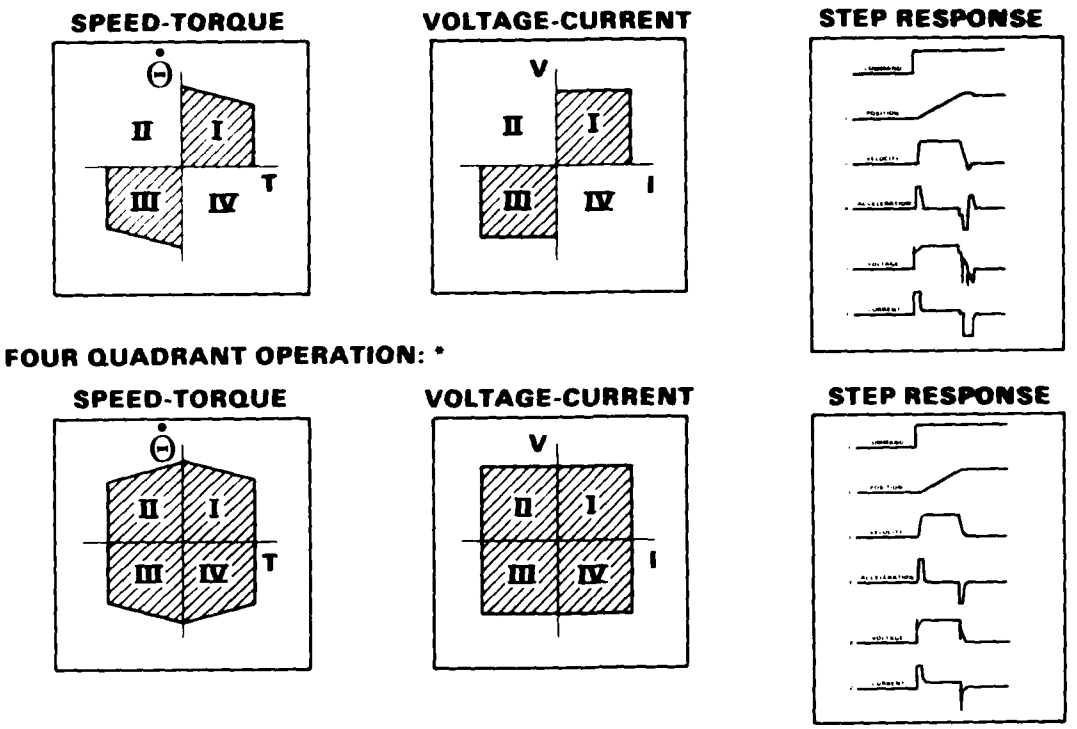

Figure 5. Two Vs-Four-Quadrant Operation

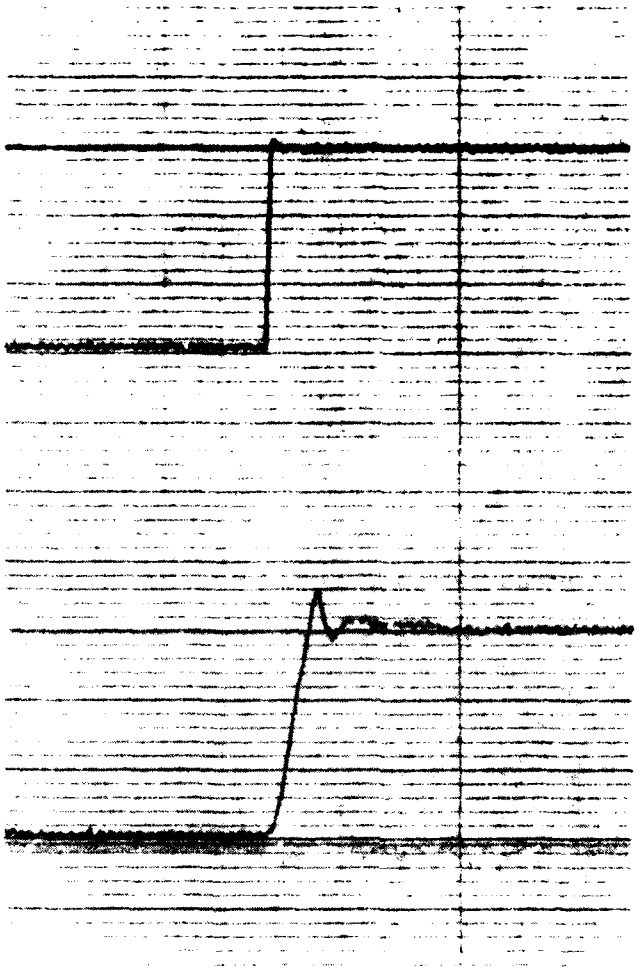

Figure 6. Typical Step Response

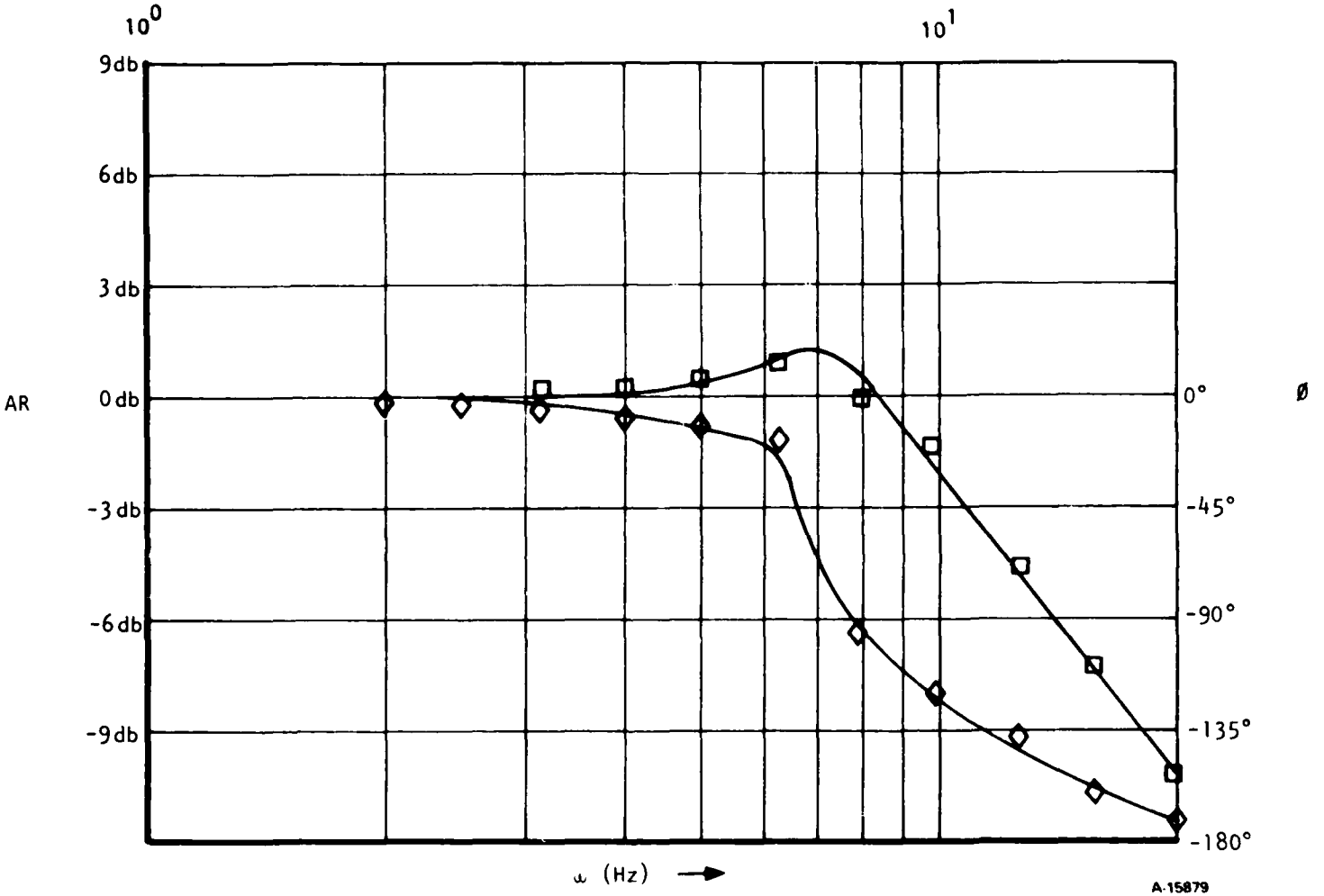

$\pm 2^0$ Amplitude

2.55 in-lb-sec^2

Figure 7. Typical Frequency Response Plot

The peaking during frequency response was attributed to the tachometer feedback loop. The cause is believed to be the result of excessive compliance in the tachometer-motor rotor coupling. Replacing the coupling with a stiffer configuration would increase the tachometer-coupling mechanical natural frequency, and thus decrease the peaking in amplitude ratio. This would also improve actuator gain and phase margins.

1.4.3 Performance

Performance was considerably improved over that of previous configurations (References 11 and 12). Both steady-state and dynamic performance were improved.

Steady-state performance was improved by an increase in no-load actuator rate. The previous configurations had utilized a forward loop limiter, which held the maximum actuator rate to 80 deg-sec^{-1}. The present configuration allows the motor to run at whatever the bus voltage dictates, up to 10 krpm. Thus, no load rate is approximately 95 deg-sec^{-1}.

Dynamic performance was evaluated primarily from frequency response data. Bandwidth was considerably increased, from 8 Hz to approximately 13 Hz. This bandwidth corresponds to $\pm 1°$ at 0 db, and should be maintained at -3 db if peaking attenuation was incorporated.

System performance data is presented in Table 1.

1.5 RECOMMENDATIONS

The following recommendations are based on test results from the subject program.

1.5.1 Sensors

Sensor interface (tachometer, rotor position) is critical because of its influence on system performance and stability. Excessive compliance or the presence of backlash in a sensor's coupling can seriously impair actuator performance.

Also, sensor characteristics (linearity, noise, accuracy) must be considered carefully in terms of the application. No existing sensors are totally satisfactory for use in advanced EMAS.

It is recommended that additional R&D be committed to sensor development and application. Ideally, a combined tachometer/rotor position sensor could be developed and tested, specifically for brushless dc-pm motor applications.

1.5.2 Controls

The four-quadrant control, as previously discussed, operated satisfactorily and improved EMAS performance. Specifically, linear operation in all four voltage-current quadrants eliminated the need for several control modes and the resulting control discontinuities.

The controls utilized in the present actuation system are built up mostly from analog components. It is believed that use of digital components and digital control techniques would provide a more flexible controller mechanization. This is especially true for a microprocessor based controller.

It recommended that a microprocessor-based controller be examined for use in EMAS applications. A prototype microprocessor controller would be very useful in evaluating digital control techniques.

1.5.3 Flight Test

EMAS will never be fully accepted until a comprehensive flight test program has been performed. This is reasonable, in light of flight control system (FCS) criticality.

It is recommended that a flight test program be funded for the purpose of realistically demonstrating EMAS feasibility. Such a program would encompass as a minimum: problem definition, EMAS fabrication, aircraft modification, safety-of-flight testing, flight test, and test data reduction.

2. PROGRAM HISTORY

As stated in the introduction, the subject program was an extension of two previous studies. Both the current and past programs have been referred to as the electromechanical actuation development program (EADP). EADP was an outgrowth of a previous study performed by AiResearch in 1975 for AFFDL (Reference 1). Feasibility studies for the use of EMAS in aircraft primary FCS was the principal objective of that study. State-of-the-art (1975) technology was reviewed in areas of motor design, electrical power conditioning techniques, servo control mechanization, mechanical drive techniques, and actuator/aircraft interface.

The purpose of this section is to provide a brief overview of the EADP for both past and present programs.

2.1 DEVELOPMENT PROGRAM (1976 THROUGH 1978)

EADP began in 1976 shortly after a feasibility study. The program objectives were to design, develop, and test a prototype actuation system based on a problem statement from the feasibility study (Reference 1). Table 2 shows a summary of the problem statement. Complete documentation of the program may be found in Reference 11.

The design of the actuation system began with the configuration shown in Figure 8. An actuator capable of satisfying the requirements of Table 3 was designed, and is shown in Figure 9. In addition, a controller/inverter compatible with the actuator requirements using microprocessor based servo control was designed.

Hardware for the actuator was fabricated, and component tests were performed to verify design predictions. Figure 10 shows the assembled actuator, and Figure 11 shows the motor used in the actuator. Concurrently, a breadboard controller/inverter was fabricated and tested.

Development testing of the EMAS began after system component checkout. During development, design and control problems surfaced requiring several EMAS configuration changes. Briefly, development testing revealed the need for the following changes:

(a) Rate feedback was necessary for servo stability and desirable transient response characteristics, when actuating large inertial loads.

(b) Analog controller circuitry was found to be more practical for development use, due to programming complexity of the microprocessor, and memory/speed requirements beyond microprocessor capabilities.

TABLE 2

EADP PROBLEM STATEMENT

Vehicle Application Interfaces	
Structurally integrated, rotary hingeline actuator	
3 hp available at control surface, max.	
115/200-vac, 3-phase power supply	
Fail-operational (two-channel)	
Actuation Goals	
Stall hinge moment	37,575 in-lb
No-load rate	80 deg-sec^{-1}
Bandwidth	4 to 12 Hz at $\pm$1 deg amplitude
Load inertia	46.6 in-lb-sec^2
Duty cycle	Continuous operation at a minimum of 20 percent peak torque

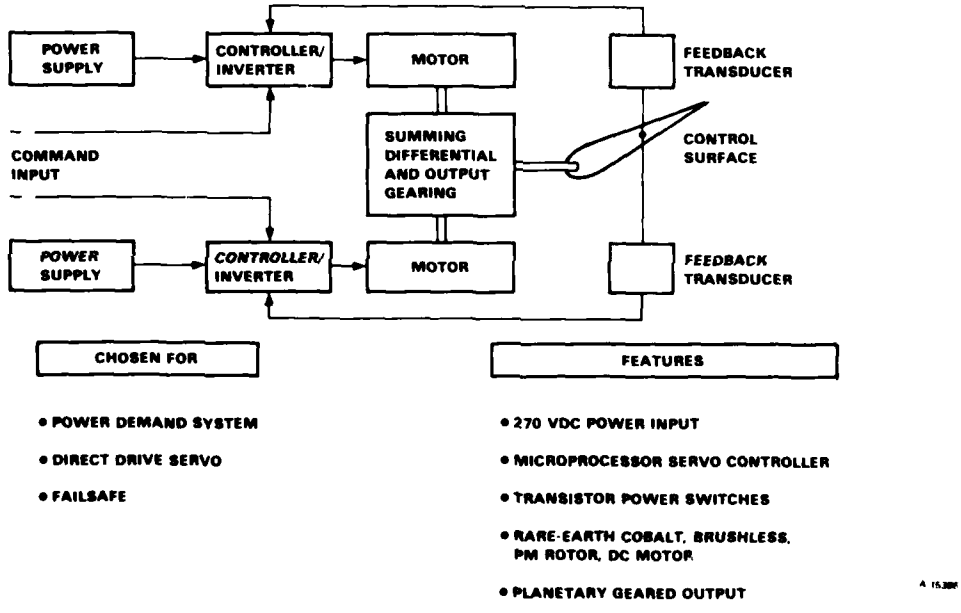

Figure 8. Prototype EMAS Configuration

TABLE 3

SUMMARY OF PERFORMANCE GOALS AND TEST RESULTS

Characteristics	Specified	Test Results
Output stroke	±30 deg	±30 deg
Output velocity (no load)	80 deg-sec^{-1}	80 deg-sec^{-1}
Output torque (stall)	37,575 in-lb	--*
Hysteresis	0.5 percent full stroke	0.5 percent
Frequency response	4 to 12 Hz -3 db, -90°	8 Hz -3 db, -60°
Position null	0.5 percent	0.5 percent

*Not tested or verified with motor and gearbox data.

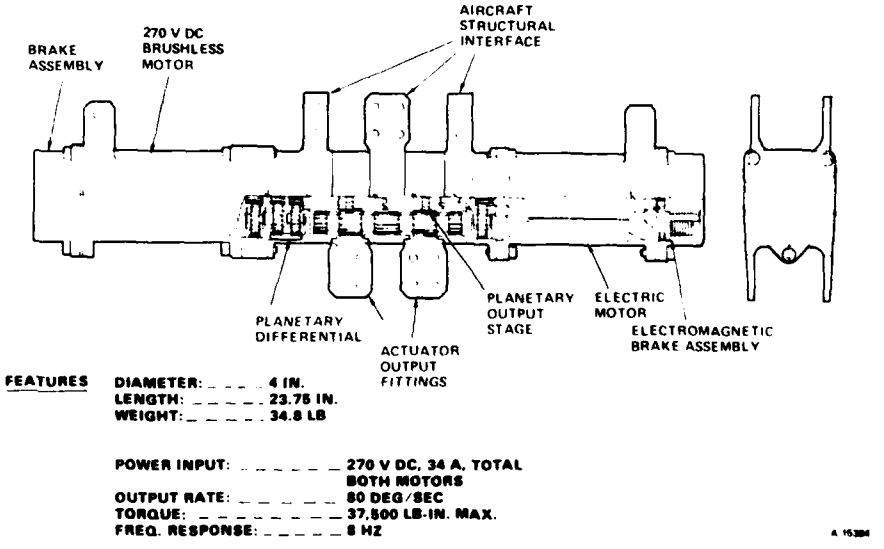

Figure 9. Actuator Design

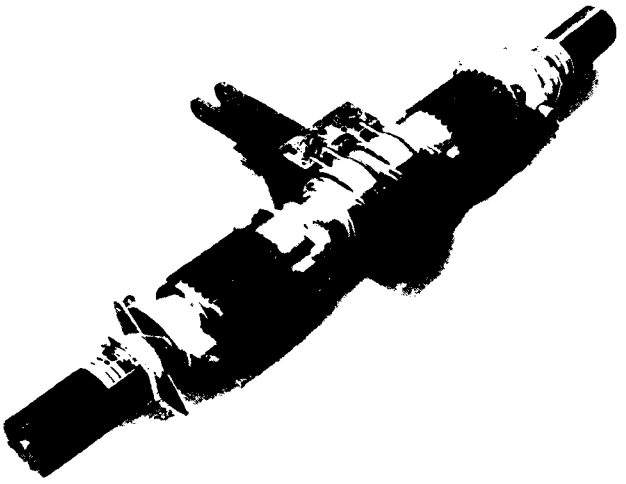

Figure 10. Development Actuator

F 35011

Figure 11. Development Motor

(c) The digital encoder was found to have insufficient resolution when directly driven by the actuator, but was satisfactory when driven through step-up gearing; it was unnecessary once a decision was made to proceed with analog controls.

Several configurations were developed to investigate digital and analog control mechanizations. Satisfactory performance and adequate stability were obtained using the analog system of Figure 12.

Testing was performed using this EMAS configuration for the balance of the program. Performance data measured using this configuration is tabulated in Table 3.

2.2 FOLLOW-ON PROGRAM (1979 TO 1980)

During the program time frame, significant advances in high voltage-high current transistors were made, and new devices became available. In order to capitalize on this technology, a follow-on program was pursued from 1979 to 1980 with the intention of increasing inverter current rating and of improving actuator performance. In addition, limited environmental testing was planned as part of the follow-on, in order to evaluate system performance and component operation. A block diagram of the EMAS is shown in Figure 12. Program documentation may be found in Reference 12.

A 30-amp inverter was constructed for use with the existing actuator. New controller electronics were also breadboarded, including an improved current limiting technique (based on average rather than peak current), and new servo control/compensation circuitry. A tachometer was not used for rate feedback in this configuration during most of the follow-on program, requiring the use of lower loop gain. Figure 13 shows the breadboard inverter.

Performance and environmental testing of the EMAS was performed at temperatures of -65°, 70°, and 250°F. Figure 14 shows the actuator installed in an environmental chamber. Figure 15 shows the follow-on EMAS block diagram. Performance data are tabulated in Table 4. The EMAS operated satisfactorily at all temperatures; however, performance of the system was not improved over the previous configuration in all of the areas anticipated.

This, and other EMAS anomalies, led to a thorough review of component designs and system control. The review was accomplished after the follow-on program, and resulted in the following conclusions:

(a) Motor rotor position sensing was not completely satisfactory because of a low signal-to-noise ratio and ramping during sensor state changes (see Figure 16A). The effect produces an inverter "firing angle" (commutation) that is not at the optimum value, thus reducing peak motor running torque (see Figure 16C).

(b) Motor tachometers previously examined were nonlinear at low speeds, and noisy at all speeds, making use of the signal difficult

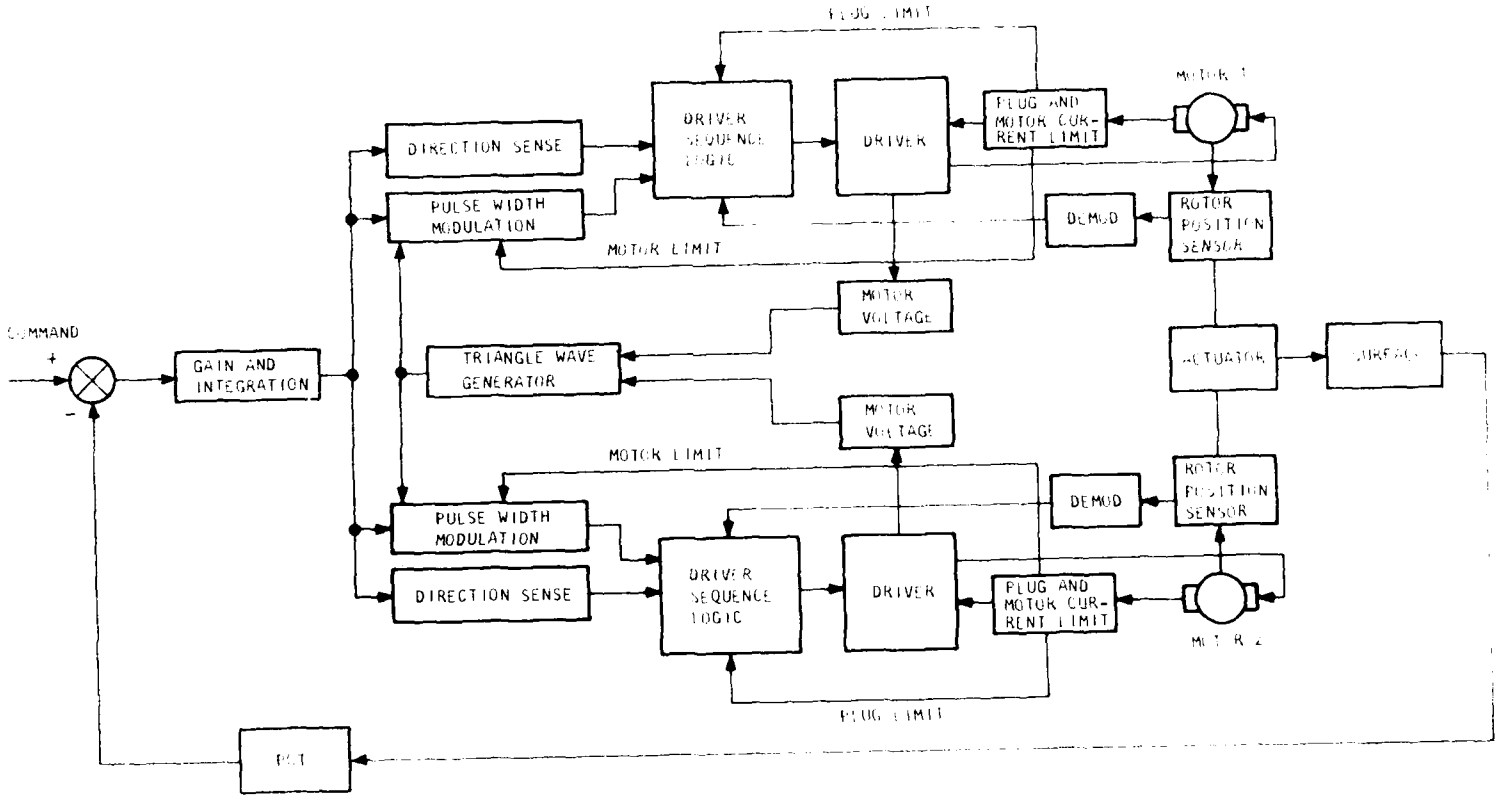

Figure 12. EMA, Block Diagram

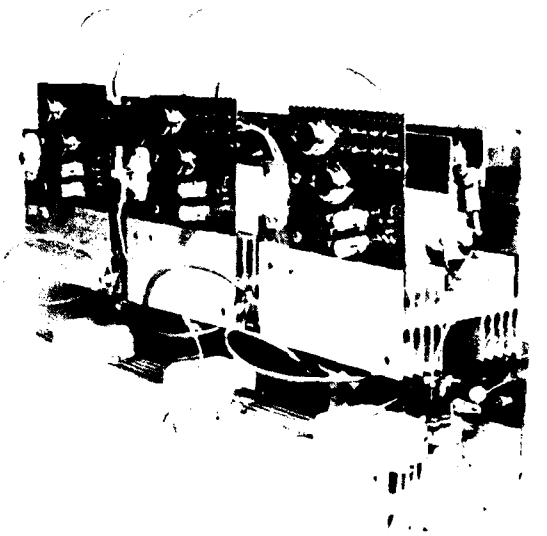

Figure 13. 4-Amp Inverter

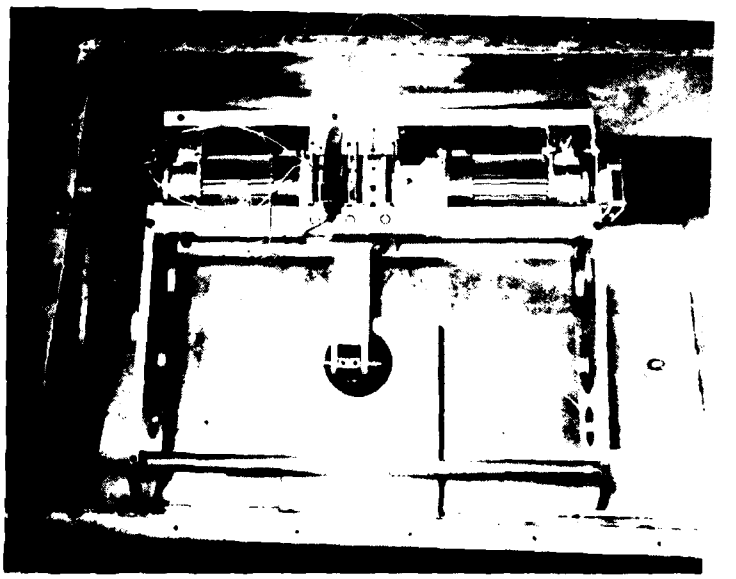

F-35009

Figure 14. Environmental Test Chamber with Actuator Installed

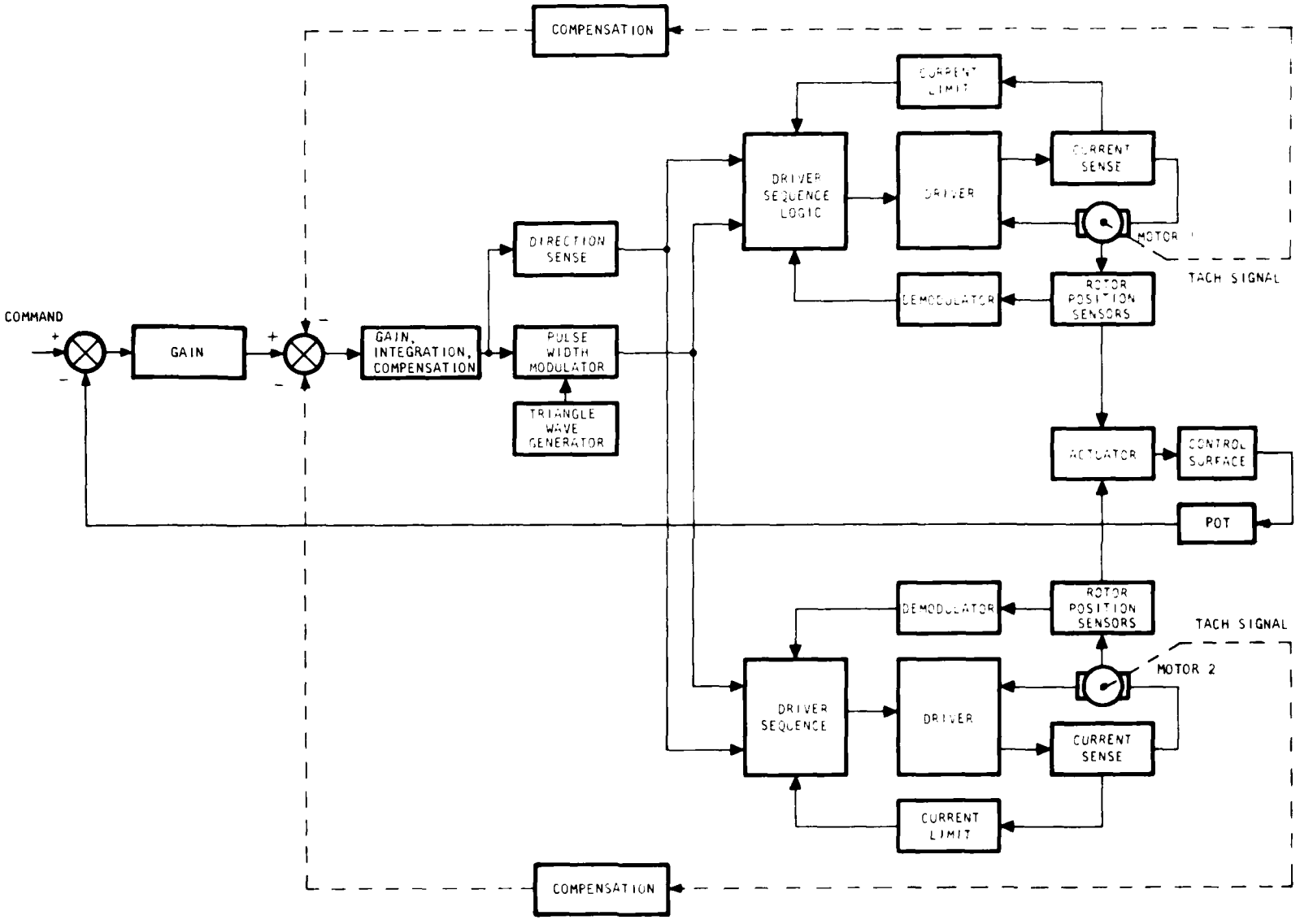

S 29790 A

Figure 15. Follow-on EMAS Block Diagram

TABLE 4

TEST DATA SUMMARY

Characteristics	Test Results
Output velocity (no-load)	80 deg-sec^{-1}
Output torque (stall)	70, 400 in-lb*
Frequency response	
• -65°F	8 Hz, -3 db, -60°
• 70°F	8 Hz, -3 db, -60°
• 250°F	8 Hz, -3 db, -80°
Thermal evaluation (motor end turns)	
• -65°F, 23 amp (rms)	0°F at 75 sec
• 70°F, 18 amp (dc)	300°F at 250 sec
• 250°F, 23 amp (rms)	385°F at 60 sec

*Not tested, verified with motor and gearbox

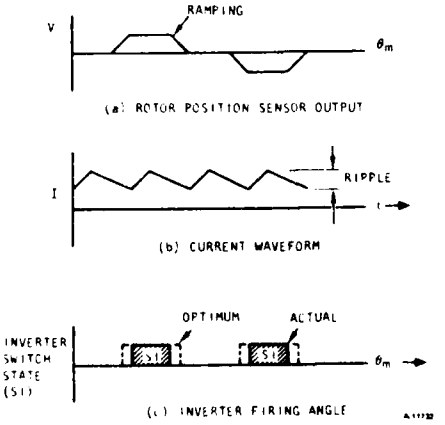

Figure 16. Sensor/Control Characteristics

(c) Motor current limiting was not as precise as desired due to significant "ripple" in the current waveform caused by inverter control technique (see Figure 16B).

(d) Although minimum performance requirements were met, it was recognized that the increased torque (current) capability affored by the Westinghouse D60T power transistors was not being used to the maximum advantage with the two-quadrant control scheme. This was evidenced by system instability at high gain levels, thus limiting system frequency response.

2.3 FOLLOW-ON PROGRAM (1980 TO 1981)

Using these conclusions as a basis, a revised EMAS controller and inverter control circuitry were designed, and new motor sensors were incorporated. This design formed the basis for a follow-on program from 1980 to 1981.

The controller design is new, and employs four-quadrant control in lieu of the previous two-quadrant control. A block diagram of the EMAS is shown in Figure 3. The system utilizes velocity and current minor loops for motor speed and current control, respectively, which provides a linear, four-quadrant servo control.

The system of Figure 3 was fabricated and tested during 1981. This system is the subject of the present report, and is discussed exclusively in Sections 3 and 4.

3. SYSTEM MODIFICATIONS

Modifications were made to the existing actuation system for the purpose of improving operation and performance. Elements of the actuation system that were modified included the controller, inverter, and actuator sensors. No modifications were made to the actuator itself.

3.1 SYSTEM

The actuation system was modified to the configuration shown in Figure 3. Notable features are current and rate minor loops; a commutation circuit; and an ac synchro and tachometer for motor rotor position-sensing and rate feedback, respectively.

A block diagram for one channel of the system is shown in Figure 17. This diagram illustrates in greater detail the portion of Figure 3 from the position command/feedback summing junction to the inverter input.

3.2 CONTROLLER

THe controller is configured to allow linear operation in all four motor voltage-current and speed-torque quadrants (see Figure 18). This permits the actuator to approach ideal response characteristics.

Linear operation is obtained by using both rate and current feedback, permitting direct control of both variables. Additionally, logic analogous to a non-linear amplifier is used for current control within the current loop. This logic provides an input to the commutation logic and determines the sign of the current feedback. This mechanization allows the motor to transition from one quadrant to any other quadrant, both voltage-current and speed-torque.

Current limiting is obtained by a limiter in the forward loop and is set for $\pm$30 amp.

3.3 INVERTER

Minor modifications were made to the inverter. Modifications were limited to the inverter commutation logic. The basic bridge remained unchanged.

The previous current limit was mechanized by monitoring the current level, and if it exceeded the maximum allowed, the motor drive was turned off for 100 usec. Turning off the drive for 100 usec caused excessive ripple in the current

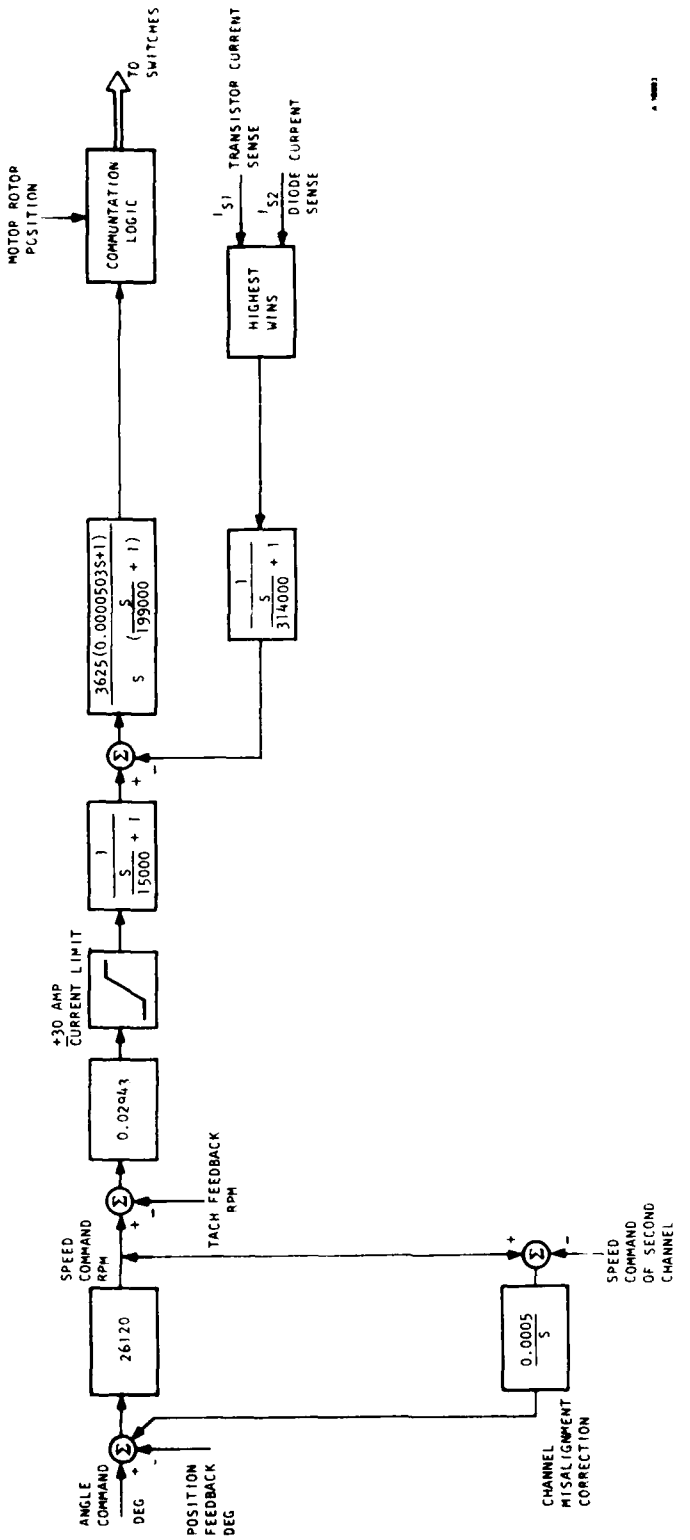

Figure 17. Detailed Block Diagram (Single-Channel)

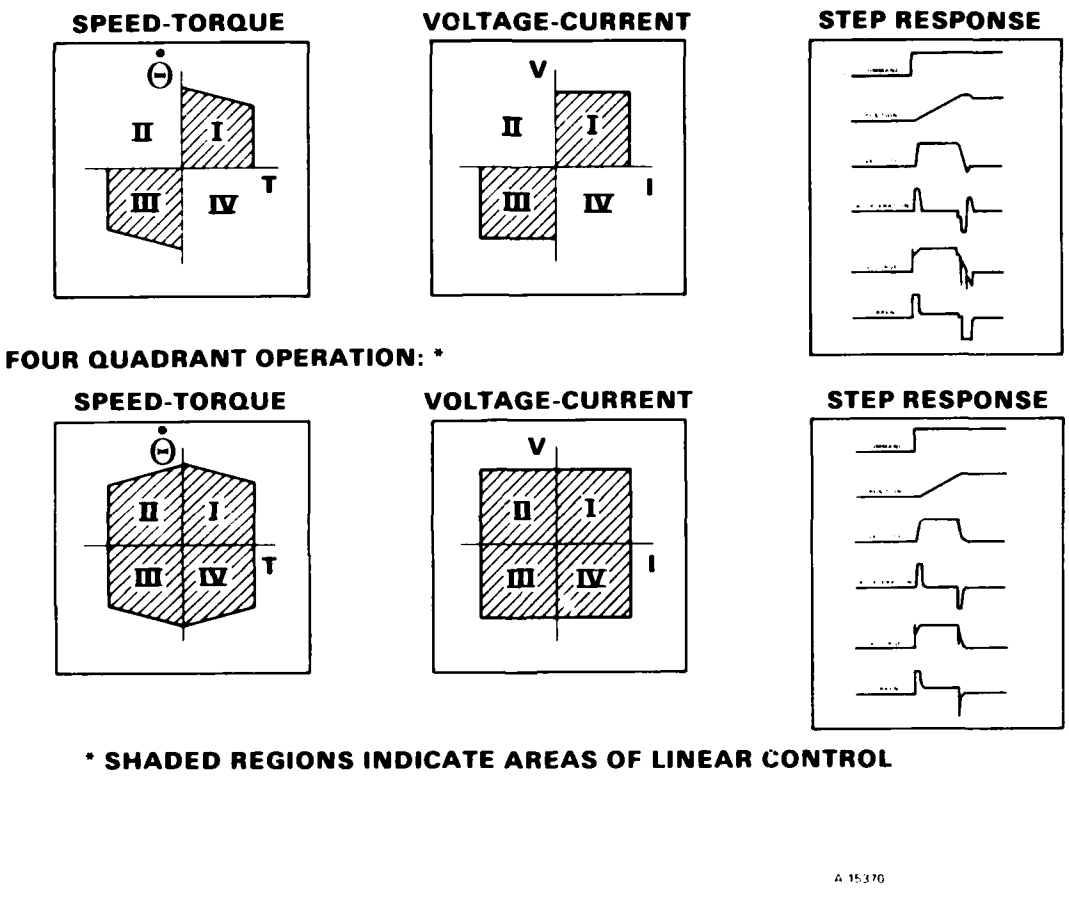

Figure 18. Four-Quadrant Operation

during current limiting. By using an active current control during current limiting, the ripple is greatly reduced. The active control of current limit is independent of the four-quadrant operation.

The four-quadrant operation allows the voltage applied to the motor to be any value between ±270 v. With a two-quadrant drive there are inequalities imposed on the voltage to prevent voltage/current combinations from entering the second and fourth quadrants:

$$\text{If } I > 0 \text{ then } V \geq V_{BEMF} + I R_{MOTOR} + L \frac{di}{dt}$$

$$\text{If } I < 0 \text{ then } V \leq V_{BEMF} + I R_{MOTOR} + L \frac{di}{dt}$$

With a two-quadrant drive, the inequalities are imposed as a result of how the switches are driven, rather than calculating the inequality and then driving the switches.

5.4 SENSORS

Both the motor position sensor and tachometer were replaced. The motor position sensor was changed to improve position accuracy and signal-to-noise ratio. The motor tachometer was changed to improve linearity in the rate feedback loop.

The motor position sensor utilized during the program was an ac synchro, as shown in figure 19. The synchro outputs three phase ac, and zero-crossing detection of the phases is used for position sensing.

The motor tachometer utilized during this program was an ac generator, as shown in figure 20. The tachometer output is single phase ac, which is demodulated and used as the rate feedback.

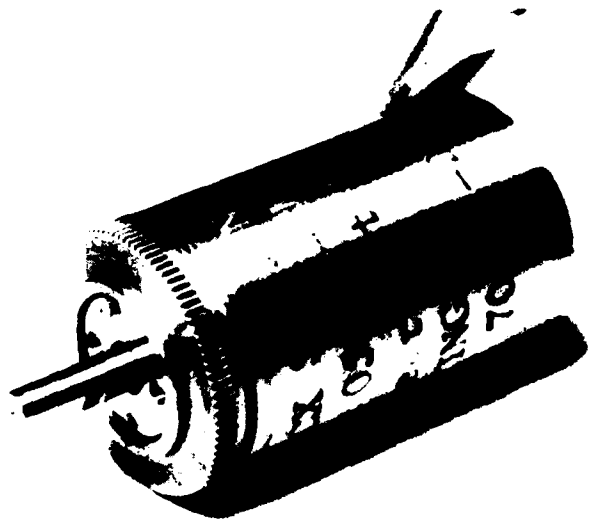

Figure 19. Motor Position Sensor

F 35008

Figure 20. Motor Tachometer

4. SYSTEM TESTING

The modified EMAS, as described in Section 3, was subjected to the testing required by the program test plan. The test plan and EMAS testing are discussed in this section. Test data are evaluated, and conclusions drawn.

4.1 TEST PLAN

A test plan was developed by AiResearch and reviewed by the customer. The approved procedure is contained in Appendix A.

Three specific tests are required by the test plan. They are:

(a) Stability assessment (para. 3.1)

(b) Frequency response (para. 3.2)

(c) Increased system inertia (para. 3.3)

The objectives of the above tests were to evaluate EMAS performance and stability.

4.2 TESTING

Testing was performed in accordance with the test plan of Appendix A. Test data were recorded and may be found in Appendix B.

Individual tests are discussed in the following paragraphs.

4.2.1 Stability Assessment (Para. 3.1)

Step and square wave inputs were applied to the actuation system. Both loaded and unloaded test runs were made. Actuator loading was accomplished with a linear spring, having a stiffness of 130 in.-lb-deg $^{-1}$.

Test data may be found in Appendix B. Test numbers corresponding to this paragraph are 1 through 16 of Appendix B.

4.2.2 Frequency Response (Para. 3.2)

A sinusoidal input was applied to the actuation system, a frequency sweep performed from 1 to 25 Hz. This was accomplished for several input amplitudes, with the actuator loaded and unloaded. Actuator loading was accomplished via a linear spring.

Test data are [illegible] in Appendix B. Test numbers corresponding to this paragraph are [illegible] of Appendix B.

4.[illegible] Inertial Loading ([illegible])

Various inertial loads were applied to the actuator, and the frequency response of the system was evaluated. Two input amplitudes were used, ±1° and ±[illegible]°.

Test data are summarized in Appendix B, in the form of Bode plots. Test numbers corresponding to this paragraph are 25 through 30 of Appendix B.

4.3 DATA EVALUATION

Data from all three tests were evaluated for actuator performance and response characteristics.

Data from the stability assessment test indicated desirable transient response characteristics. Step responses exhibited a single overshoot and a single undershoot [illegible] settling, which is nearly ideal. [illegible] was relatively [illegible], at approximately 1°. Triangle wave responses exhibited good tracking capability of the actuation system. Some nonlinear tracking characteristics were present in the triangle wave responses, but they were not objectionable. Loading did not significantly alter any of the step or triangle responses.

Data from the frequency response test exhibited smooth tracking by the actuator at all frequencies. Waveform distortion occurred only at larger amplitudes and higher frequencies, where acceleration or rate saturation occurred. Local distortion in the regions of maximum acceleration can be seen on some of the traces (at the peaks), but this is not objectionable and becomes noticeable only when the unit is approaching acceleration saturation. Some distortion of the waveform also occurs during the loaded runs, when actuator direction changes.

Inertial loading test data revealed peaking of up to +4.[illegible] [illegible] the amplitude ratio for the maximum inertia investigated (8.04 in-lb-sec[illegible]). This is somewhat higher than [illegible], although positive gain and phase margins [illegible] (2.[illegible] and [illegible]°, respectively). It was concluded that the tachometer [illegible] coupling was the cause of the resonance. It is believed that [illegible] the coupling, and [illegible] compensation would reduce the [illegible] to [illegible] level ([illegible]) without affecting bandwidth. Bandwidth of the system is approximately [illegible] at [illegible], ±1° input.

4.4 CONCLUSIONS

The following [illegible] were reached, based on the test [illegible].

(a) Actuation system performance and operation have been [illegible] improved over previous EMAS configurations.

(b) System gain and phase margins are marginal but acceptable, [illegible] readily be [illegible] without significantly degrading [illegible].

5. REFERENCES

1. Wood, N., Echolds, F., and J. Ashmore, Electromechanical Actuation Feasibility Study, Air Force Flight Dynamics Laboratory Report AFFDL-TR-77-42.

2. Grau, R., Feasibility Investigation for Advanced Flight Control Actuation Systems; All Electric Concepts (AFCAS/AE), Naval Air Development Center Technical Report NADC 76160-30.

3. Voight, "Electric Flight Control Systems - Applicable Now," NAECON 77 Record, pp. 1094-1101.

4. Helsley, C.W., Jr., "Power by Wire for Aircraft - The All Electrical Airplane," SAE Technical Paper 771006.

5. Edge, "An Electromechanical Actuator Technology Development Program", SAE Technical Paper 780581.

6. Leonard, Sorensen, Rowe, Design Investigation of Electromechanical Rotary Actuation Concepts for V/STOL Aircraft, Naval Air Development Center Technical Report NADC 78059-60.

7. Rowe, S., " Electromechanical Airplane Actuation Trade Study," AiResearch Manufacturing Company Report No. 80-17284.

8. Heimbold, Cronin, Howison, "Application of Advanced Electric/Electronic Technology to Conventional Aircraft," National Aeronautics and Astronautics Contractor Report NAS 9-15863.

9. Cronin, "The All-Electric Airplane as an Energy Efficient Transport," SAE Technical Paper 801131.

10. Swihart, "The Next Generation of Commercial Aircraft - The Technical Imperative," Paper presented at the 12th Congress of the Internation Council of Aeronautical Sciences at Munich, F.R.G., October 12-17 1980.

11. Wood, N., and R. Lewis, "Electromechanical Actuation Development," Air Force Flight Dynamics Laboratory Report AFFDLTR-78-150.

12. Lewis, R., Gray, J., and N. Wood, "Electromechanical Actuation Development," Air Force Flight Dynamics Laboratory Report AFFDL-TR-80-3024.

APPENDIX A

TEST PLAN

AIRESEARCH MANUFACTURING COMPANY
OF CALIFORNIA

INTEGRATED HINGE (ROTARY) ELECTROMECHANICAL ACTUATION TEST PLAN

CONTRACT NO. F33615-80-C-3620

80-17331, Rev. A October 18, 1980

Number of pages 9

Original date 9-18-80

Prepared by R. A. Lewis

Approved by R. M. Belanus

Revision	Date	Pages Affected (Revised, Added, Eliminated)

INTEGRATED HINGE (ROTARY) ELECTROMECHANICAL ACTUATION TEST PLAN

1.0 PURPOSE

1.1 INTRODUCTION

This document is submitted by AiResearch Manufacturing Company in accordance with the data requirements list, Sequence No. 4, of Air Force Contract Number F33615-80-C-3620 issued by Air Force Wright Aeronautical Laboratories Flight Dynamics Laboratory. The following paragraphs describe a test plan for additional demonstration testing of the integrated hinge (rotary) electromechanical actuation unit.

1.2 SCOPE

This plan describes the tests to be conducted on the integrated hinge (rotary) electromechanical actuation unit. The actuation system will be tested under laboratory ambient conditions using the existing actuator test stand.

The components that undergo a redesign or change function will be checked out and demonstrated initially on a component level then incorporated and tested on a system level.

A major emphasis of this program will be to assess the improvement at system stability that results from 1) more sophisticated switching logic, 2) the use of pure rate feedback via a discrete tachometer mounted on the motor shaft and 3) the use of a synchro for improved motor commutation.

Further areas of interest include system operation with increased surface inertia and redundancy management. These areas will be investigated through test demonstration and system analysis.

1.3 BACKGROUND

Air Force Contract F33615-76-C-3043 has sponsored the development and test of the integrated hinge (rotary) electromechanical actuation unit designed for aircraft primary flight control. The baseline unit shown schematically in Figure 21 provides dual redundancy in the electronic control, motor drive, and mechanical elements. The actuator was designed to be in a flight configuration to illustrate hingeline structural interface capability, thermal management considerations, and servo feedback mounting and design considerations. The controller was fabricated as an engineering breadboard with two separate, rack-mounted servocircuits and power switch assemblies. This arrangement provided maximum flexibility to incorporate design improvements. Major actuation unit features are described on the following page

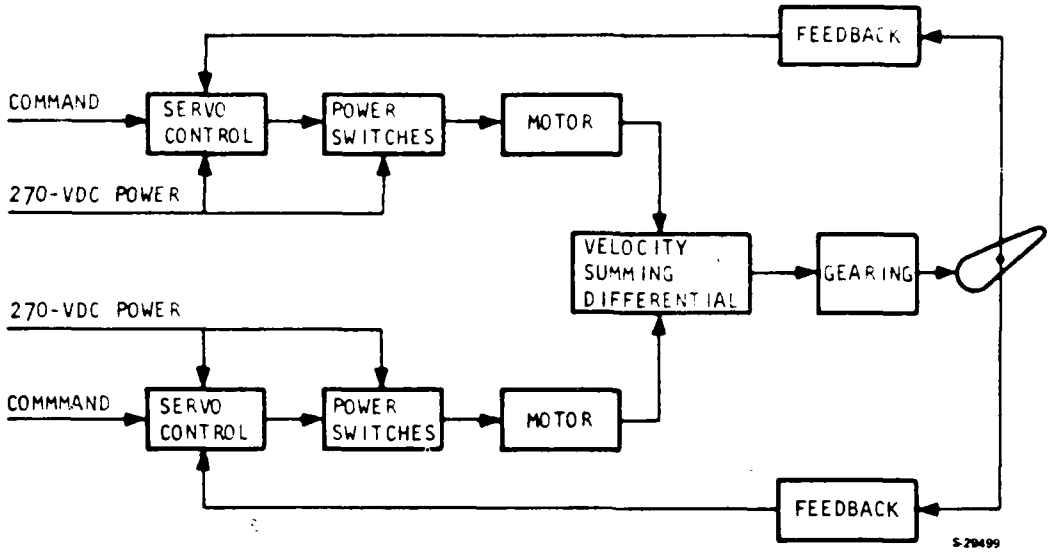

Figure 21. Electromechanical Actuation Unit Block Diagram

(a) Closed-loop position servo circuits were impelemented using both analog and digital techniques to demonstrate versatility for interfacing with various aircraft flight control systems. Optical, digital encoders, and analog potentiometers were used to monitor control surface position and are used in the servo feedback loop. Transistorized electric power switch circuits provides motor torque-rate and commutation control.

(b) Permanent-magnet, 270-vdc motors using brushless commutation and rare-earth cobalt magnets in the rotor assembly are used to achieve high acceleration and torque in minimum space and weight. Samarium cobalt and other high-energy, rare-earth-magnet materials are being used to reduce servomotor size and weight while maintaining high performance output. As a result, dc electric motors are competitive with the hydraulic motors used in primary flight control systems. The selection of 270-vdc power was based upon rectification of a standard 115/200-v, 400-Hz aircraft power source.

(c) Torque multiplication and speed reduction are accomplished through a rotary hingeline actuator that implements dual redundant drive channels, using a velocity summing planetary differential and planetary gear stages to the rotary output. The rotary actuator gear ratio matches the torque and speed requirements of the control surface to the motor output. Improved materials and manufacturing processes make use of high-strength alloys to achieve high fatigue strength, high stiffness, and ease of producibility.

This hardware has demonstrated the capability of using low-level electric signals (fly-by-wire) to control high-power electrical servomotors (power-by-wire). The following tests were performed under the basic contract, including an amendment to the contract.

- Component acceptance and functional testing
- Mechanical and electrical interface compatibility verification
- System performance (frequency response, dynamic stiffness, velocity, position resolution, and efficiency)
- System demonstration (reliability redundancy management)
- System performance at ambient temperatures (actuator only) from -65°F to + 250°F
- System performance as a function of the inverter current limit at currents up to 30 amp.
- System operation as a function of supply voltage

1.4 OBJECTIVE

The overall objective of this testing effort is to further demonstrate the feasibility of electromechanical actuation for primary flight control surfaces. This can be accomplished through dual channel stabilized control capability for high torque, high bandwidth response.

1.5 REFERENCES

1. Air Force Contract F33615-80-C-3620, Section C, Description/Specifications
2. AiResearch Proposal, 09308-13720-015, March 20, 1980. Preliminary Proposal for Integrated Hinge (Rotary) Electromechanical Actuation Testing.

2.0 TEST CONCEPTS

2.1 TEST ARTICLES

The hardware to be tested consists of components and assemblies as described below:

COMPONENT			ASSEMBLY		UNIT
ITEM	QTY	PART NO.	ITEM	PART NO.	ITEM
Motor*	2	P515018-2	Actuator	2022194	Integrated Hinge Actuation Unit
Gearbox	1	2022192			
Controller 2-channel	1	-			

*The motor includes instrumentation per Dwg. PA150920 (tachometer and synchro)

2.2 TEST PLAN

2.2.1 Special Test Equipment

For this testing effort the existing test stand and linear spring loading fixture will be utilized.

2.2.2 Schedule

The schedule of tests is presented in Figure 22. This figure also includes the time allotted to incorporate the required hardware modifications. Testing of the actuation system will require one month beginning October 1980.

2.2.3 Facilities

The test program will be conducted in the existing facilities of AiResearch Manufacturing Company. All system tests are to be performed in the electromechanical laboratory.

3.0 TESTING

This section presents descriptions of each test that is to be performed. Individual test briefs summarizing setups, procedures, and required data are presented in Section 4 of this document.

3.1 STABILITY ASSESSMENT

The objective of this test is to establish the actuation system operates in a stable manner. The system will be subjected to square waves (step) and triangular waves (ramp) input commands of various amplitudes and frequencies under loaded and unloaded conditions. Results will be recorded on an oscillograph and be available for evaluation. All tests will be performed at laboratory ambient temperature.

3.2 FREQUENCY RESPONSE TEST

The objective of this test is to determine the amplitude ratio and phase lag as a function of frequency. The system will be subjected to input commands of various amplitudes and frequencies to determine the bandwidth of the actuation unit.

3.3 INCREASED SYSTEM INERTIA

This test will investigate the effect of an increased inertial load. The output arm of the test stand will be incrementally weighted and system response will be recorded. These results will be correlated with analytical predictions. This test will be limited to demonstration only due to test stand limitations. Results of the test will determine the extent to which the output inertia is increased.

4.0 TEST PROCEDURES

This section includes test briefs describing the system demonstration tests to be performed. These briefs include the following information:

Objective

Facility

Test Setup Schematic

Equipment and Instrumentation List

Test Procedure Summary

Required data to be recorded

Criteria for acceptance or rejection of tests

Special Notes

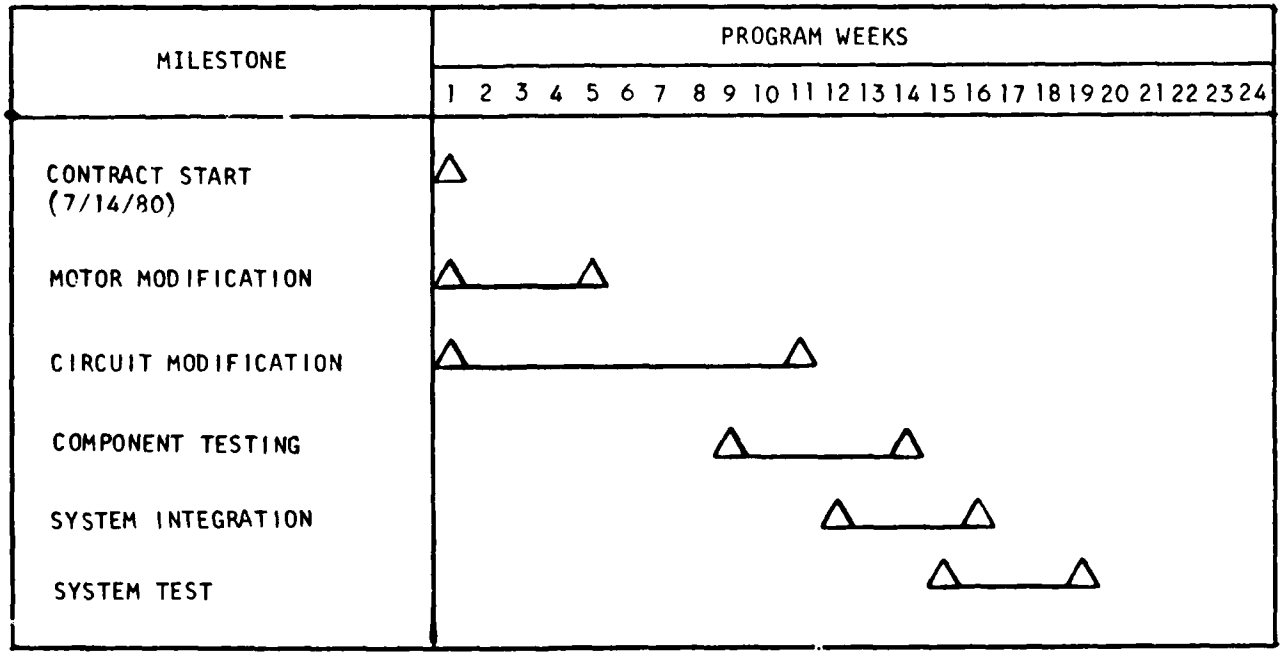

Figure 22. Program Sch

GARRETT

TEST

STABILITY ASSESSMENT

Prepared by: _____

Part No. _____

Date _____

OBJECTIVE

TO DEMONSTRATE ACCEPTABLE SYSTEM STABILITY

FACILITY

ELECTROMECHANICAL LABORATORY

SCHEMATIC

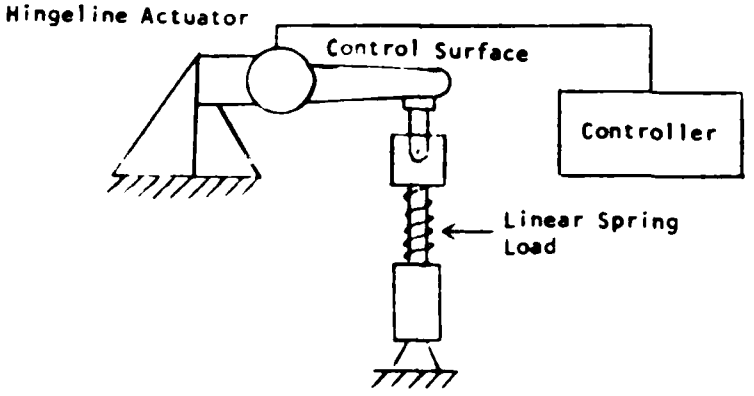

EQUIPMENT AND INSTRUMENTATION

1. OSCILLOGRAPH
2. SIGNAL GENERATOR
3. POSITION INDICATOR
4. REACTION FIXTURE

PROCEDURE

1. APPLY STEP INPUT COMMANDS OF 1, 5, AND 10 DEG AMPLITUDES - RECORD RESULTS
2. REPEAT STEP 1 FOR VARIOUS LOADS
3. APPLY RAMP (TRIANGLE) INPUT COMMANDS OF 1, 5, AND DEG AMPLITUDES - RECORD RESULTS
4. REPEAT STEP 3 FOR VARIOUS LOADS INCLUDING NO LOAD AND FREQUENCIES - FREQUENCY TO VARY BETWEEN 0.1 AND 2 HZ.

REQUIRED DATA

1. INPUT COMMAND
2. OUTPUT POSITION
3. LOAD
4. CURRENT
5. VOLTAGE

ACCEPT/REJECT CRITERIA

TEST DEMONSTRATION ONLY

NOTES

DATA TO BE COMPARED TO ANALYTICAL RESULTS

S-95237

GARRETT

TEST

FREQUENCY RESPONSE

Prepared by: _____

Part No. _____

Date _____

OBJECTIVE

TO DETERMINE BANDWIDTH OF THE ACTUATION SYSTEM

FACILITY

ELECTROMECHANICAL LABORATORY

SCHEMATIC

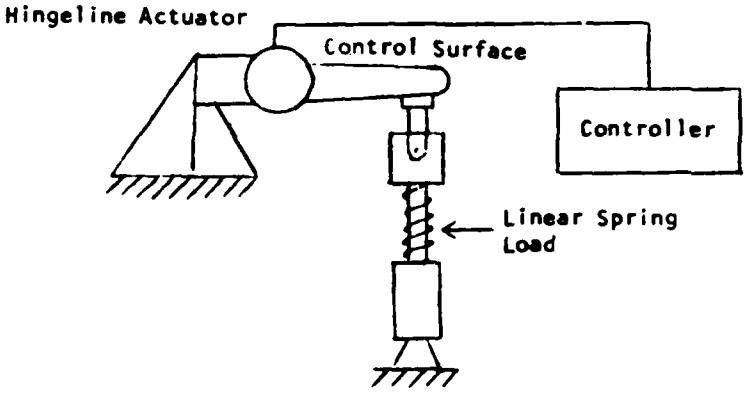

EQUIPMENT AND INSTRUMENTATION

1. OSCILLOGRAPH
2. SIGNAL GENERATOR
3. POSITION INDICATOR
4. REACTION FIXTURE

PROCEDURE

1. APPLY SINUSOIDAL INPUT COMMANDS OF AMPLITUDES OF $\pm$ 0.5 DEG AND $\pm$ 1.0 DEG AND VARY THE FREQUENCY FROM 0.5 TO 20 HZ - RECORD RESULTS
2. REPEAT STEP 1 FOR VARIOUS LOADS

REQUIRED DATA

1. INPUT COMMAND
2. OUTPUT POSITION
3. LOAD
4. CURRENT
5. VOLTAGE

ACCEPT/REJECT CRITERIA

TEST DEMONSTRATION ONLY

NOTES

DATA TO BE COMPARED TO ANALYTICAL RESULTS

S-95237

5.0 DOCUMENTATION

All documentation of test conducted for this program will be included in the final report for this contract (CDRL Sequence 6) which will be submitted March 1981. The format of test results will be determined by the nature of the individual test.

APPENDIX B

TEST DATA

APPENDIX B

TEST DATA

Guide to Test Data

Test No.	Figure No.	Description
1	23	+1° step, no load
	24	-1° step, no load
2	25	+2° step, no load
	26	-2° step, no load
3	27	+5° step, no load
	28	-6° step, no load
4	29	+10° step, no load
	30	-10° step, no load
5	31	+1° step, X_0 = 0°, loaded
	32	-1° step, X_0 = +1°, loaded
	33	-1° step, X_0 = 0°, loaded
	34	+1° step, X_0 - -1°, loaded
6	35	-2° step, X_0 = +2°, loaded
	36	-2° step, X_0 = 0°, loaded
	37	+2° step, X_0 = -2°, loaded
7	38	+5° step, X_0 = 0°, loaded
	39	-5° step, X_0 = 5°, loaded
	40	-5° step, X_0 = 0°, loaded
	41	+5° step, X_0 - -5°, loaded
8	42	+10° step, X_0 = 0°, loaded
	43	-10° step, X_0 = +10°, loaded

Test No.	Figure No.	Description
8	44	-10° step, X_0 = 0°, loaded
	45	+10° step, X_0 = -10°, loaded
9	46	±1° triangle, 1 Hz, no load
	47	±1° triangle, 2 Hz, no load
10	48	±2° triangle, 0.1 Hz, no load
	49	±2° triangle, 1 Hz, no load
	50	±2° triangle, 2 Hz, no load
11	51	±5° triangle, 0.1 Hz, no load
	52	±5° triangle, 1 Hz, no load
	53	±5° triangle, 2 Hz, no load
12	54	±10° triangle, 0.1 Hz, no load
	55	±10 triangle, 2 Hz, no load
13	56	±1° triangle, 0.1 Hz, loaded
	57	±1° triangle, 1 Hz, loaded
	58	±1° triangle, 2 Hz, loaded
14	59	±2° triangle, 0.1 Hz, loaded
	60	±2° triangle, 1 Hz, loaded
	61	±2° triangle, 2 Hz, loaded
15	62	±5° triangle, 0.1 Hz. loaded
	63	±5° triangle, 1 Hz loaded
	64	±5° triangle, 2 Hz, loaded
16	65	±10° triangle, 0.1 Hz, loaded
	66	±10° triangle, 1 Hz, loaded
	67	±10° triangle, 2 Hz, loaded
17	68	±1° sine, 1 Hz, no load

Test No.	Figure No.	Description
17	69	±1° sine, 2 Hz, no load
	70	±1° sine, 4 Hz, no load
	71	±1° sine, 8 Hz, no load
	72	±1° sine, 16 Hz, no load
18	73	±2° sine, 1 Hz, no load
	74	±2° sine, 2 Hz, no load
	75	±2° sine, 4 Hz, no load
	76	±2° sine, 8 Hz, no load
	77	±2° sine, 16 Hz, no load
19	78	±5° sine, 1 Hz, no load
	79	±5° sine, 2 Hz, no load
	80	±5° sine, 4 Hz, no load
	81	±5° sine, 8 Hz, no load
	82	±5° sine, 16 Hz, no load
20	83	±10° sine, 1 Hz, no load
	84	±10° sine, 2 Hz, no load
	85	±10° sine, 4 Hz, no load
	86	±10° sine, 8 Hz, no load
	87	±10° sine, 16 Hz, no load
21	88	±1° sine, 1 Hz, loaded
	89	±1° sine, 2 Hz, loaded
	90	±1° sine, 4 Hz, loaded
	91	±1° sine, 8 Hz, loaded
	92	±1° sine, 16 Hz, loaded
22	93	±2° sine, 1 Hz, loaded

Test No.	Figure No.	Description
22	94	±2° sine, 2 Hz, loaded
	95	±2° sine, 4 Hz, loaded
	96	±2° sine, 8 Hz, loaded
	97	±2° sine, 16 Hz, loaded
23	98	±5° sine, 1 Hz, loaded
	99	±5° sine, 2 Hz, loaded
	100	±5° sine, 4 Hz, loaded
	101	±5° sine, 8 Hz, loaded
	102	±5° sine, 16 Hz, loaded
24	103	±10° sine, 1 Hz, loaded
	104	±10° sine, 2 Hz, loaded
	105	±10° sine, 4 Hz, loaded
	106	±10° sine, 8 Hz, loaded
	107	±10° sine, 16 Hz, loaded
25	108	Frequency response, ±1°, 2.55 in.-lb-sec^2
26	109	Frequency response, ±2°, 2.55 in.-lb-sec^2
27	110	Frequency response, ±1°, 4.34 in.-lb-sec^2
28	111	Frequency response, ±2°, 4.34 in.-lb-sec^2
29	112	Frequency response, ±1°, 8.04 in.-lb-sec^2
30	113	Frequency response, ±2°, 8.04 in.-lb-sec^2

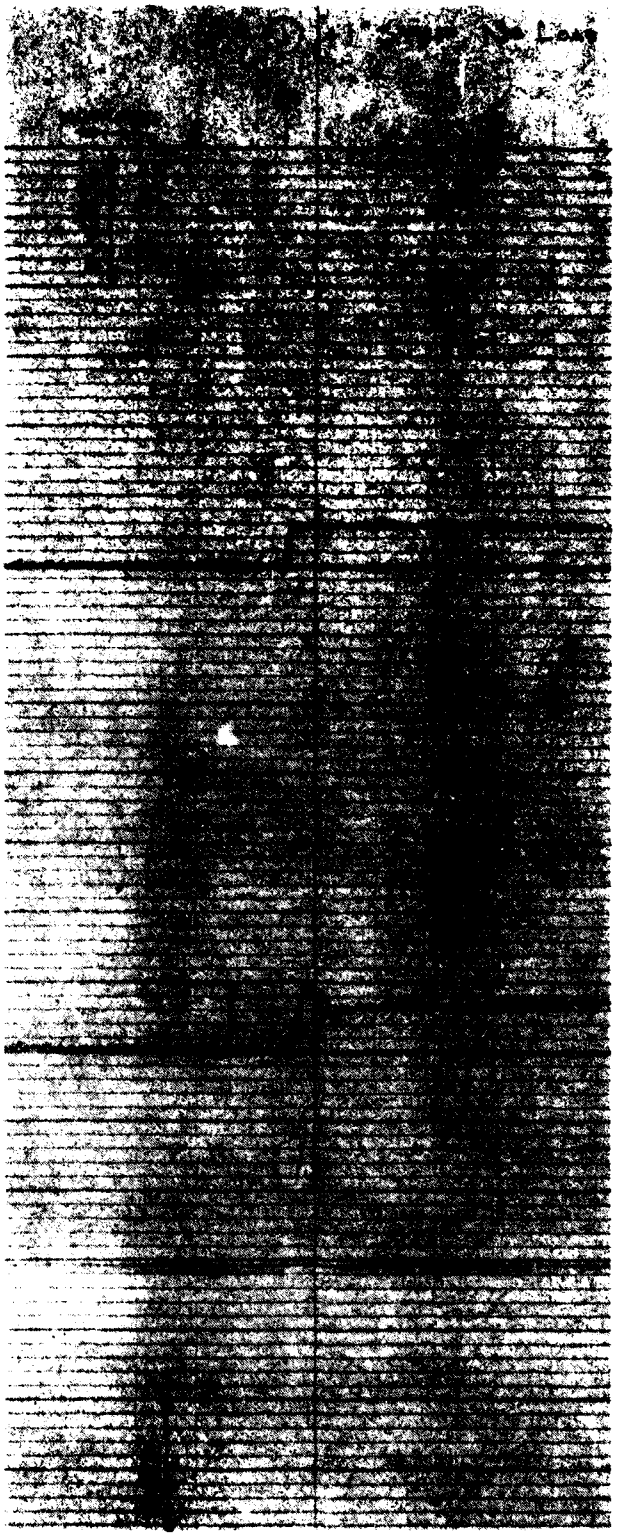

Figure 23. Test 1, 11° step, 2a [illegible]

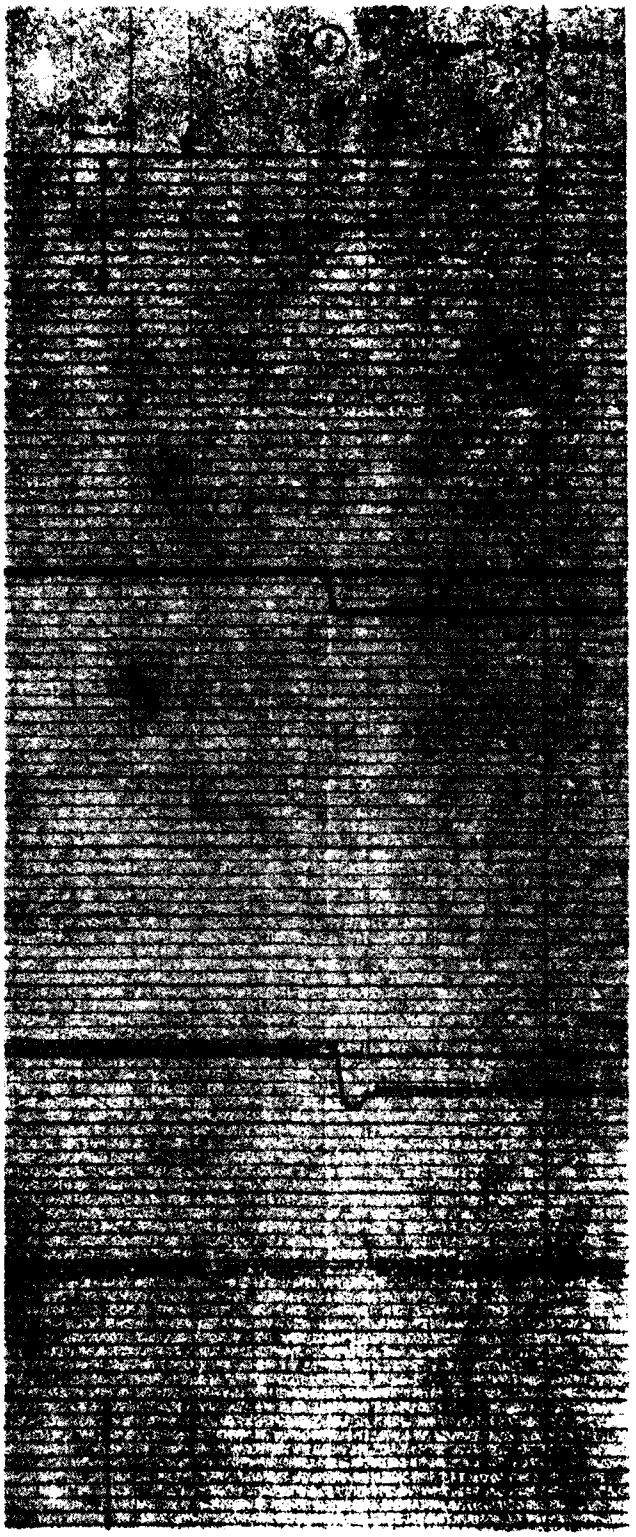

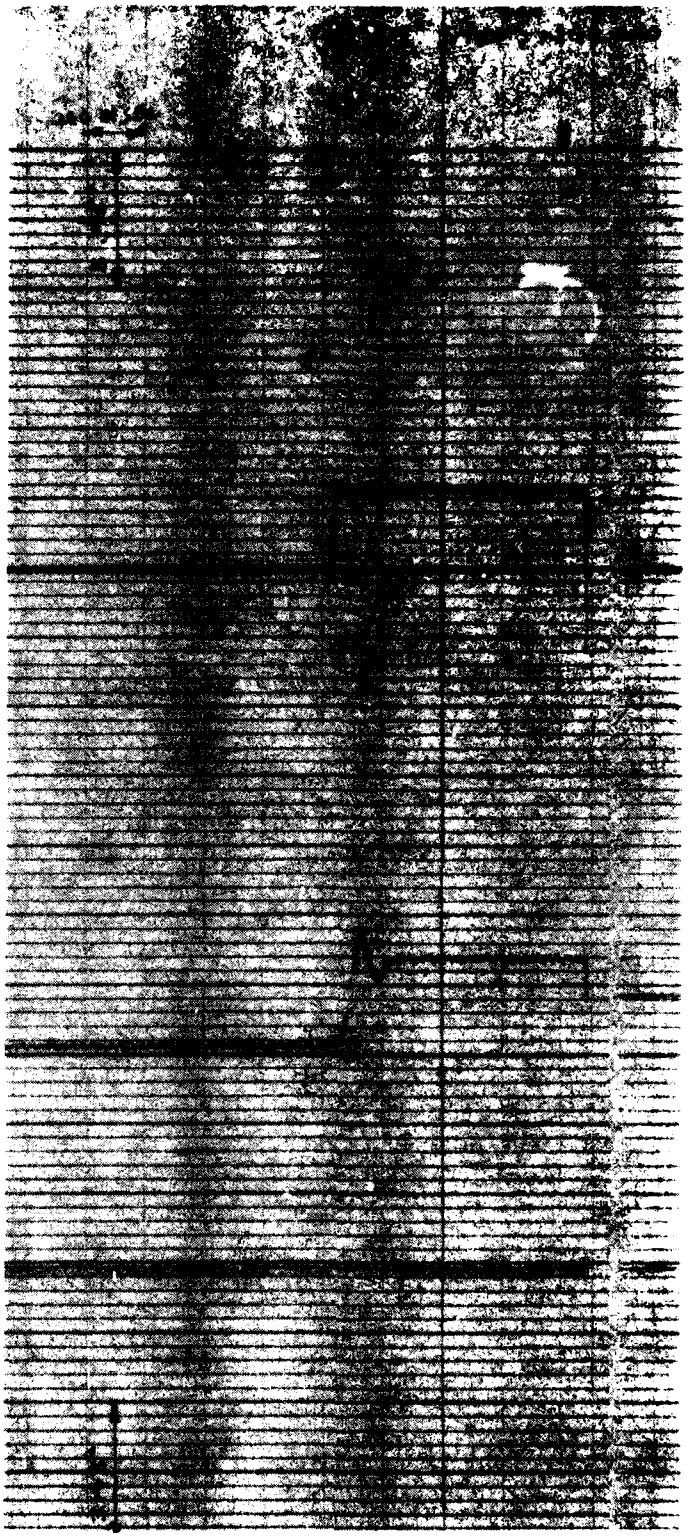

Figure 25. Test 3, 6° step, [illegible]

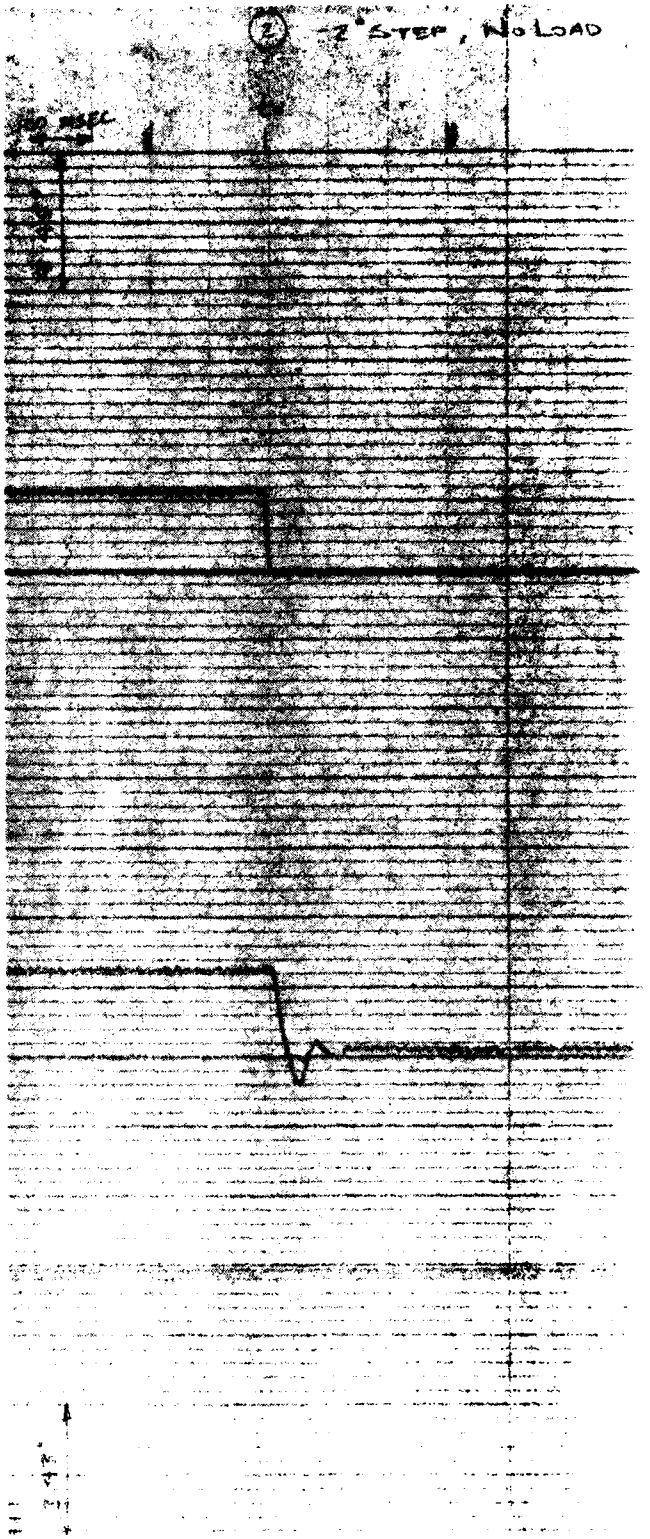
(2) -2° STEP, NO LOAD
100 MSEC

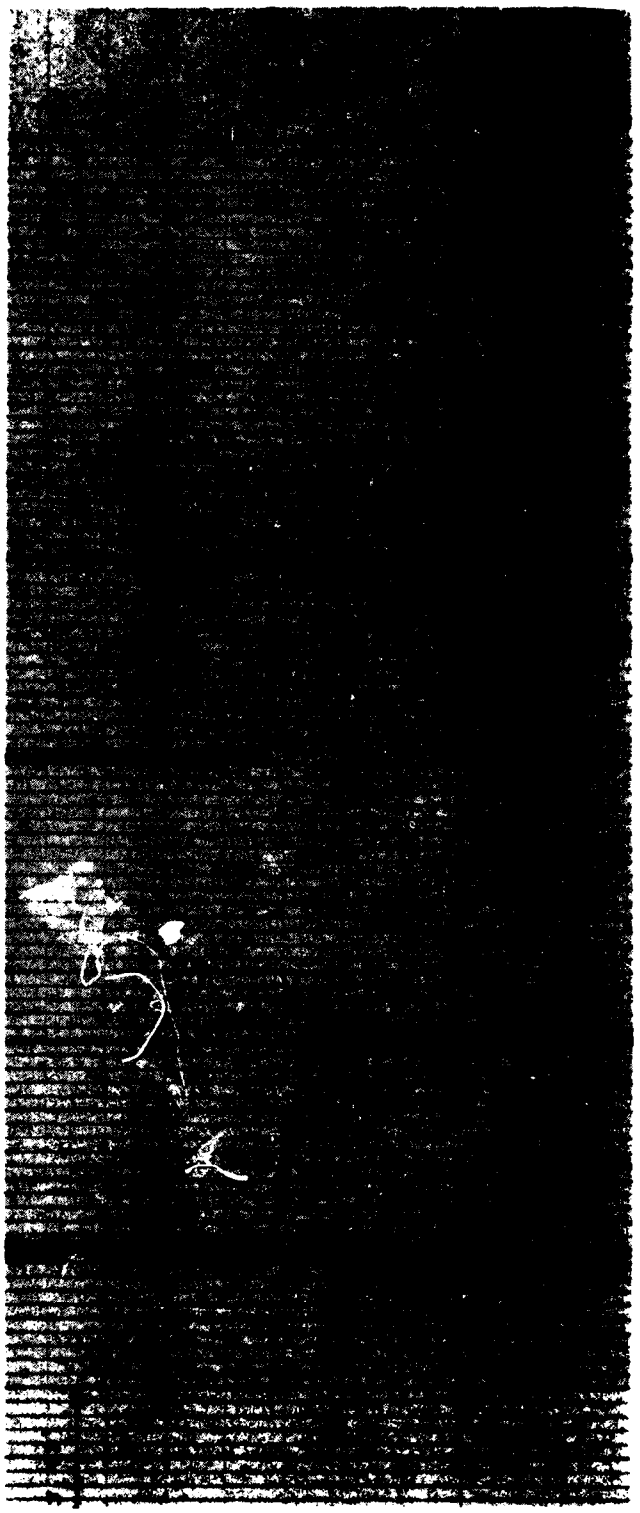

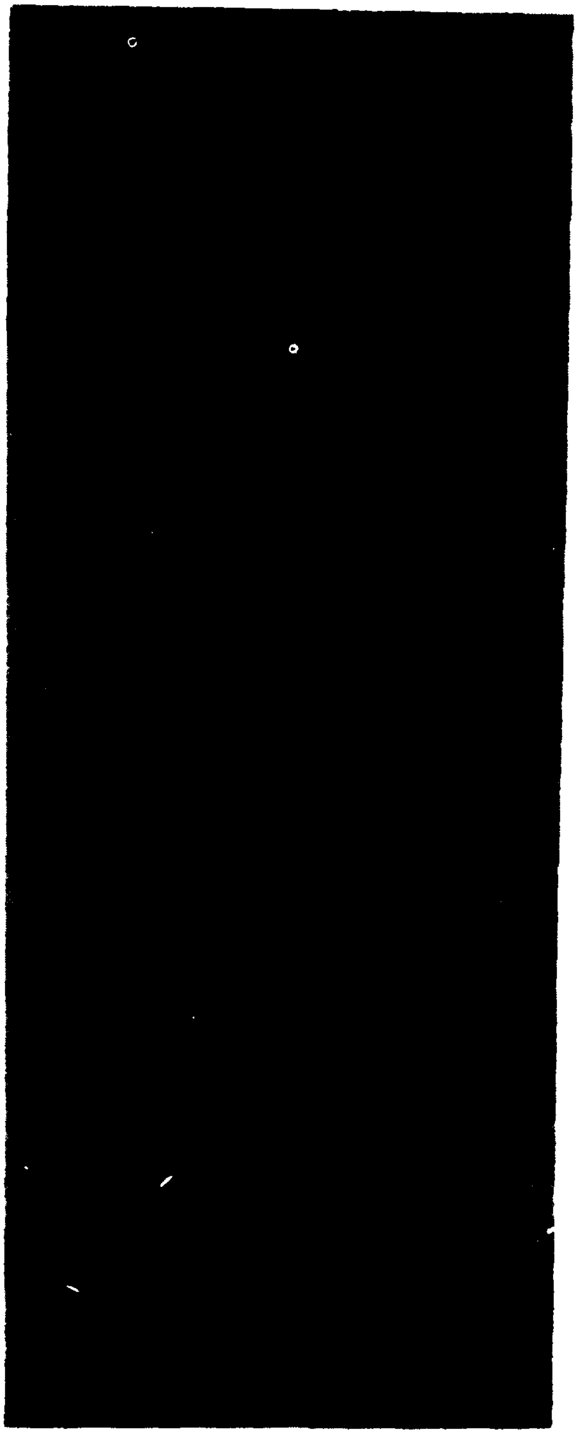

Figure [illegible]. Test [illegible], –[illegible]° [illegible], [illegible]

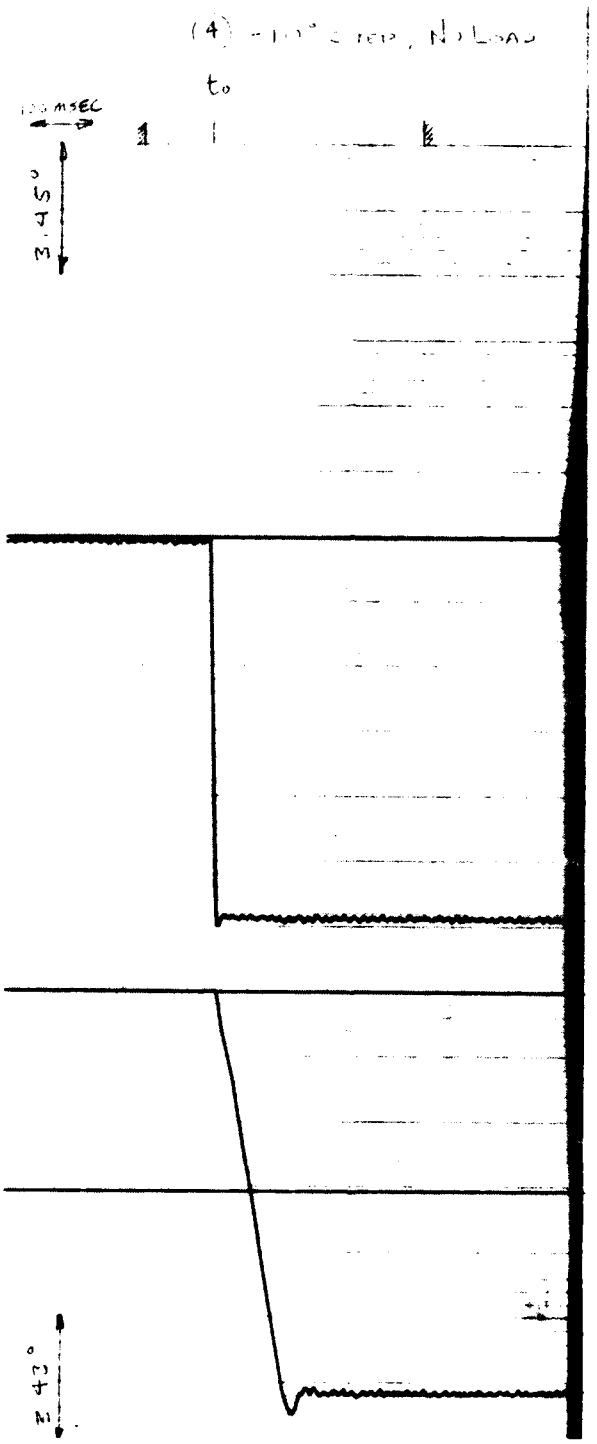

Figure 30. Test 4, -10° Step, No Load

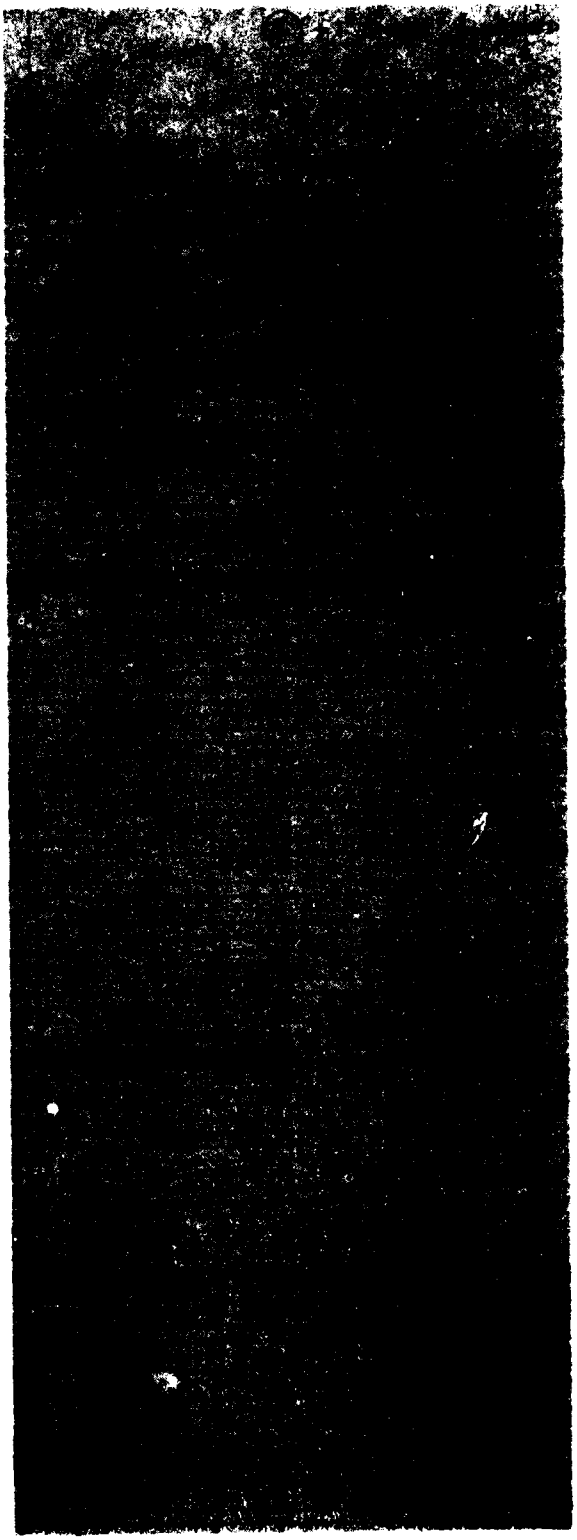

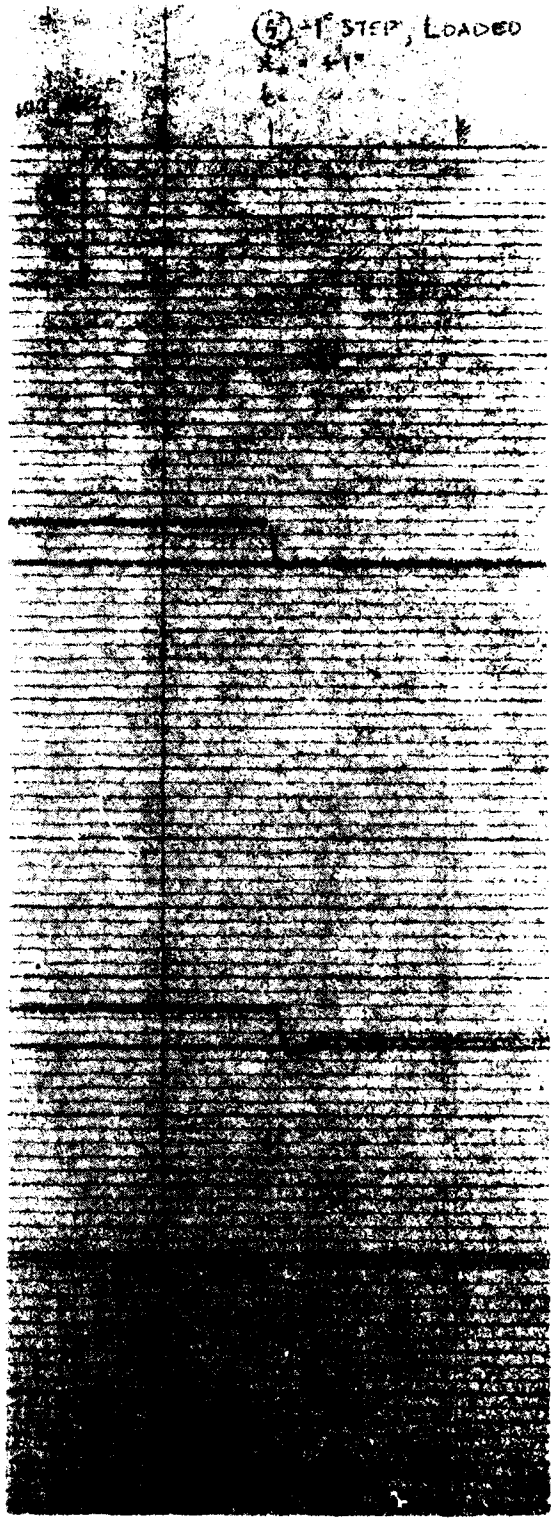
(5) -1° STEP, LOADED

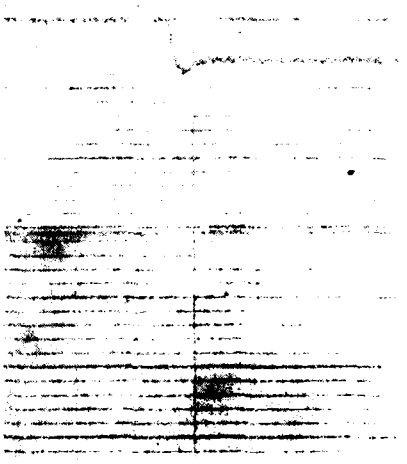

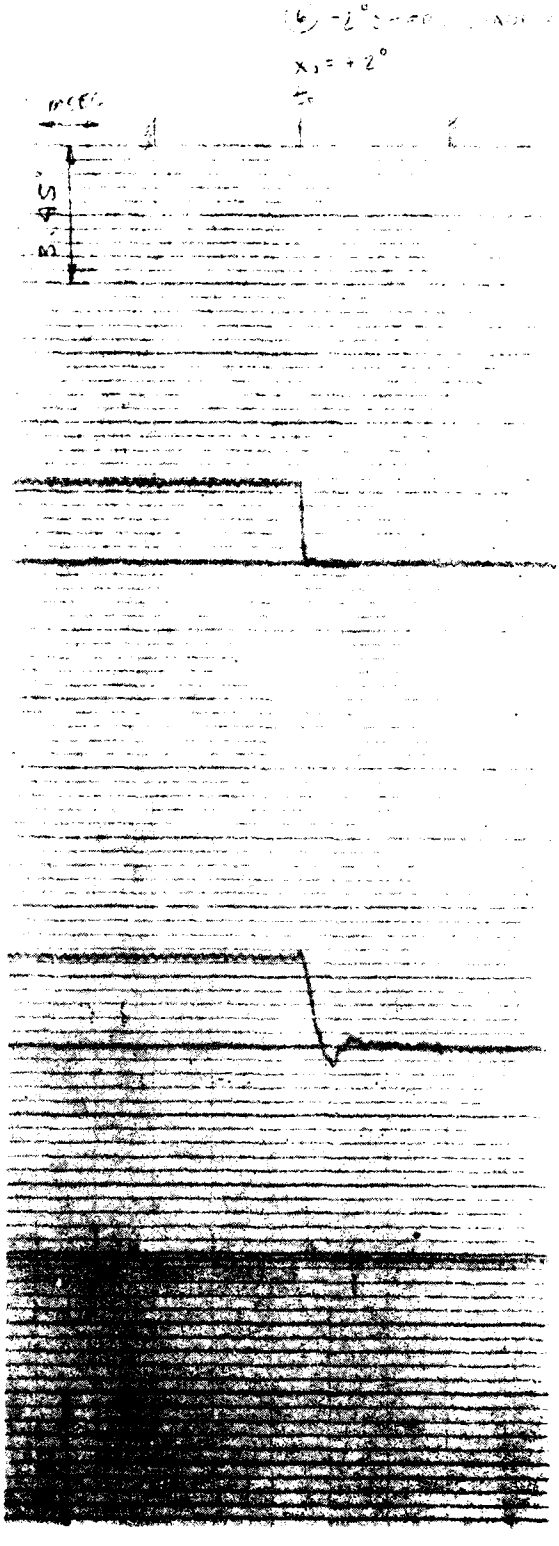

Figure 45. Test 6, -2° step, x_c = +2°,

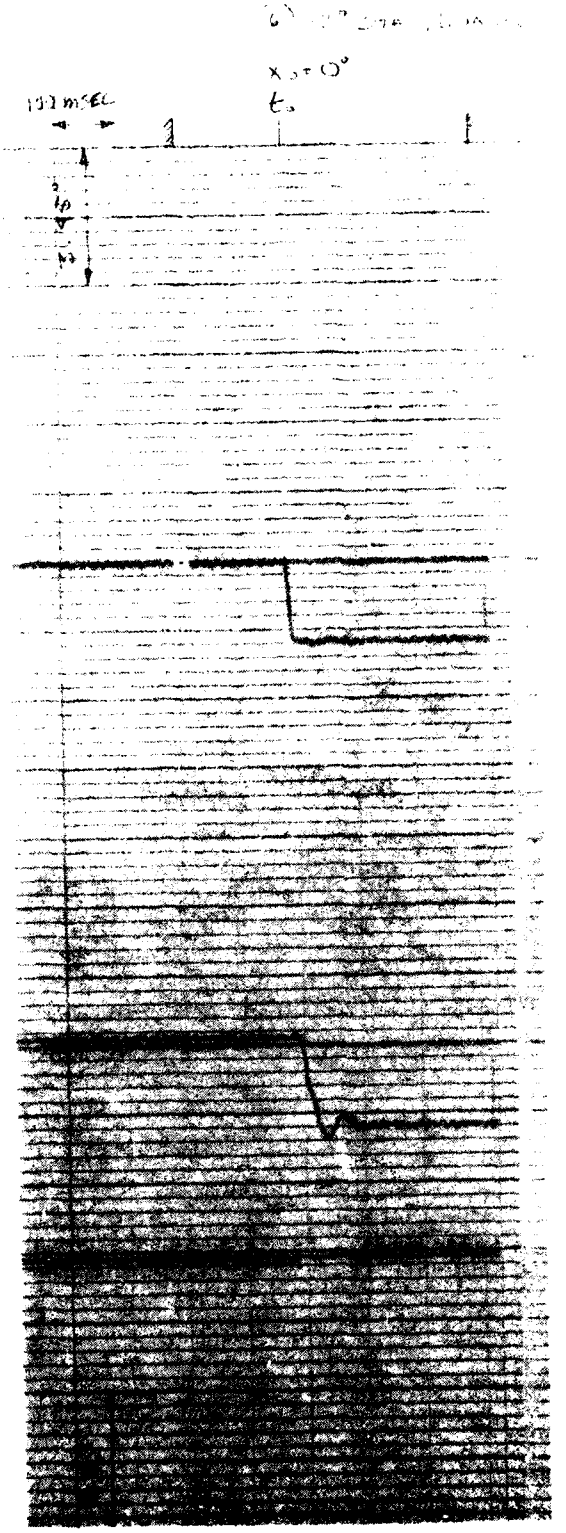

Figure 46. Test 6, -2° Step, X_{cg} = 0°, Loaded

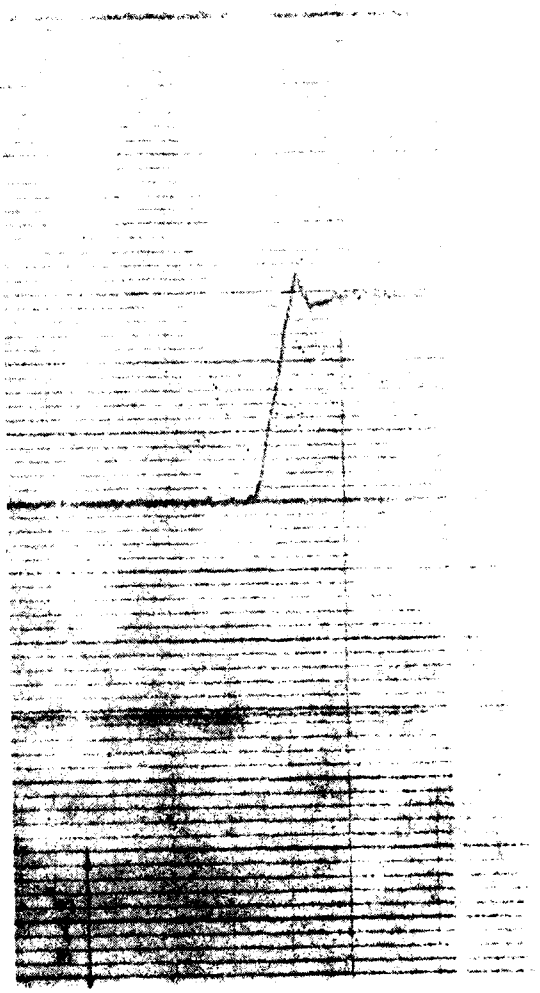

Figure 9. Test 7, [illegible]

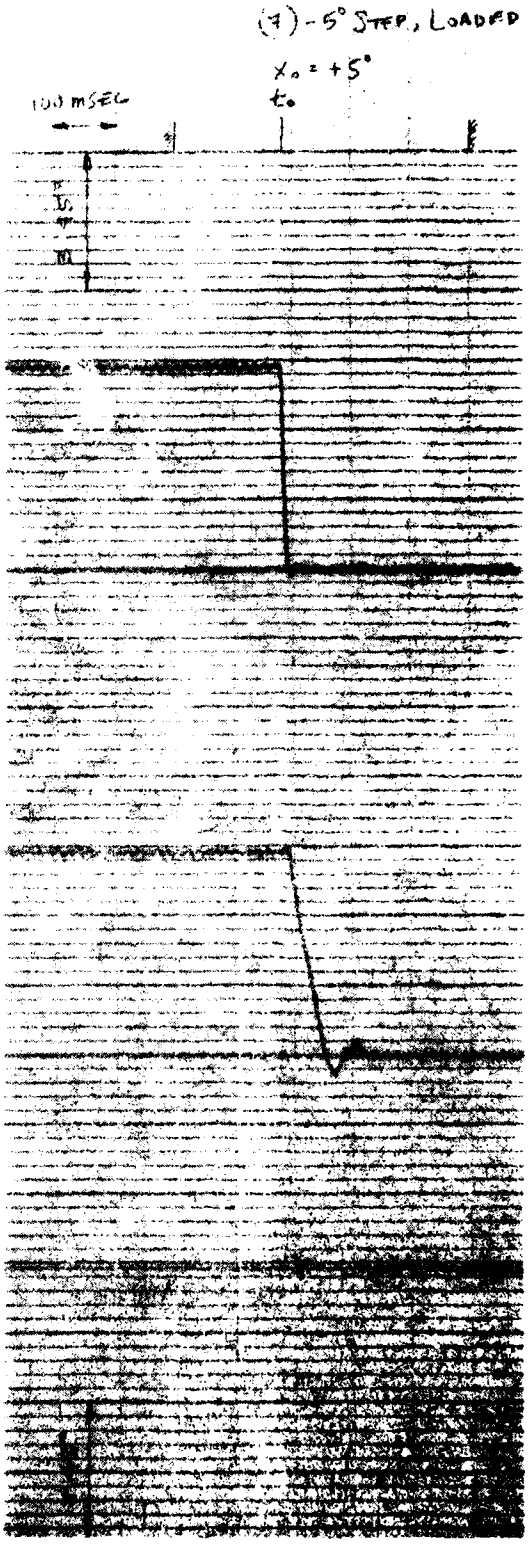

Figure 39. [illegible]

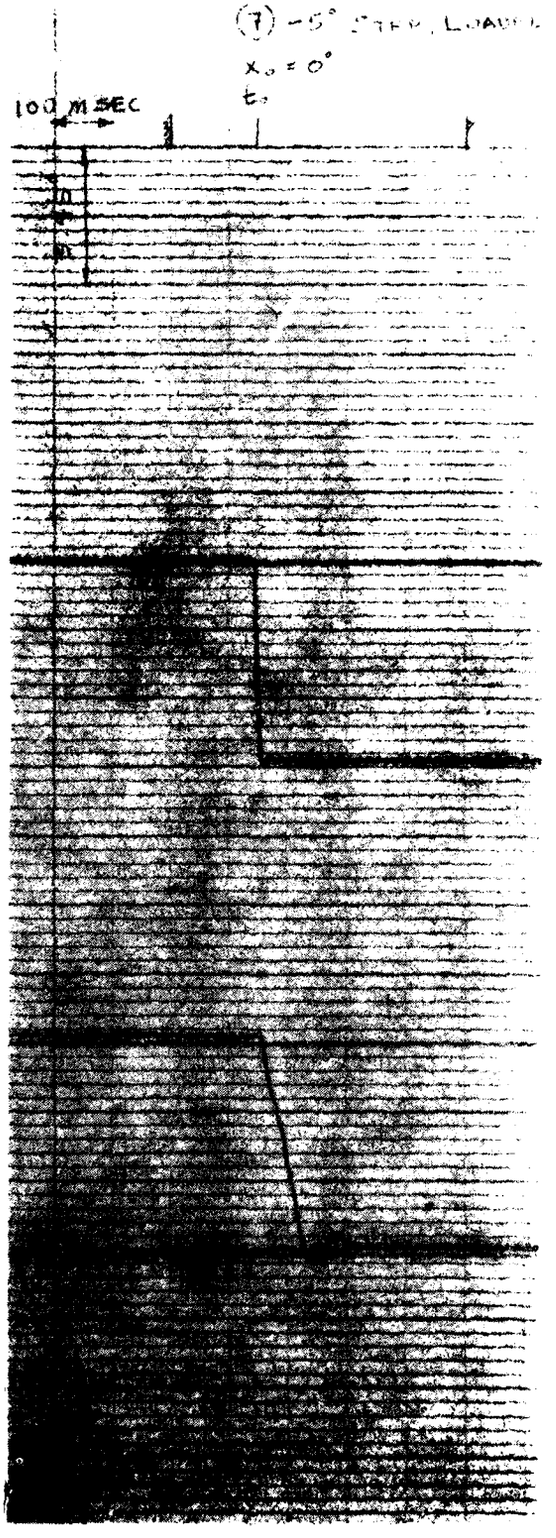

Figure 4(. Test ', -°° step, x_0 = °,

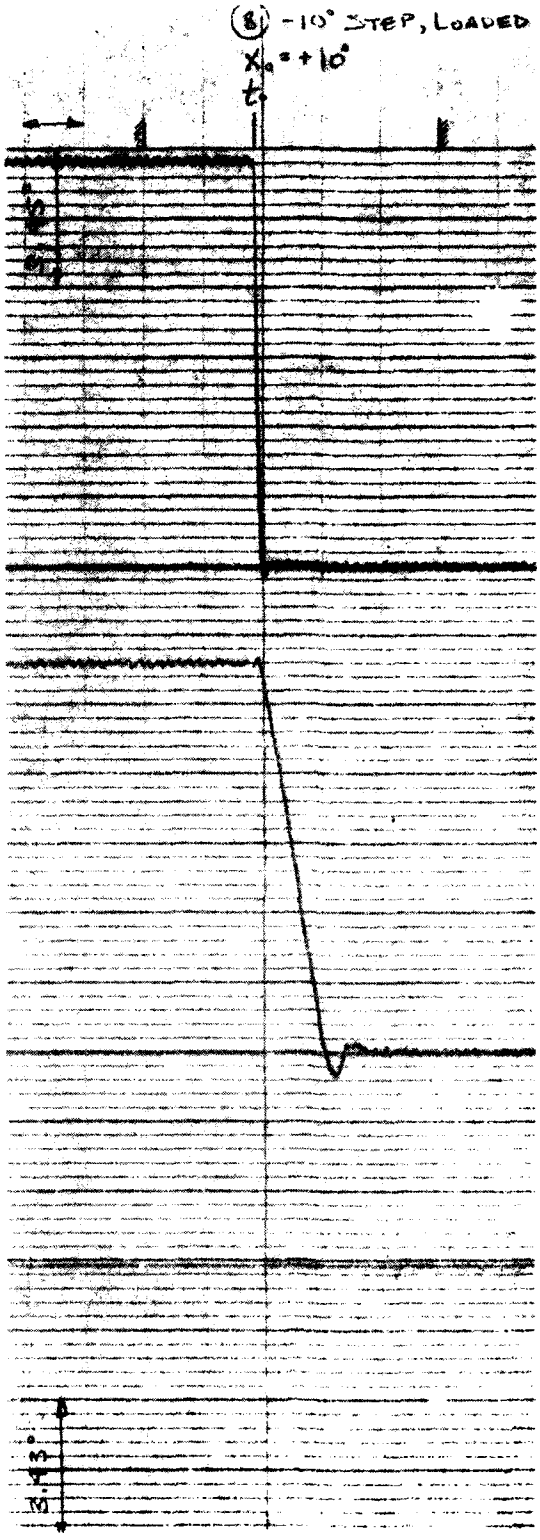
(8) -10° STEP, LOADED
$X_0 = +10°$
t_0

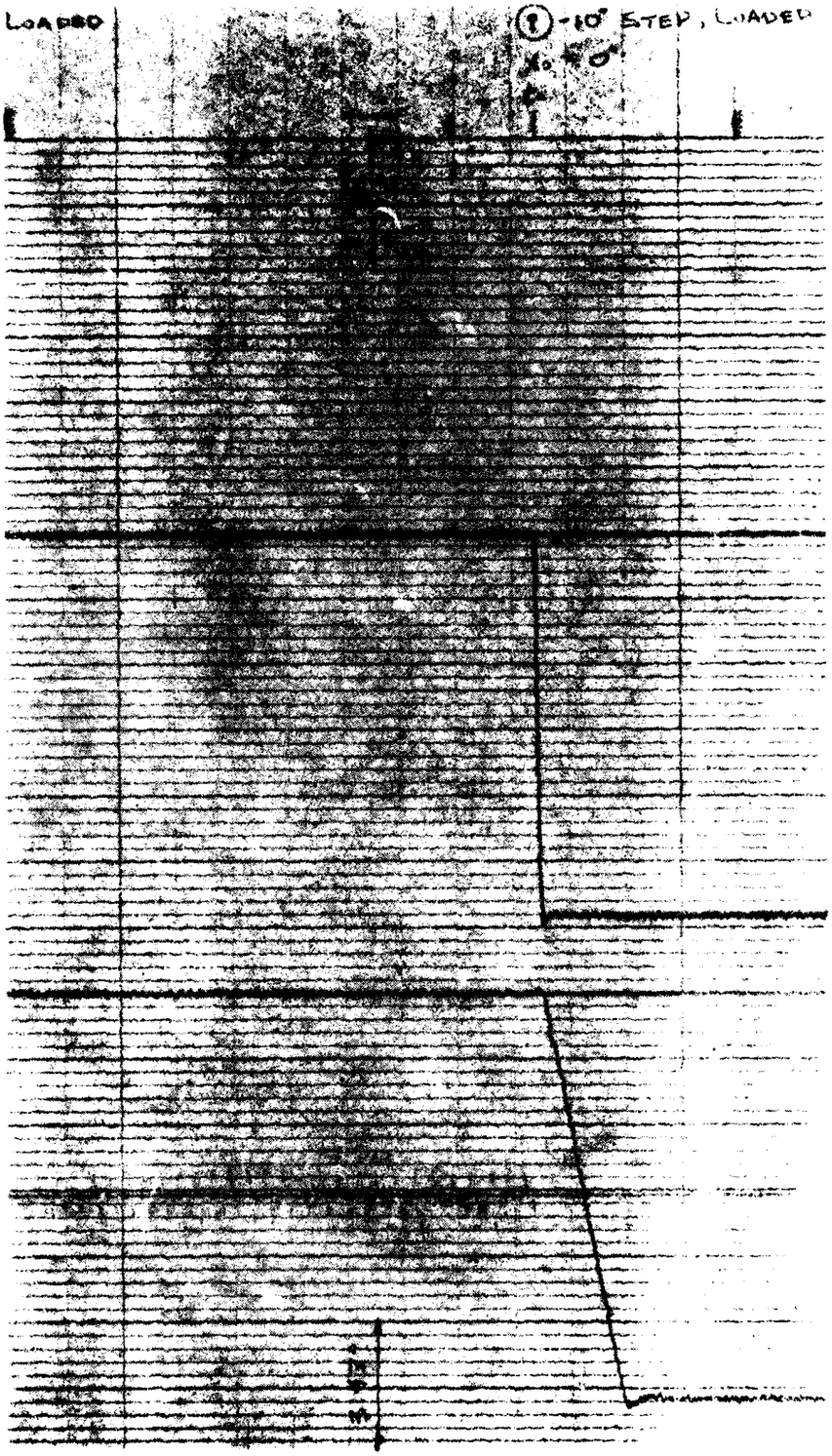
LOADED
-10° STEP, LOADED

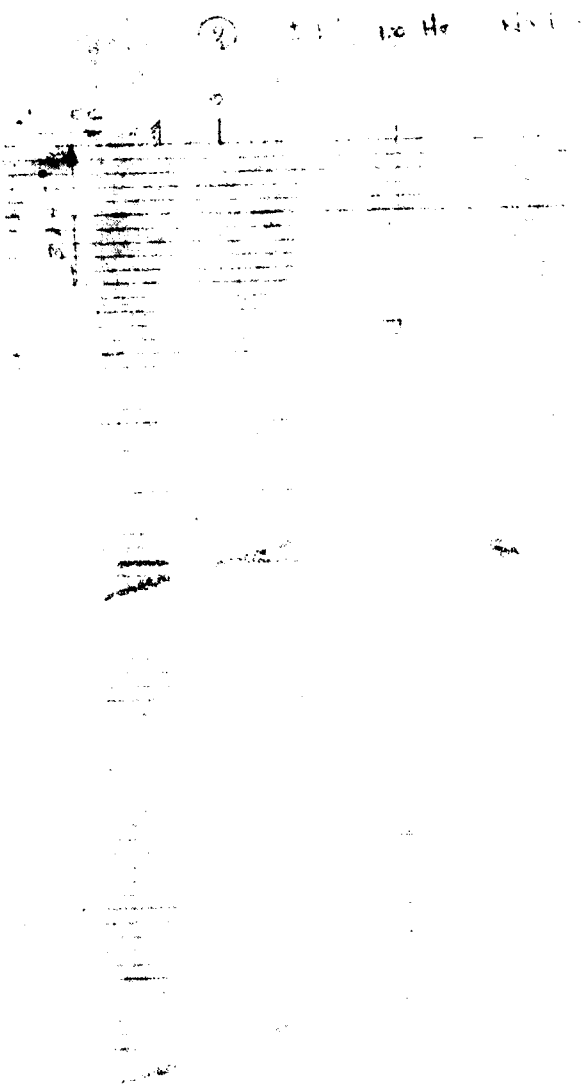

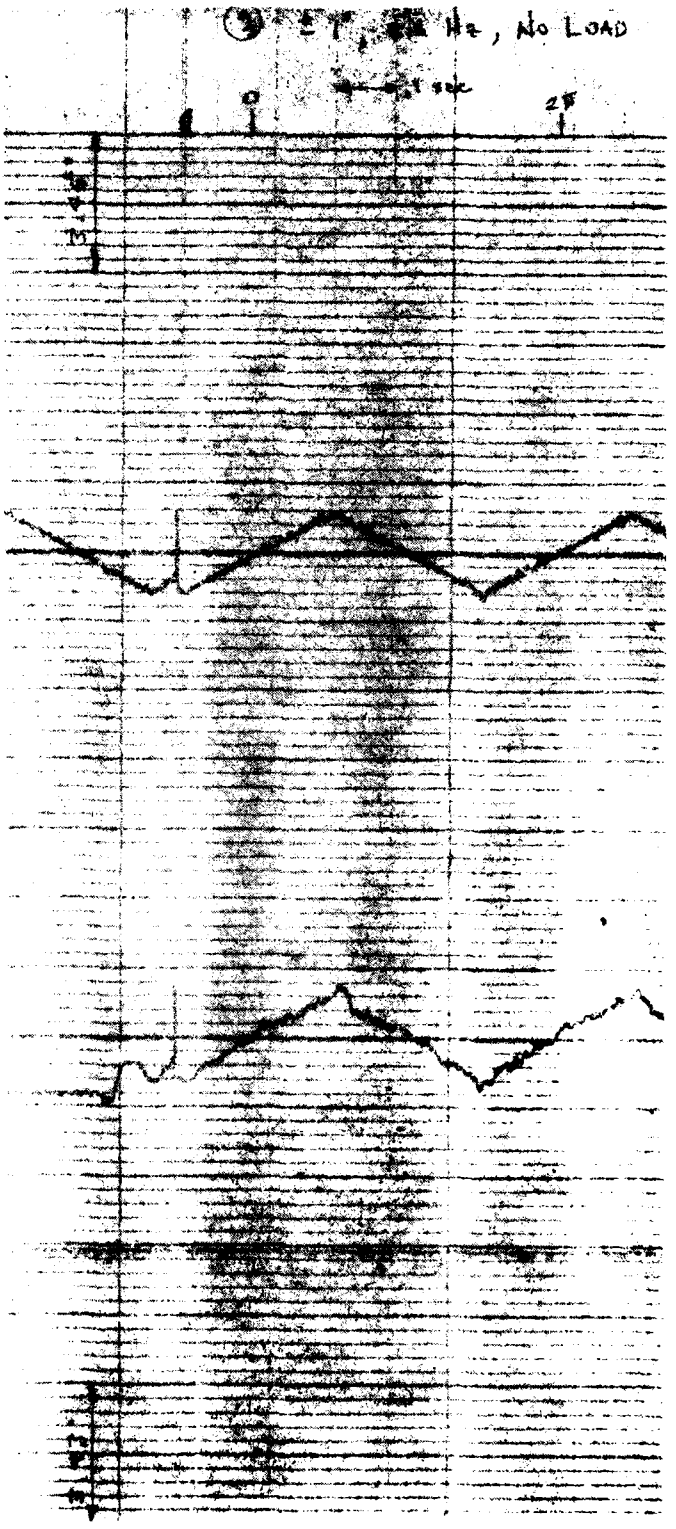
, No Load
1 sec
0
25

(10) ± 2° AT 1 HZ, NO LOAD

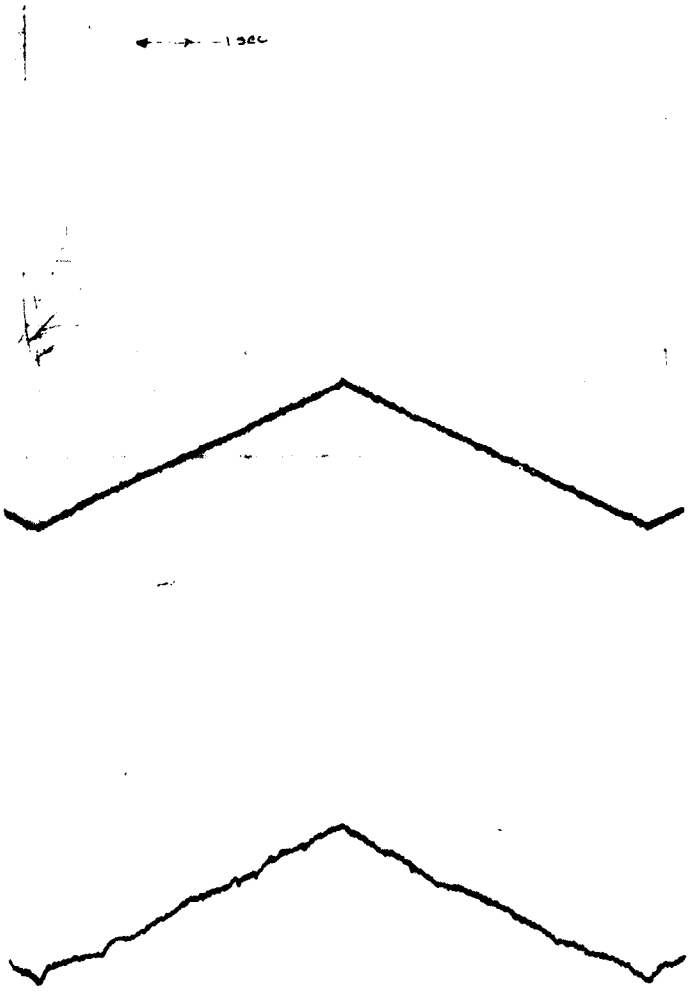

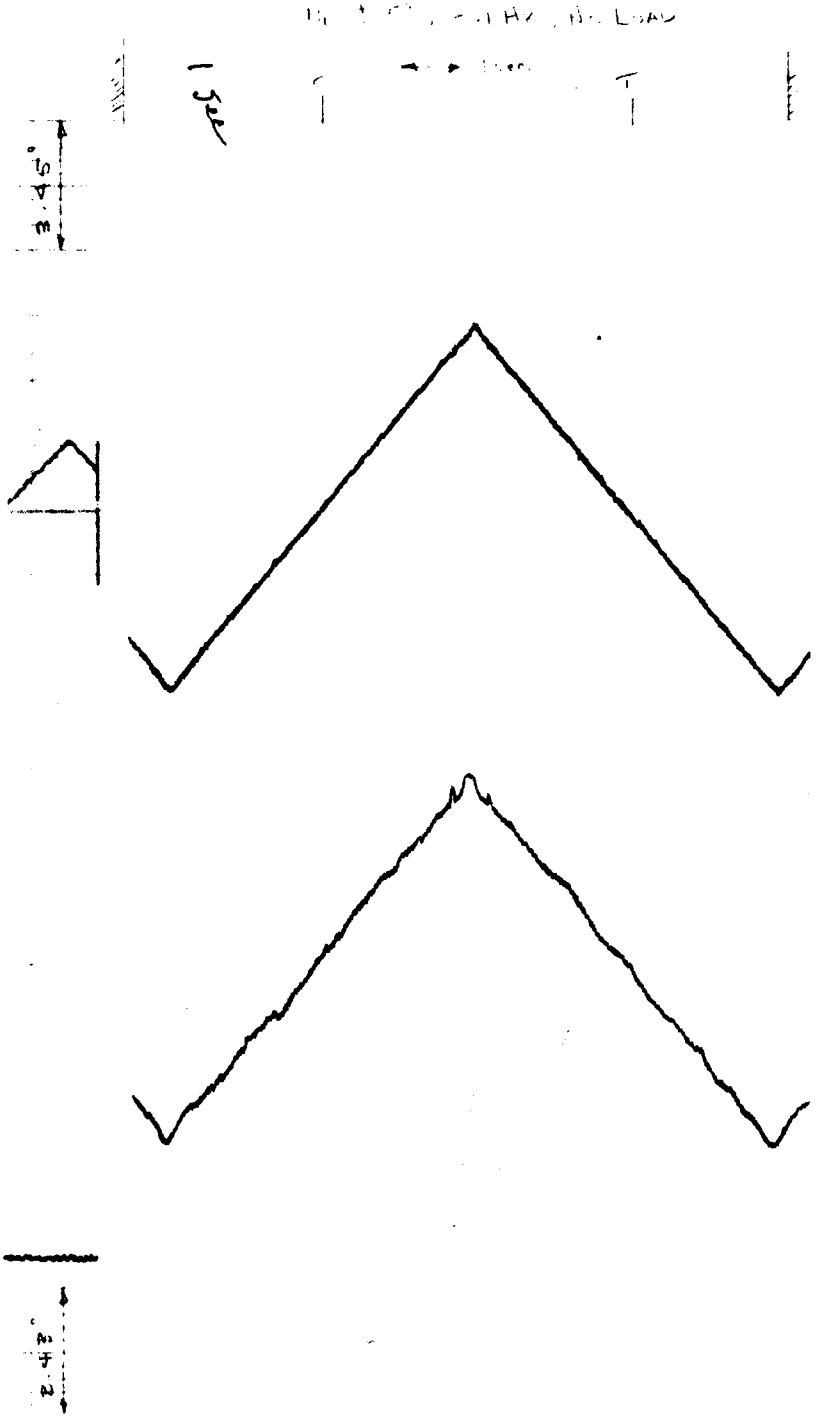

Figure 51. Test 11, [illegible] Triangle, [illegible] Hz, No Load

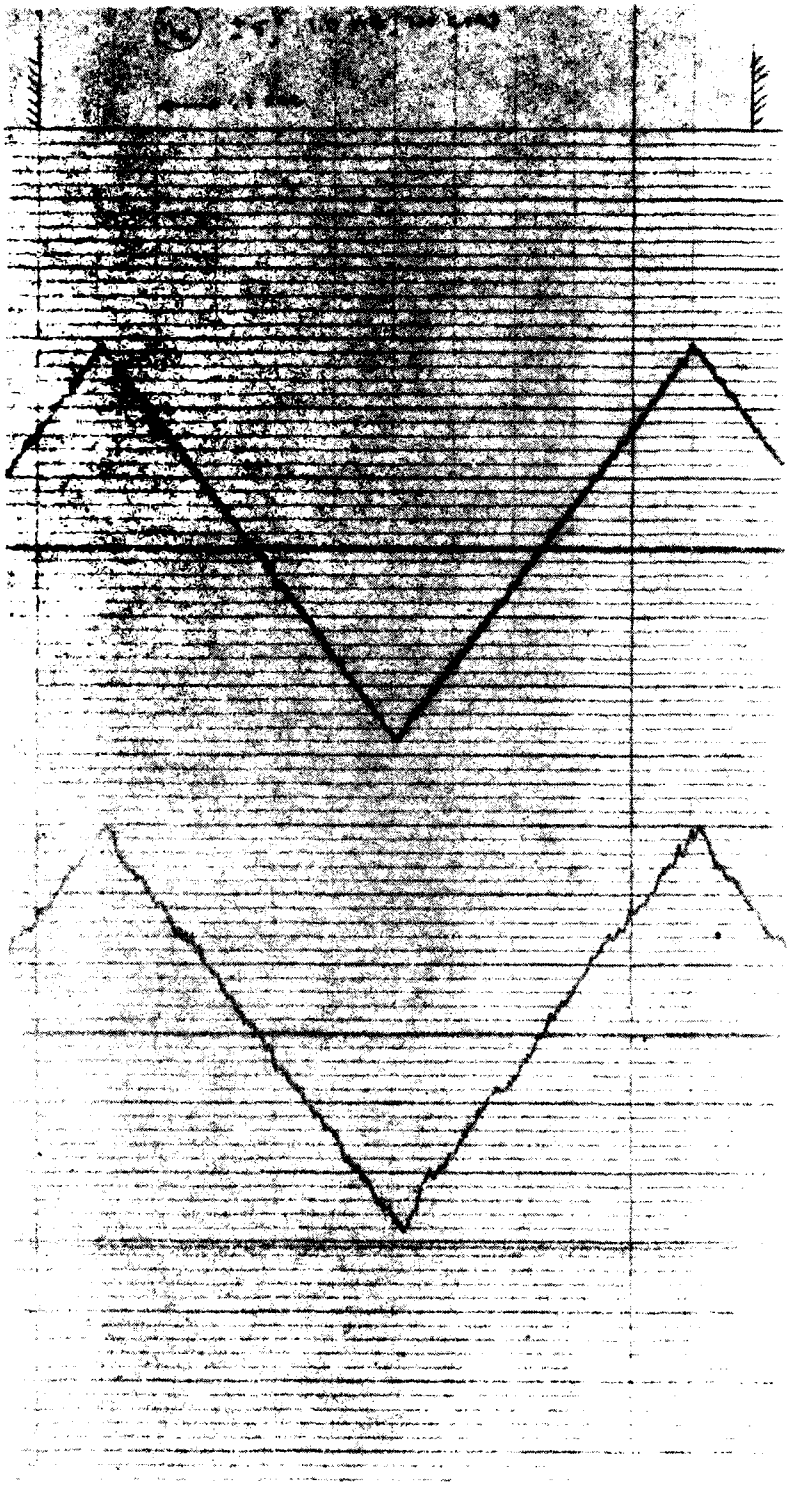

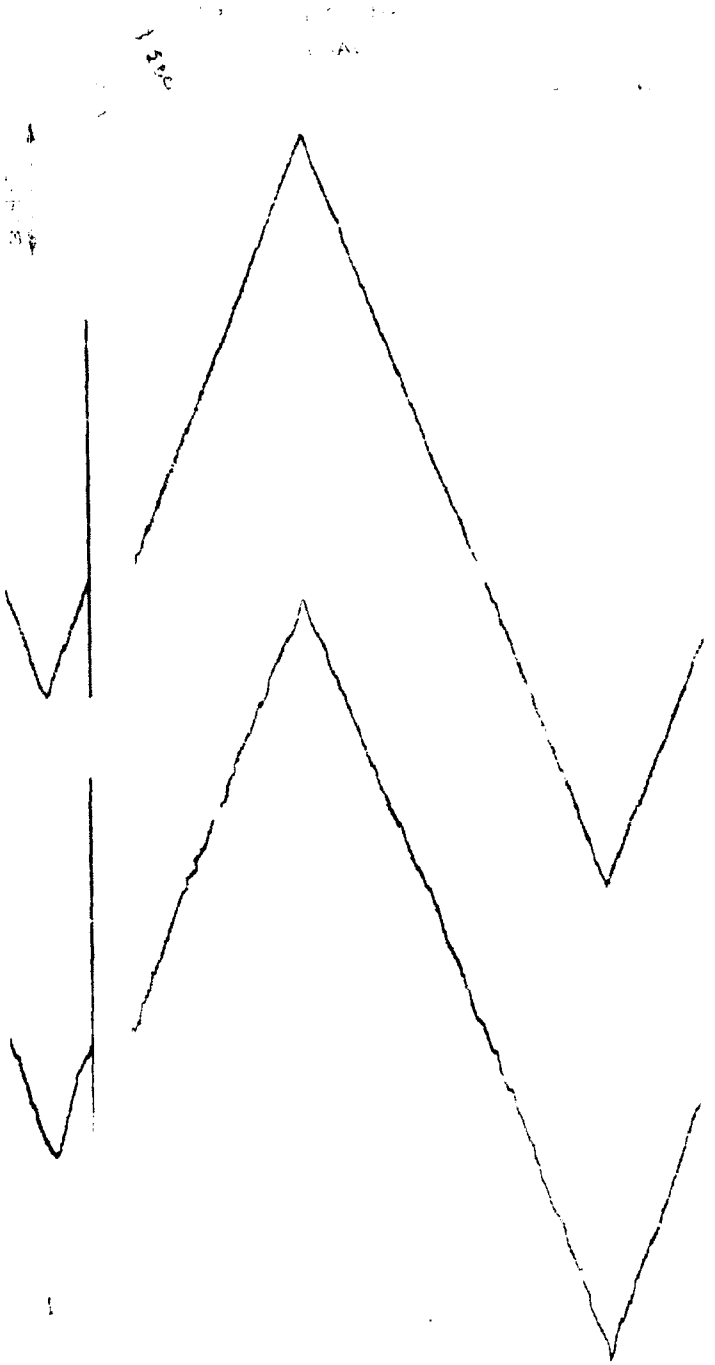

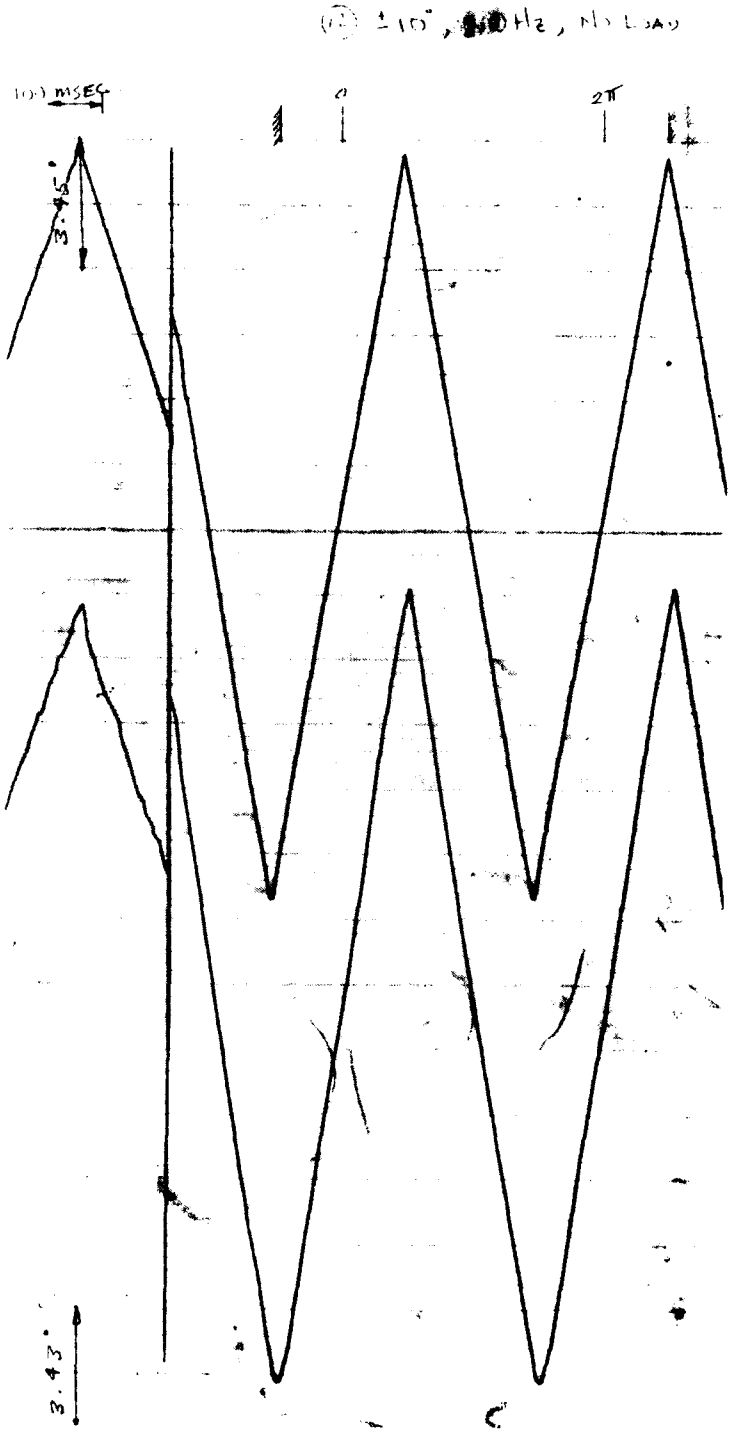

Figure 9. Test 12, the triangle, [illegible]

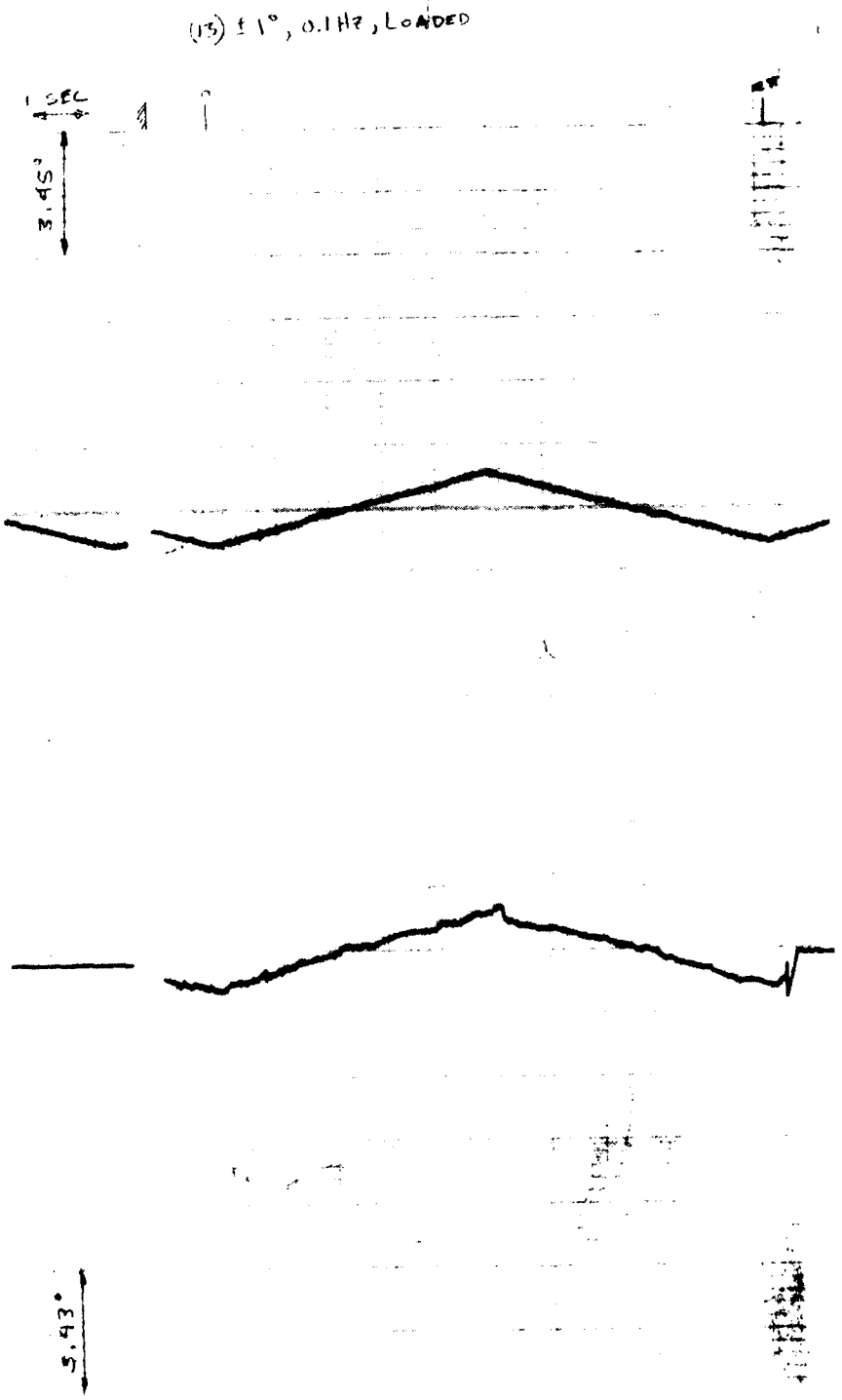

Figure 56. Test 14, ±1° Triangle, 0.1 Hz, Loaded

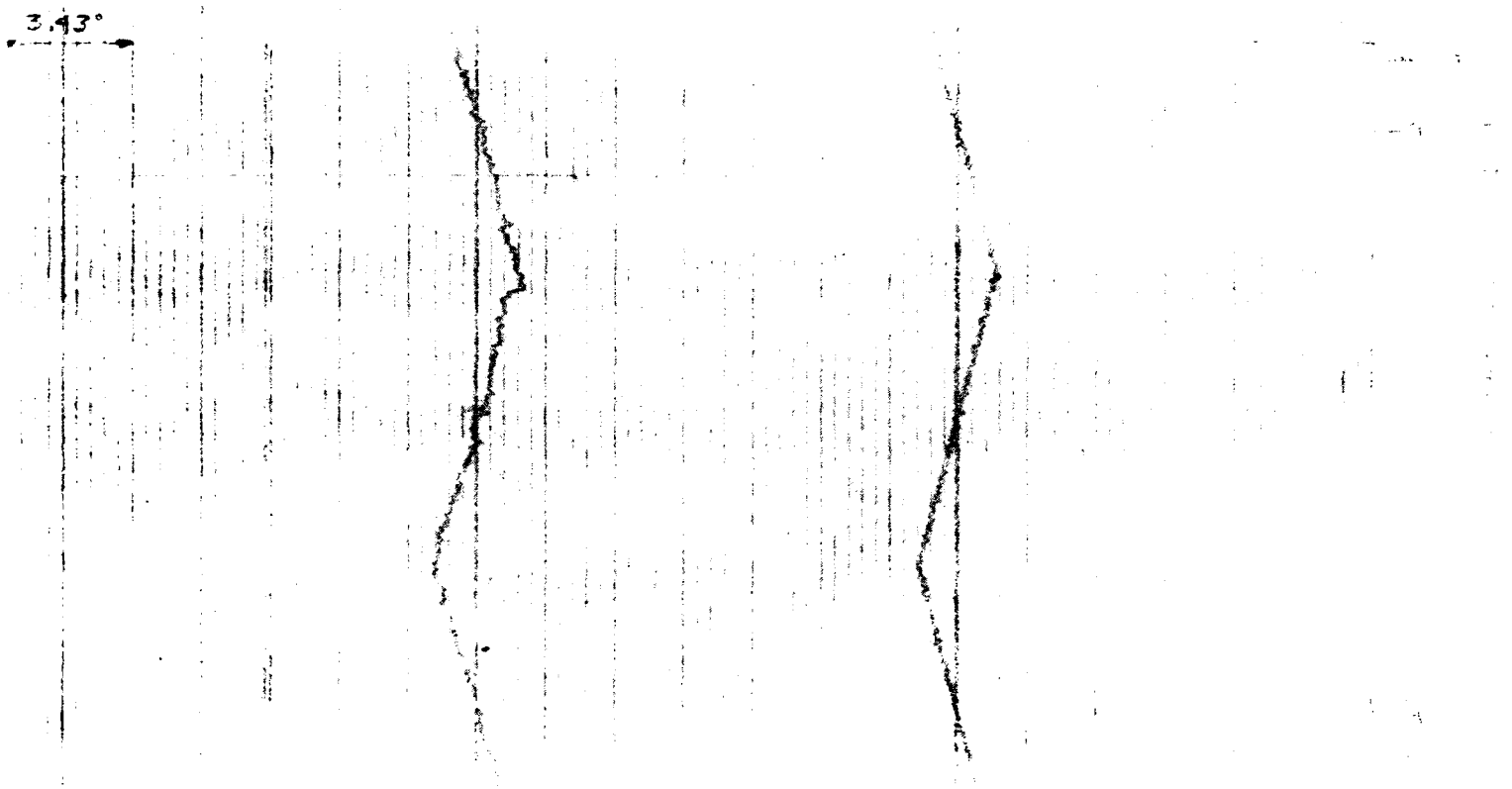
3.43°

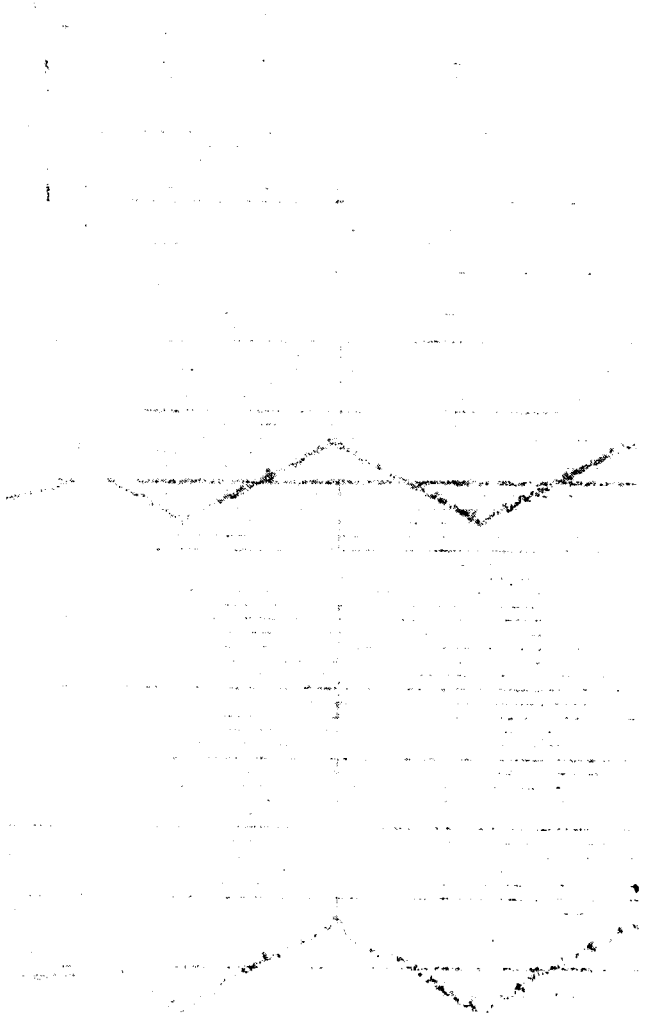

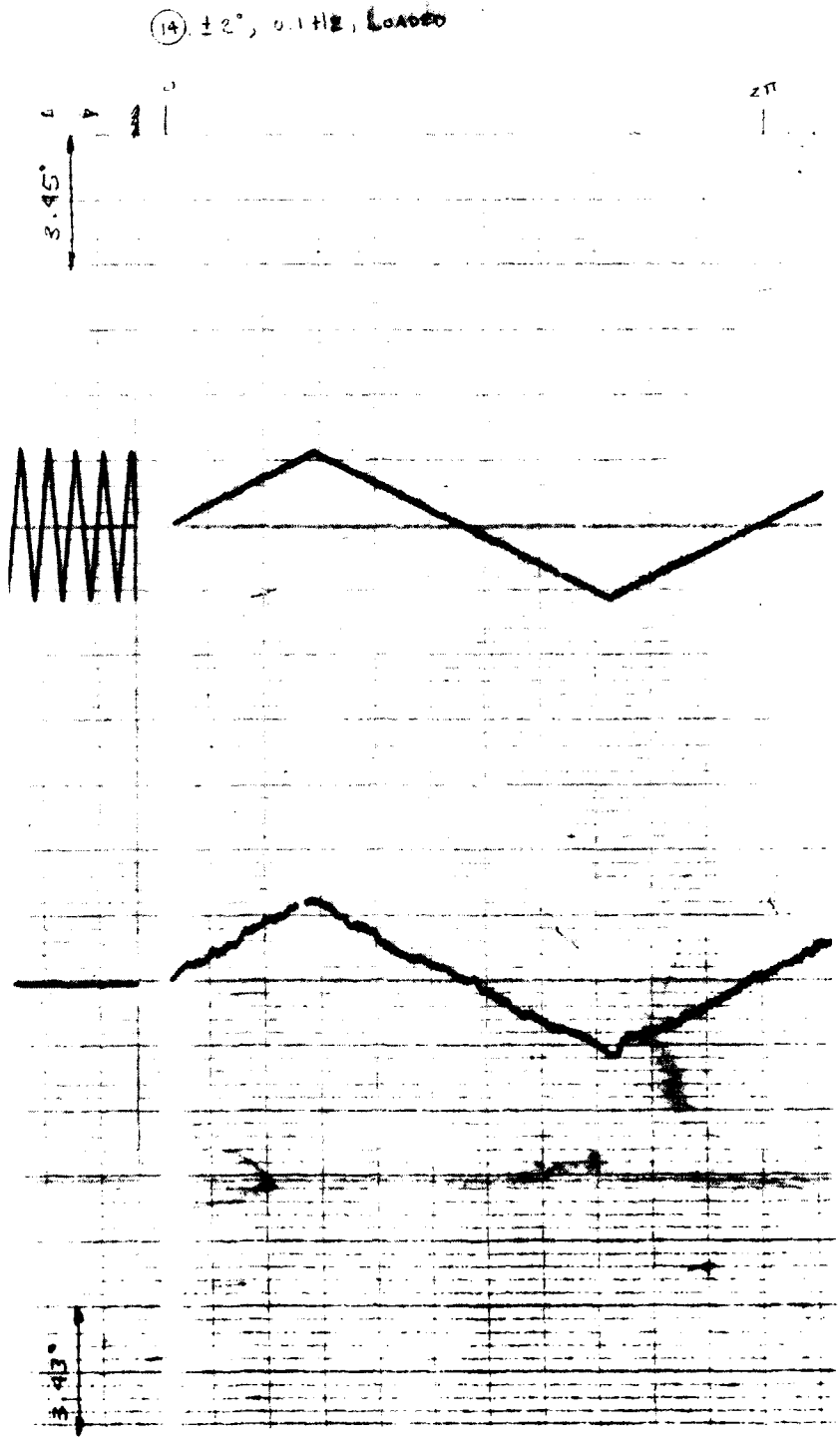

Figure 50. Test 14, ±2° Triangle, 0.1 Hz, Loaded

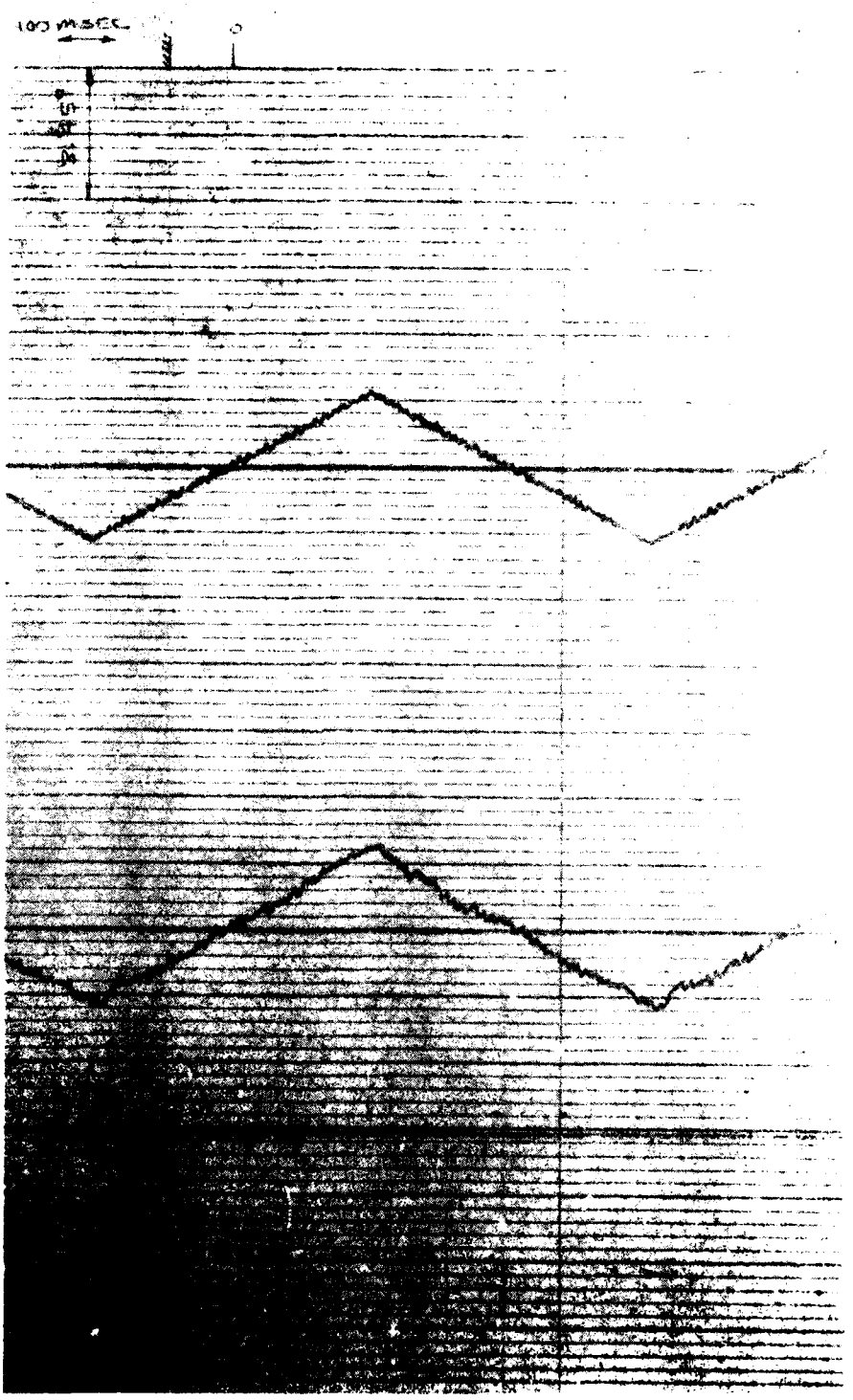
100 msec

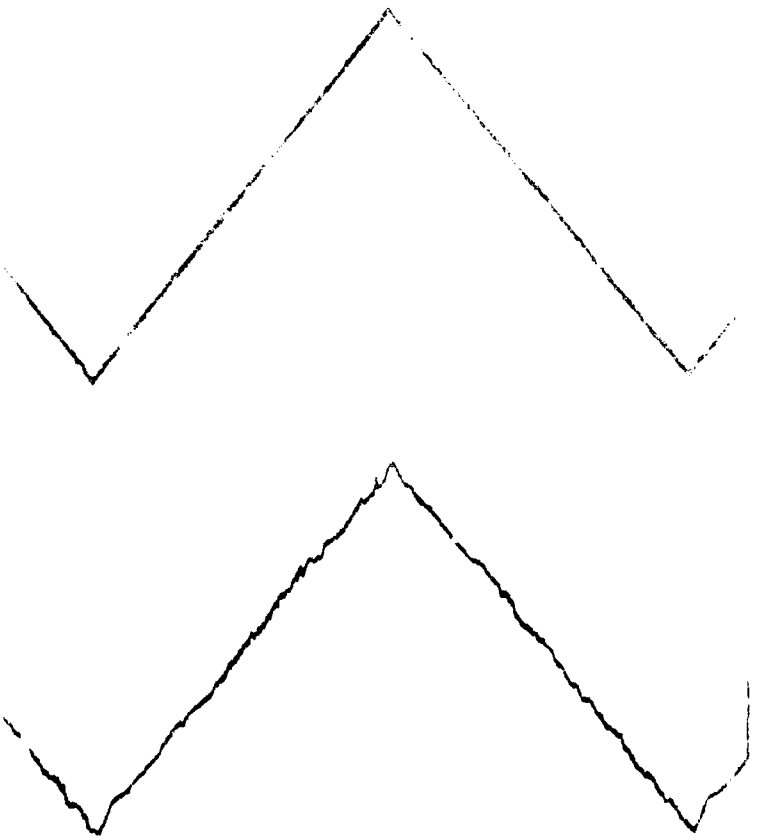

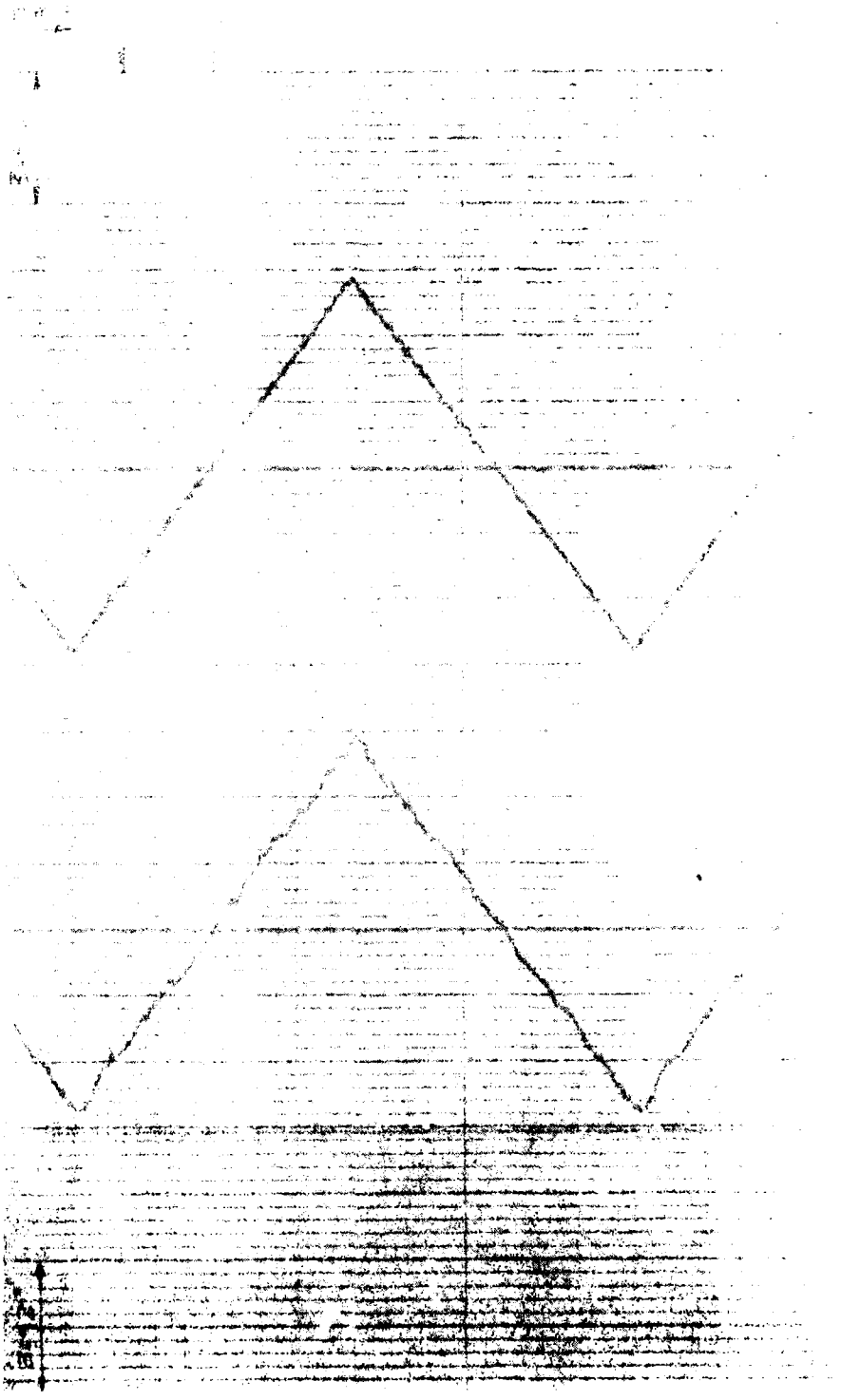

AD-A116 126 AIRESEARCH MFG CO OF CALIFORNIA TORRANCE F/G 20/3
ELECTROMECHANICAL ACTUATION DEVELOPMENT PROGRAM (EADP), POWER C--ETC(U)
SEP 81 S ROWE, D BAILEY, R BELANUS F33615-80-C-3620
UNCLASSIFIED 81-18106 AFWAL-TR-81-3106 NL

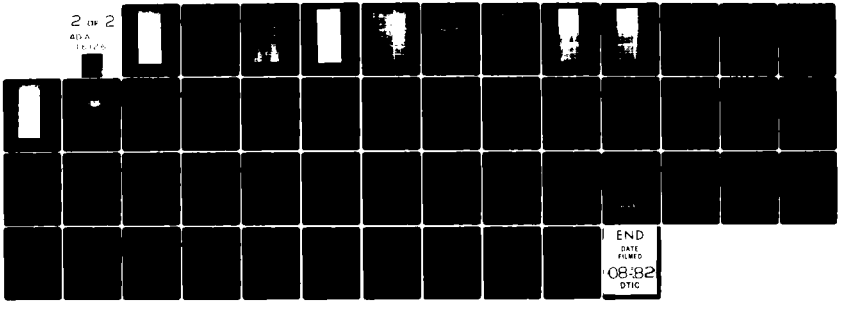

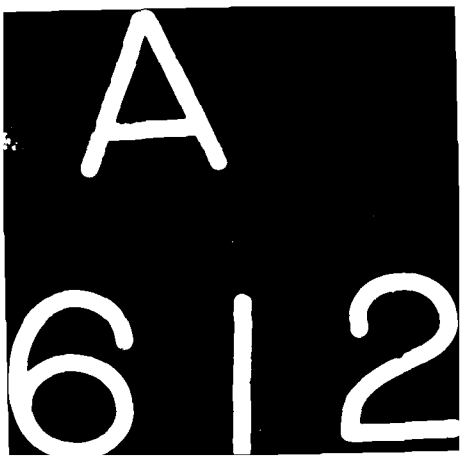
A
612

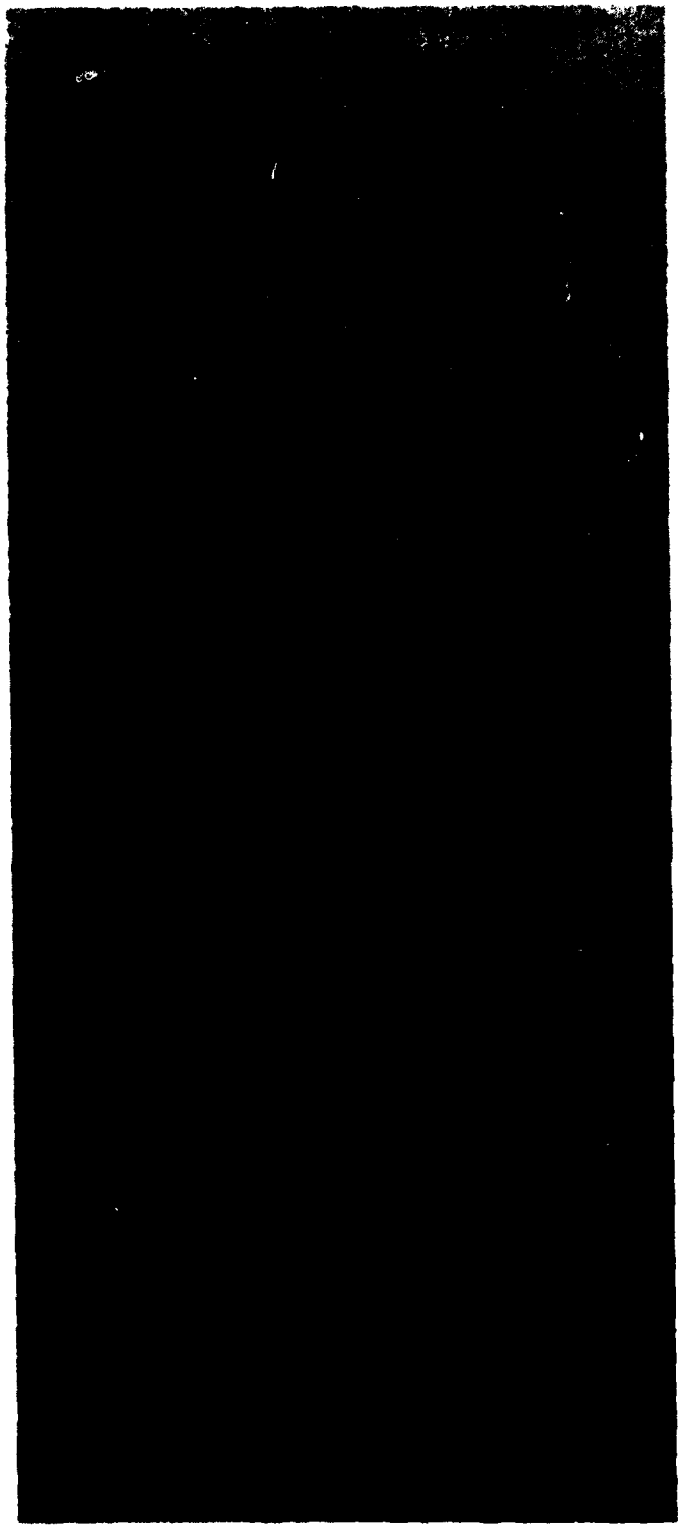

Figure 64. Test 15, ±5° Triangle, 2 Hz, Loaded

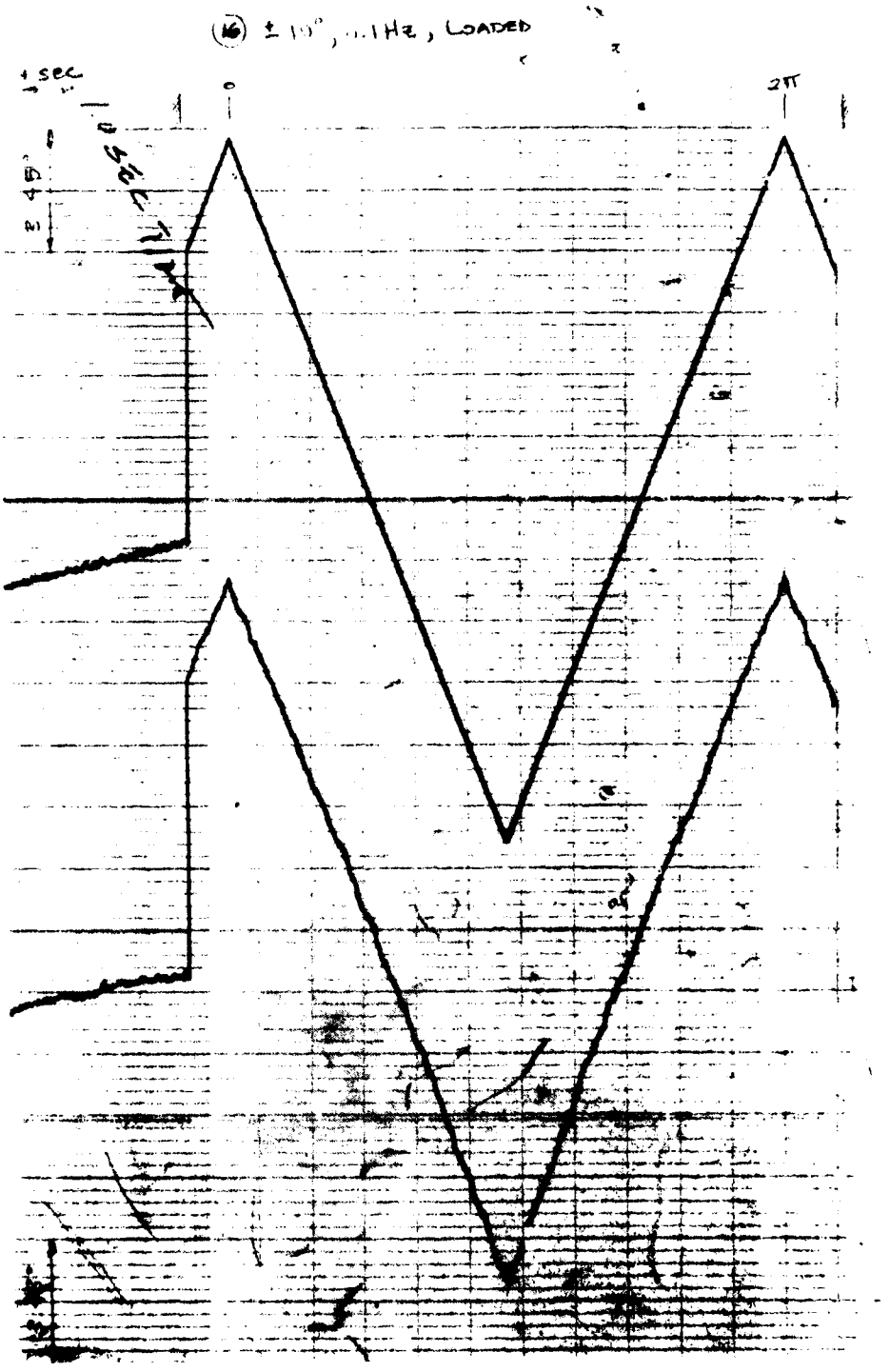

Figure 65. Test 16, ±10° Triangle, 0.1 Hz, Loaded

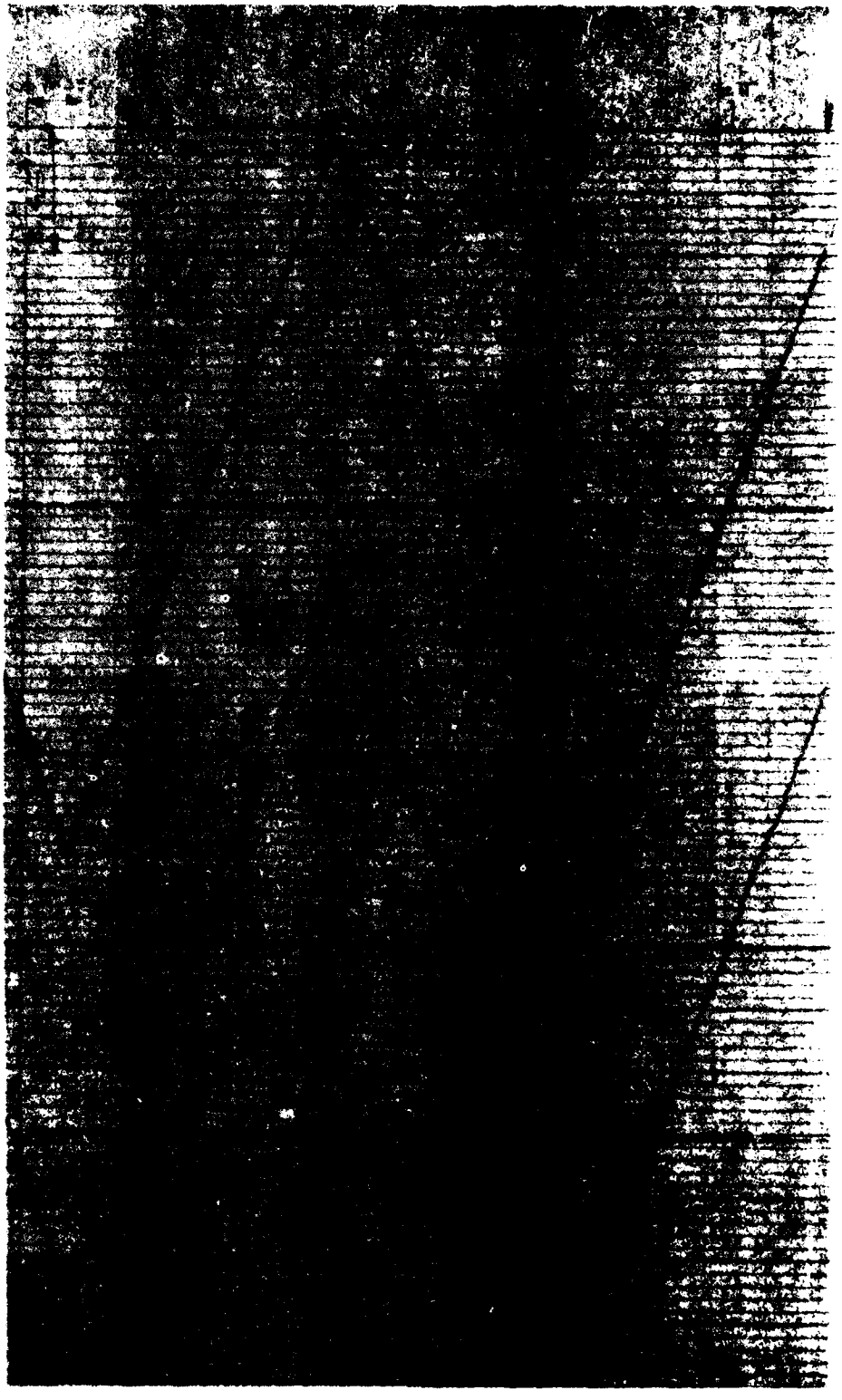

Figure 66. Test 16, ±10° Triangle, 1 Hz, Loaded

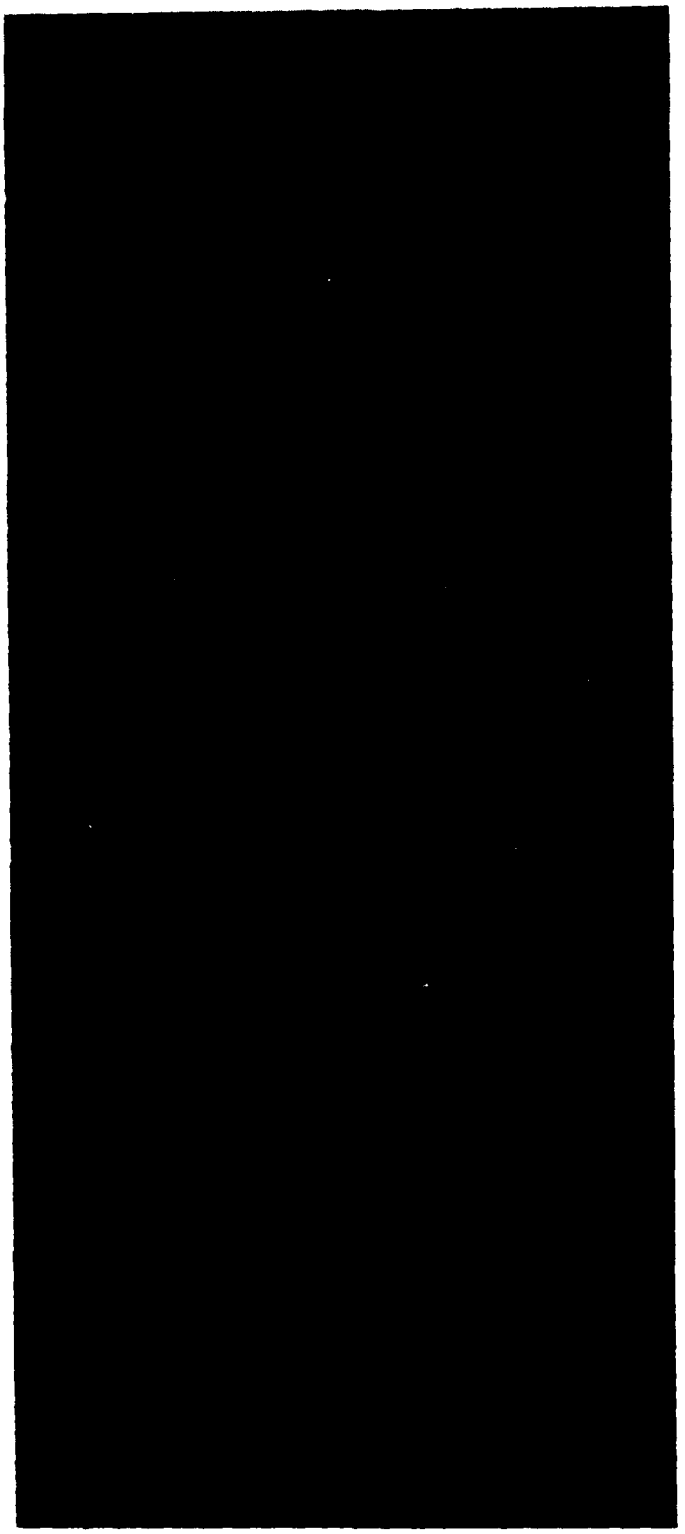

Figure 67. Test 16, ±10° Triangle, 2 Hz, Loaded

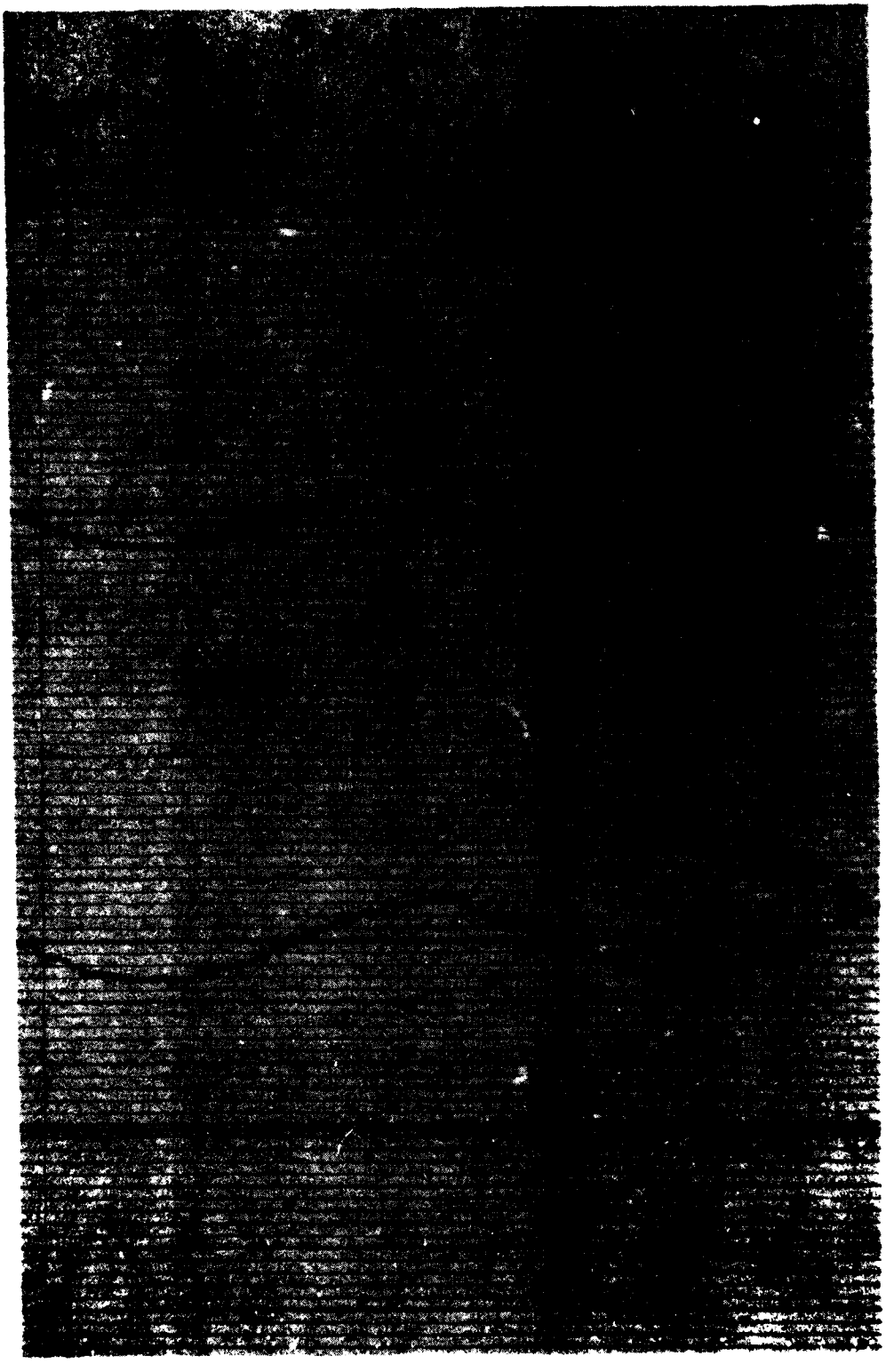

Figure 68. Test 17, ±1° Sine, 1 Hz, No Load

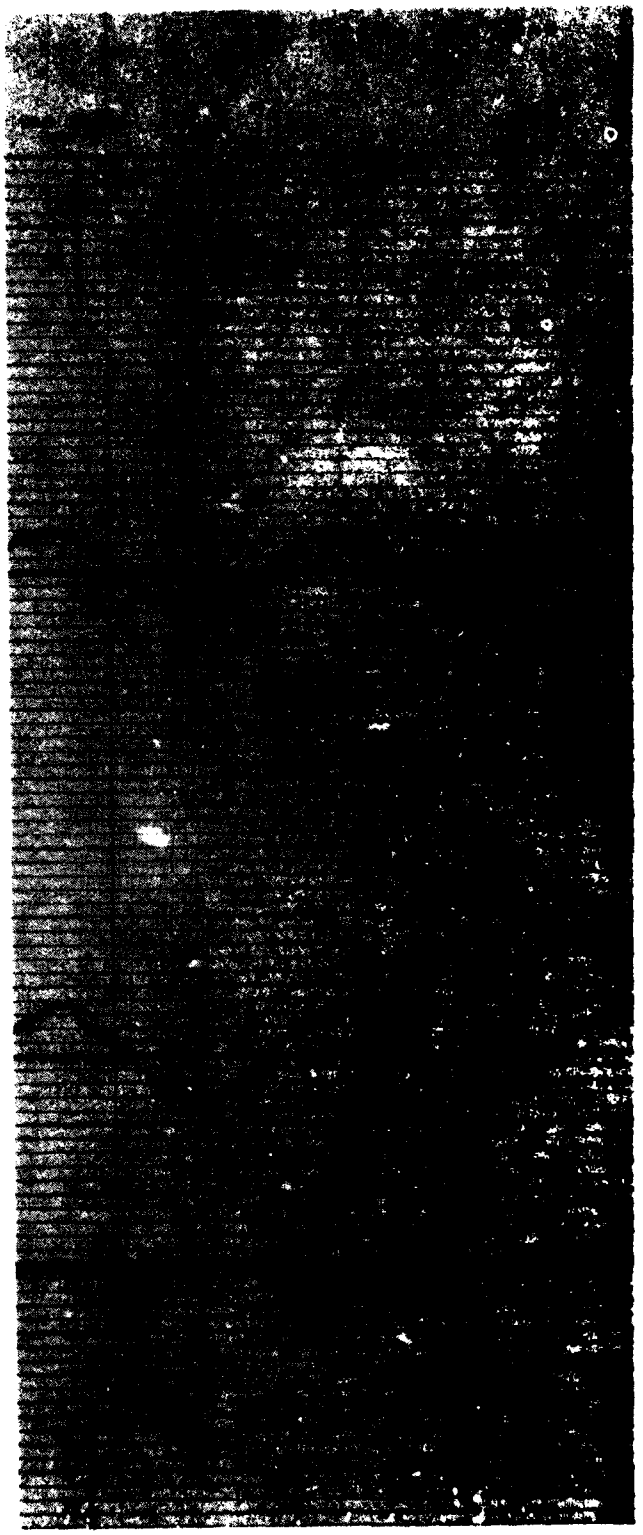

Figure 69. Test 17, ±1° sine, [illegible]

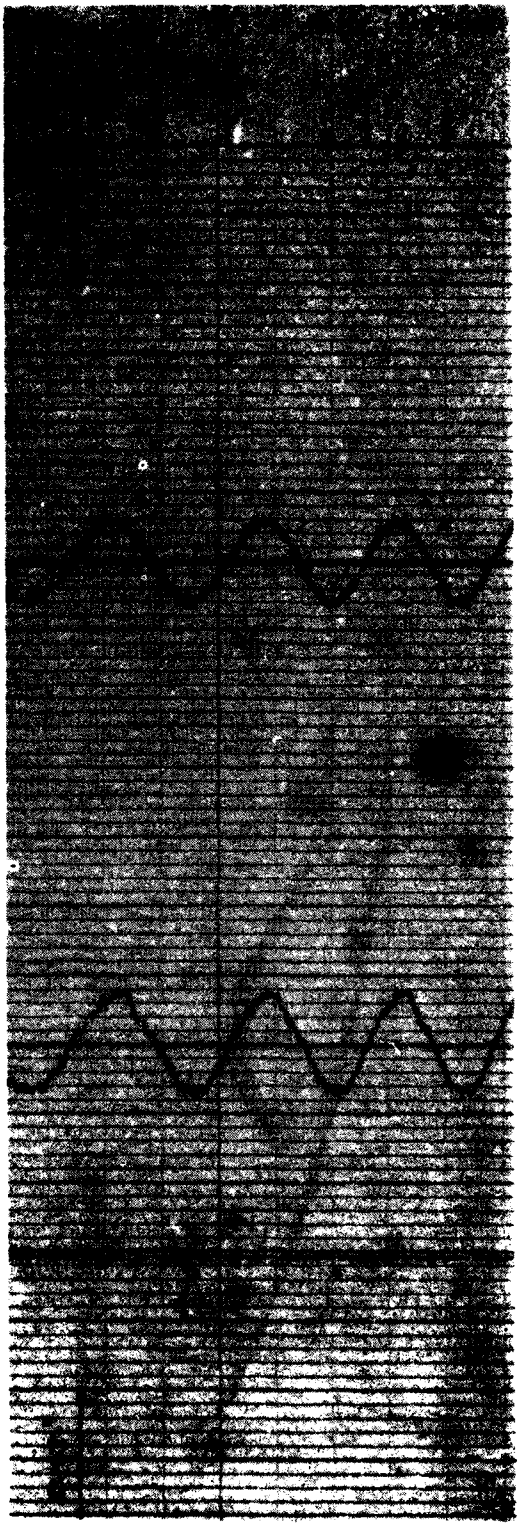

Figure 70. Test 17, ±1° Sine, 4 Hz, No Load

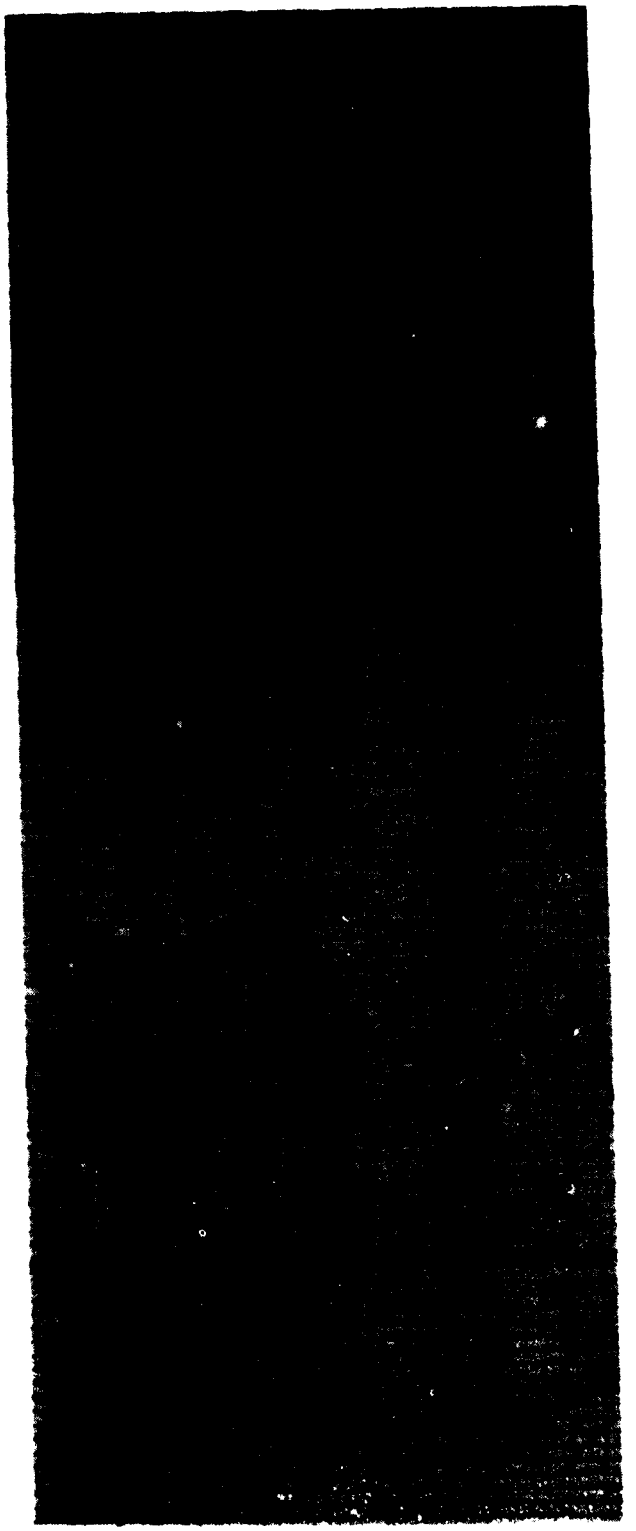

Figure 71. Test 17, ±1° Sine, 8 Hz, No Load

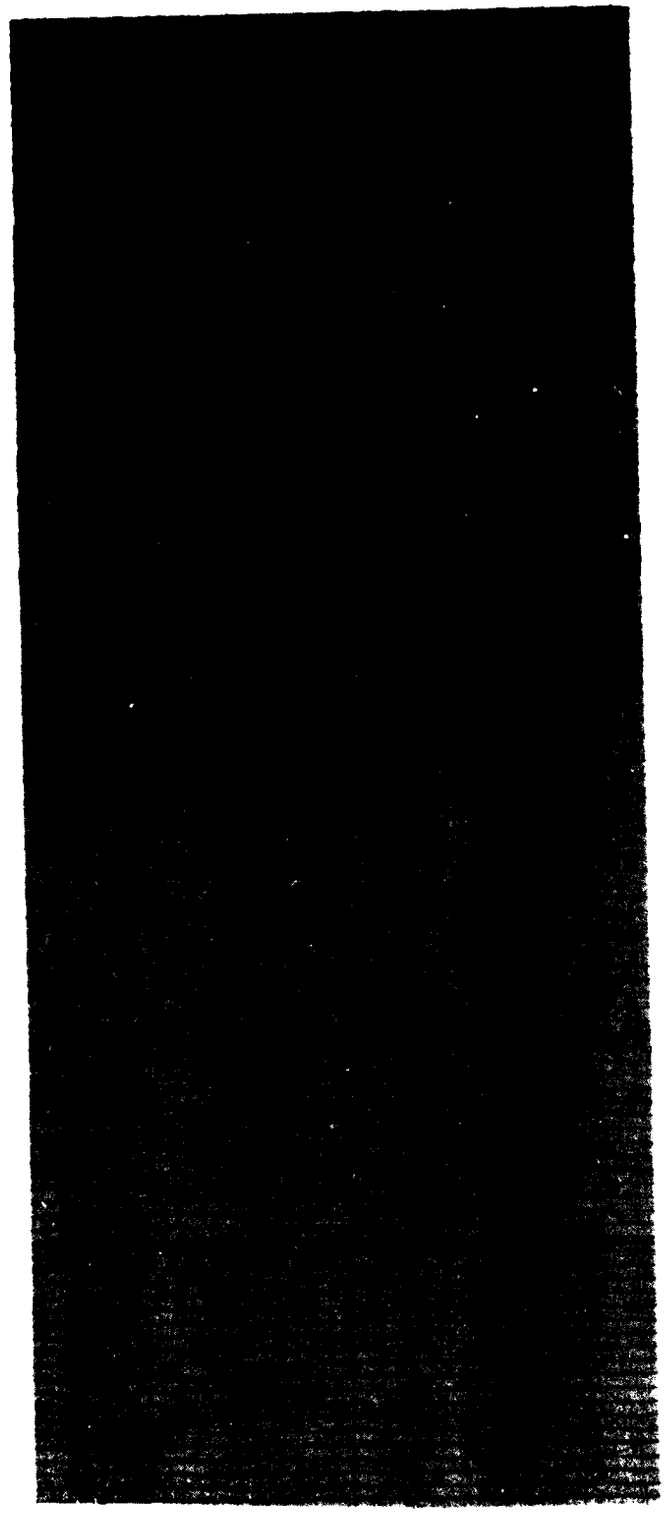

Figure 72. Test 17, ±1° Sine, 16 Hz, No Load

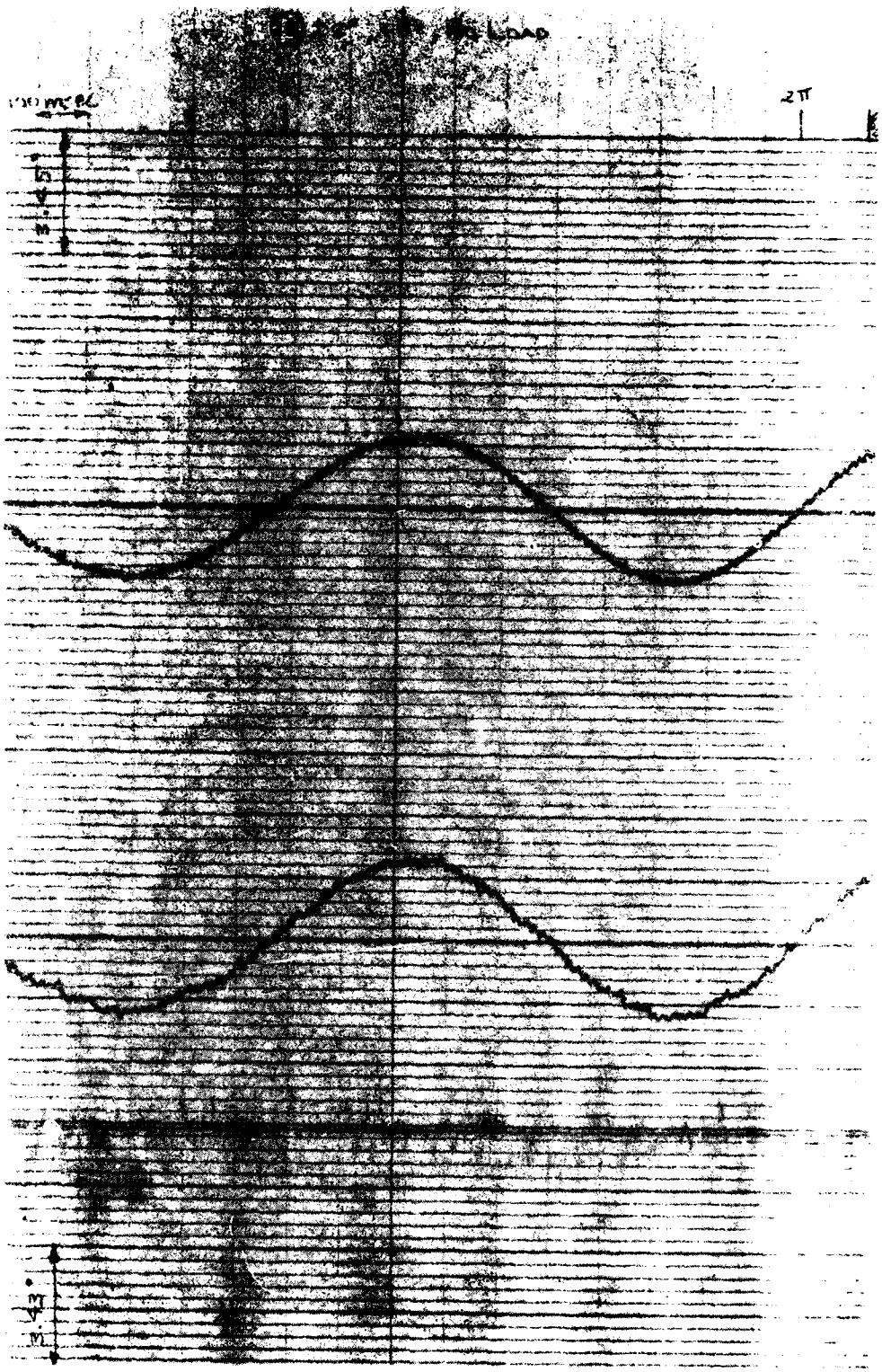

Figure 74. Test 18, [illegible]° Sine, [illegible], [illegible] Load

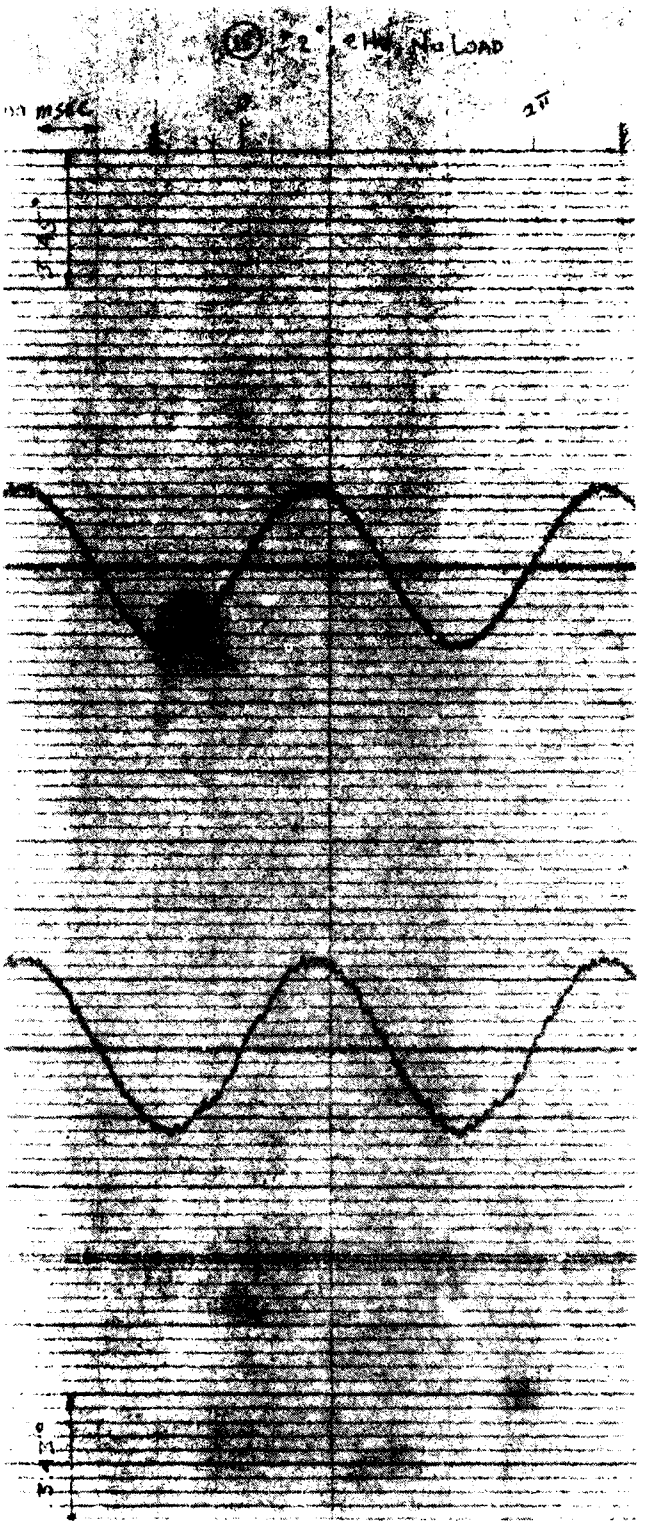

Figure 24. Test 18, [illegible]

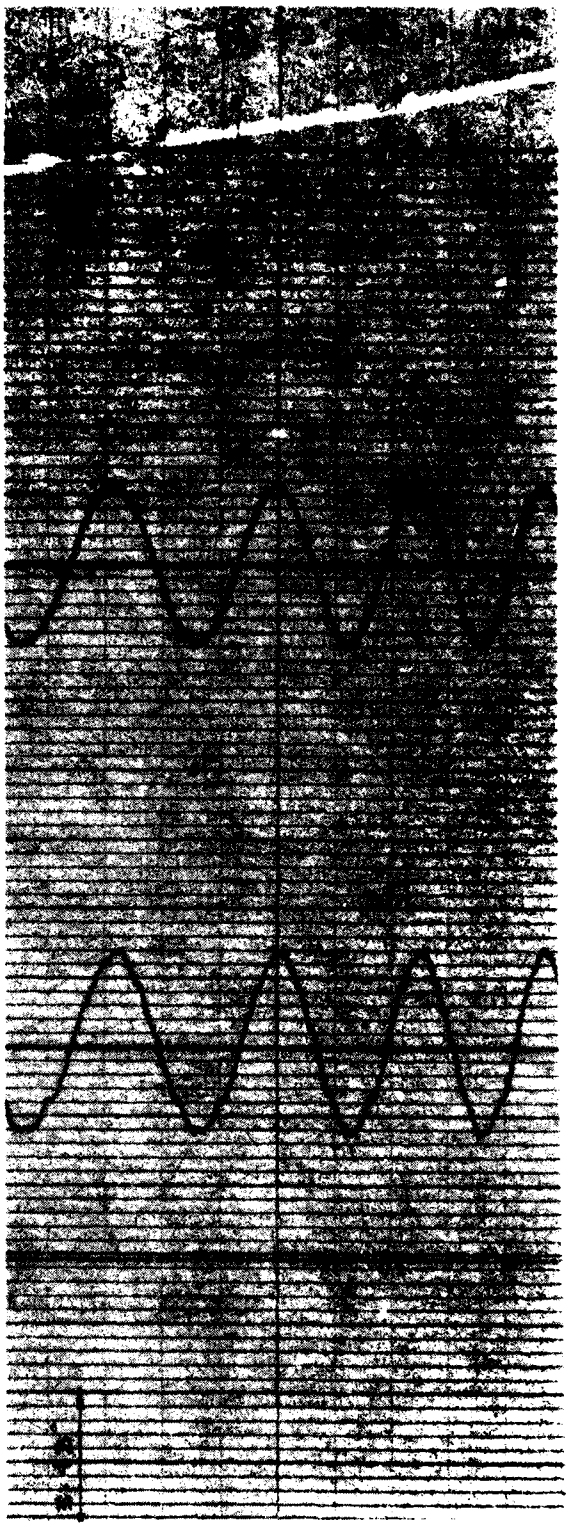

Figure [illegible]. Test 15, ±[illegible]° sine, [illegible]

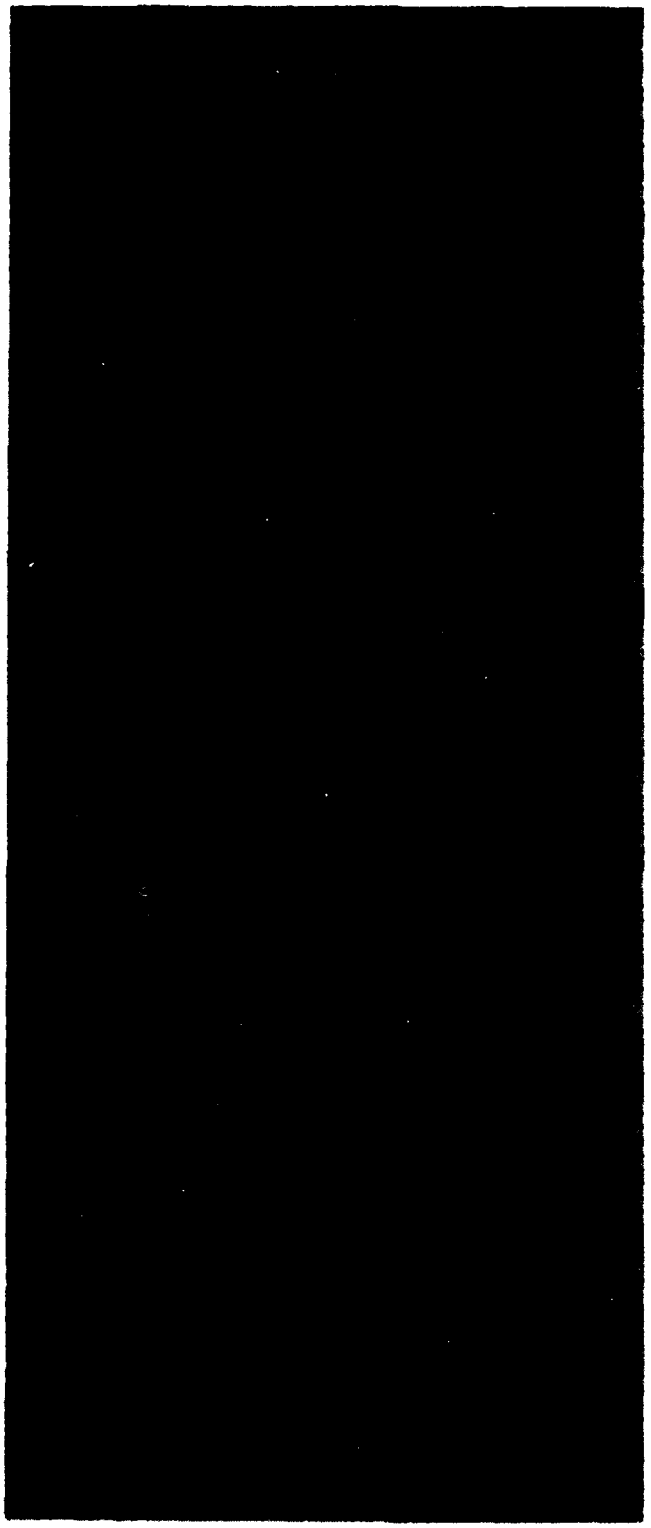

Figure 76. Test 18, ±2° Sine, 8 Hz, No Load

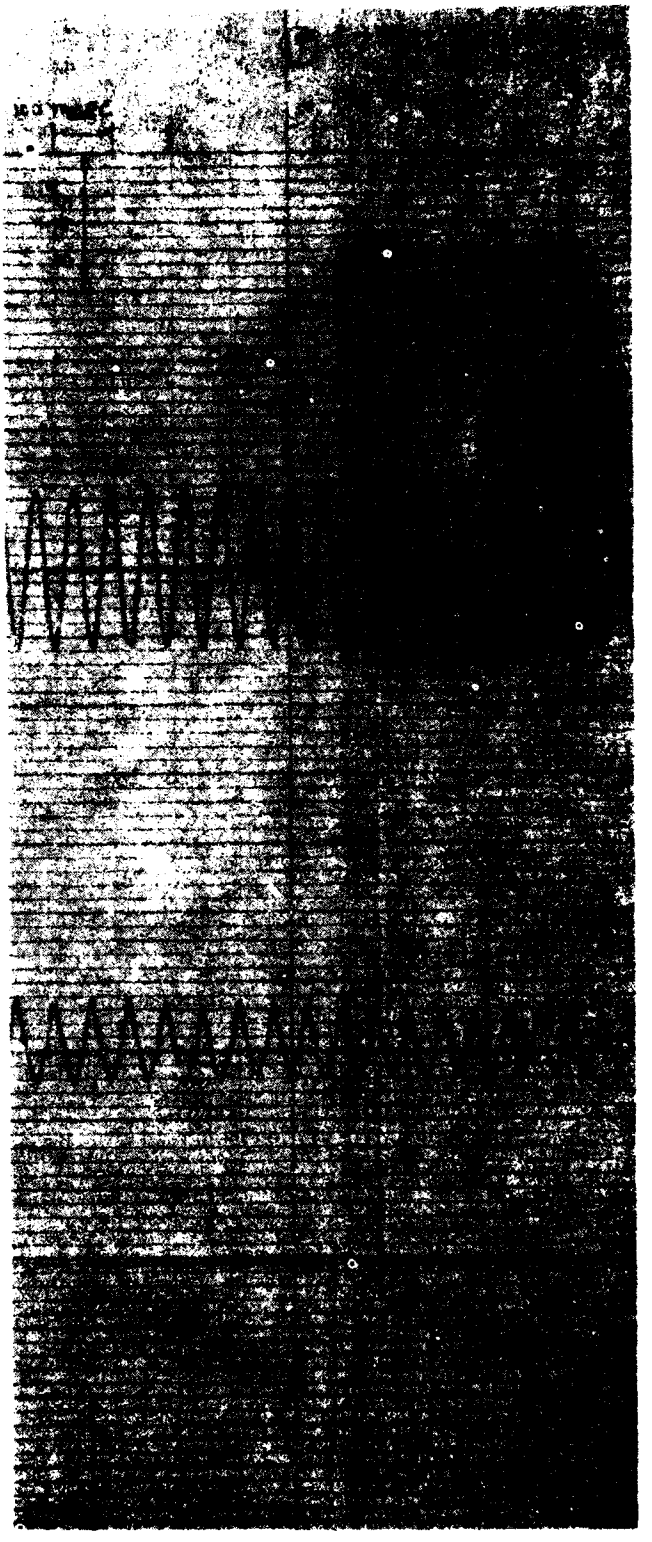

Figure 7. Test 18, ±2° Sine, 10 Hz, No Load

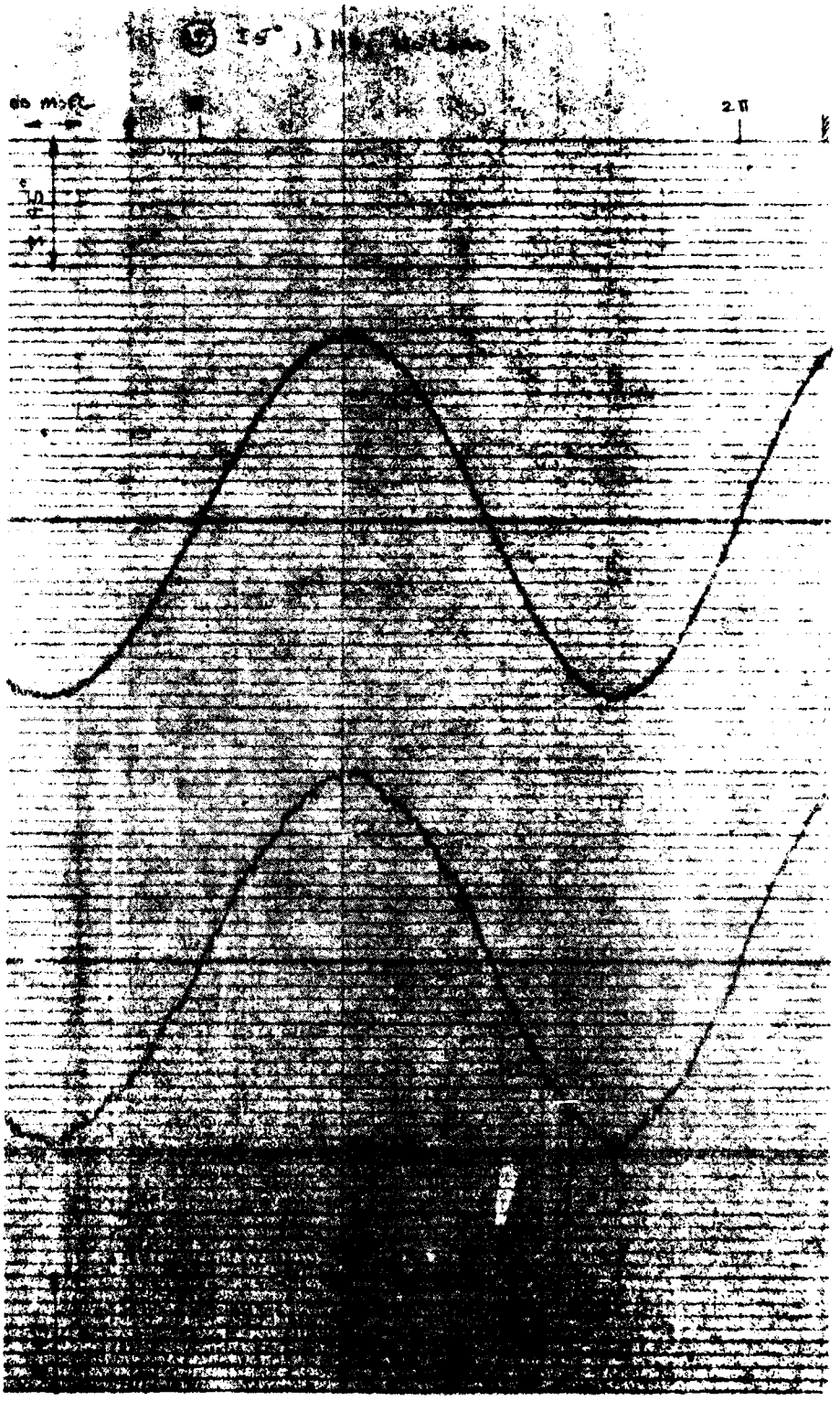

Figure 38. Test 19, ±5° Sine, [illegible]

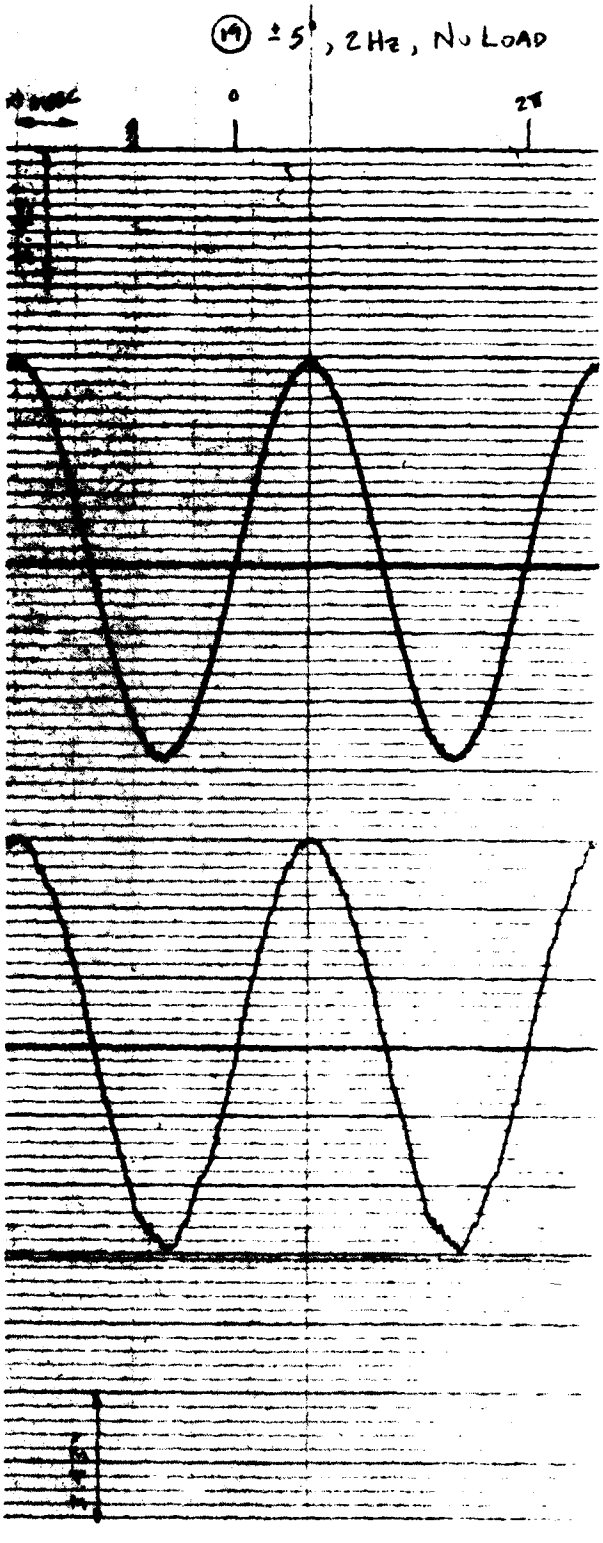

Figure 79. Test 19, ±5° Sine, 2 Hz, No Load

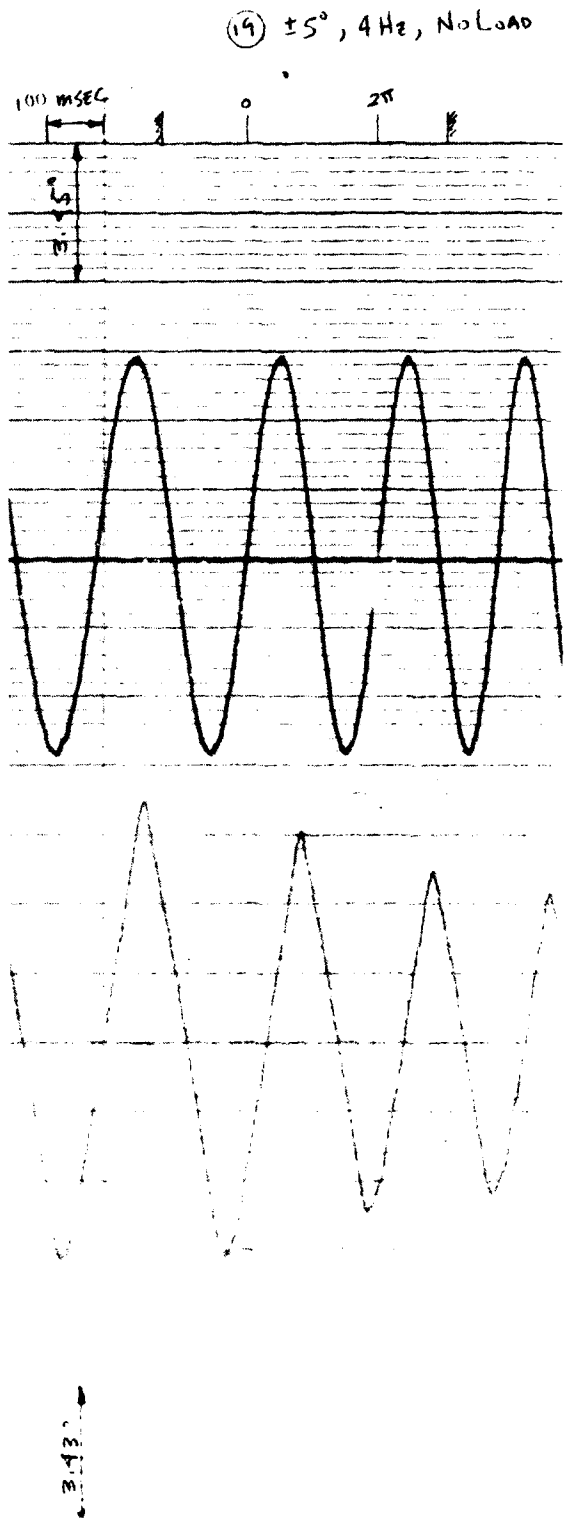

Figure 80. Test 19, ±5° Sine, 4 Hz, No Load

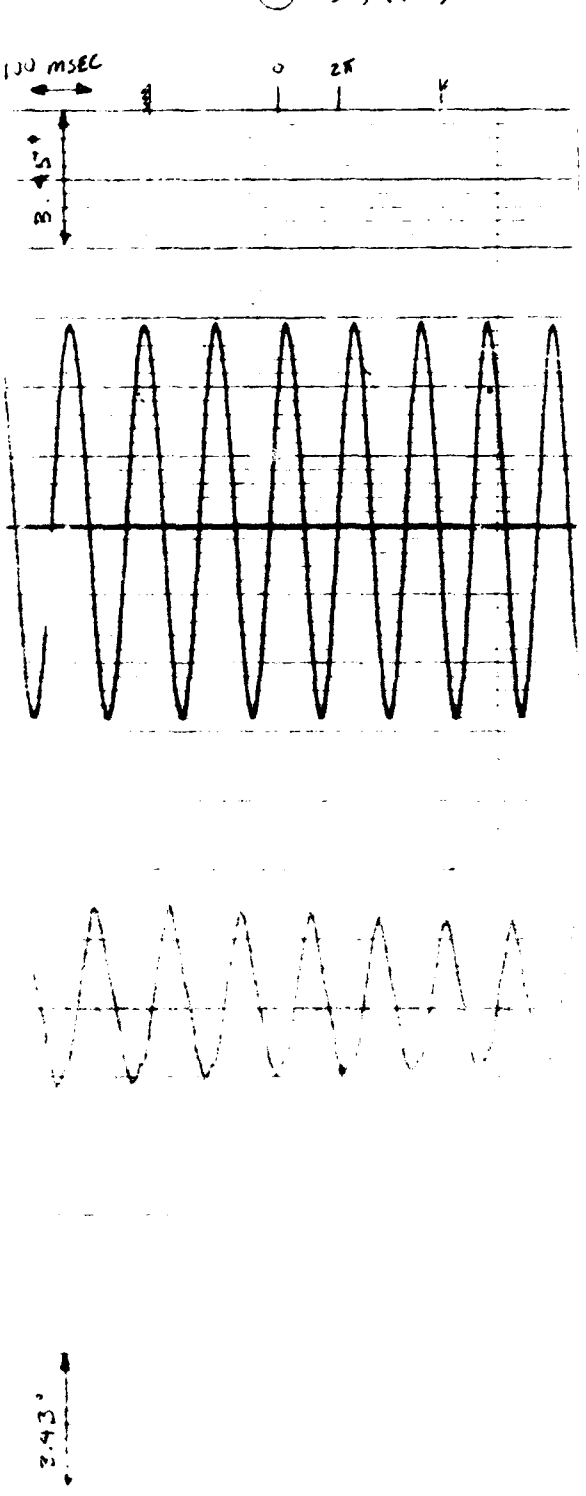

Figure 3.1. Test 19, ±5° Sine, 2 Hz, No Load

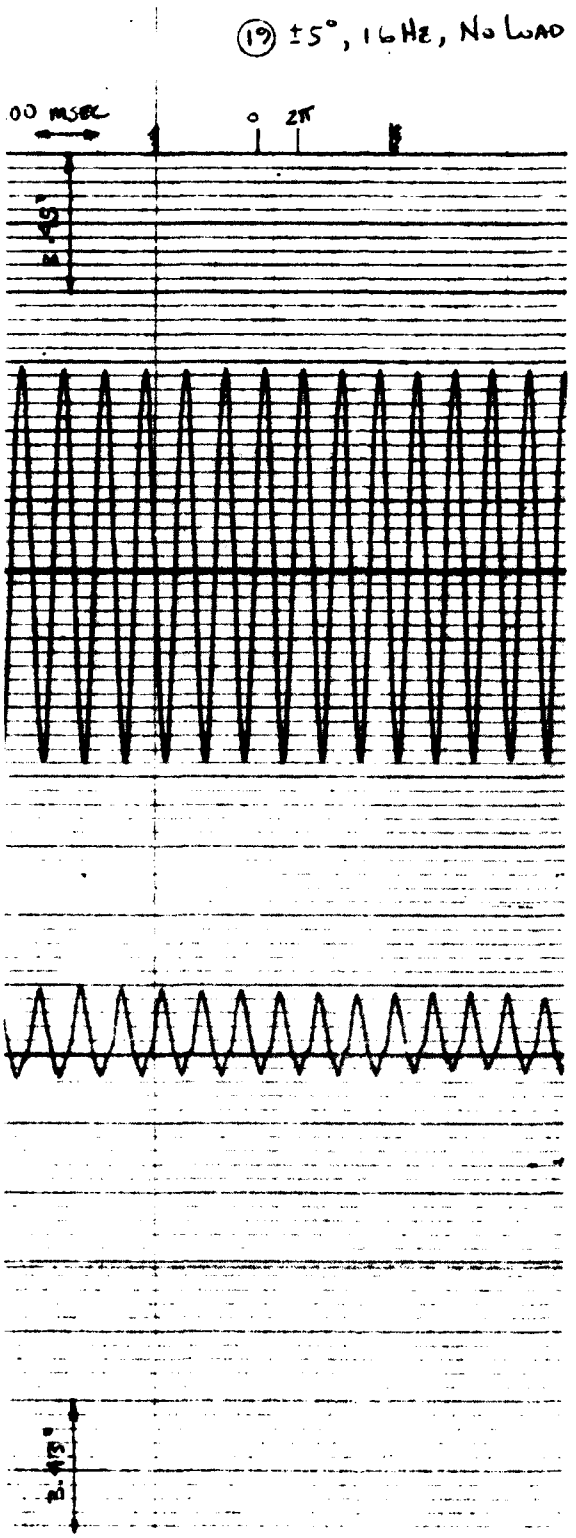

Figure 82. Test 19, ±5° Sine, 16 Hz, No Load

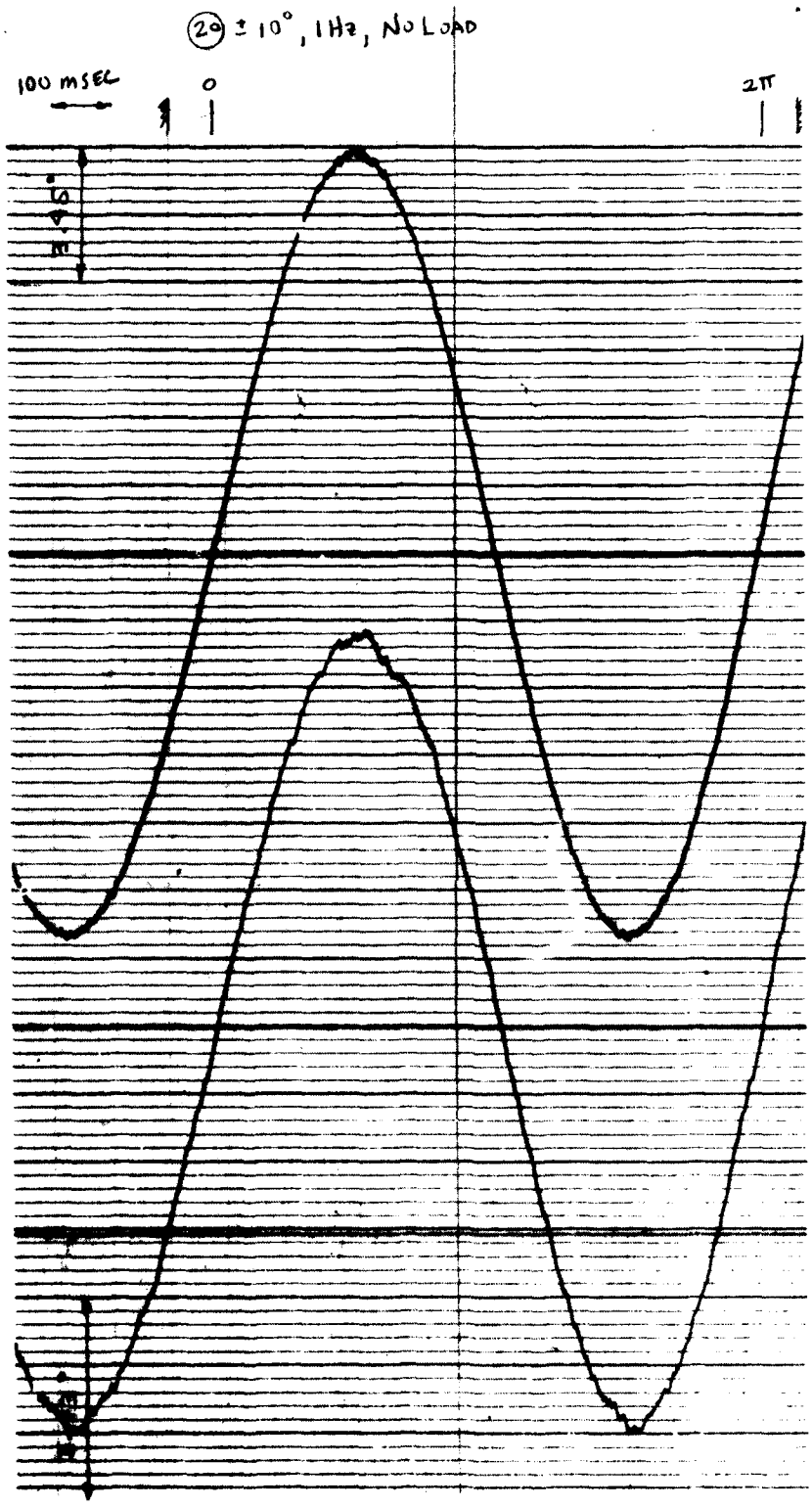

Figure 83. Test 20, ±10° Sine, 1 Hz, No Load

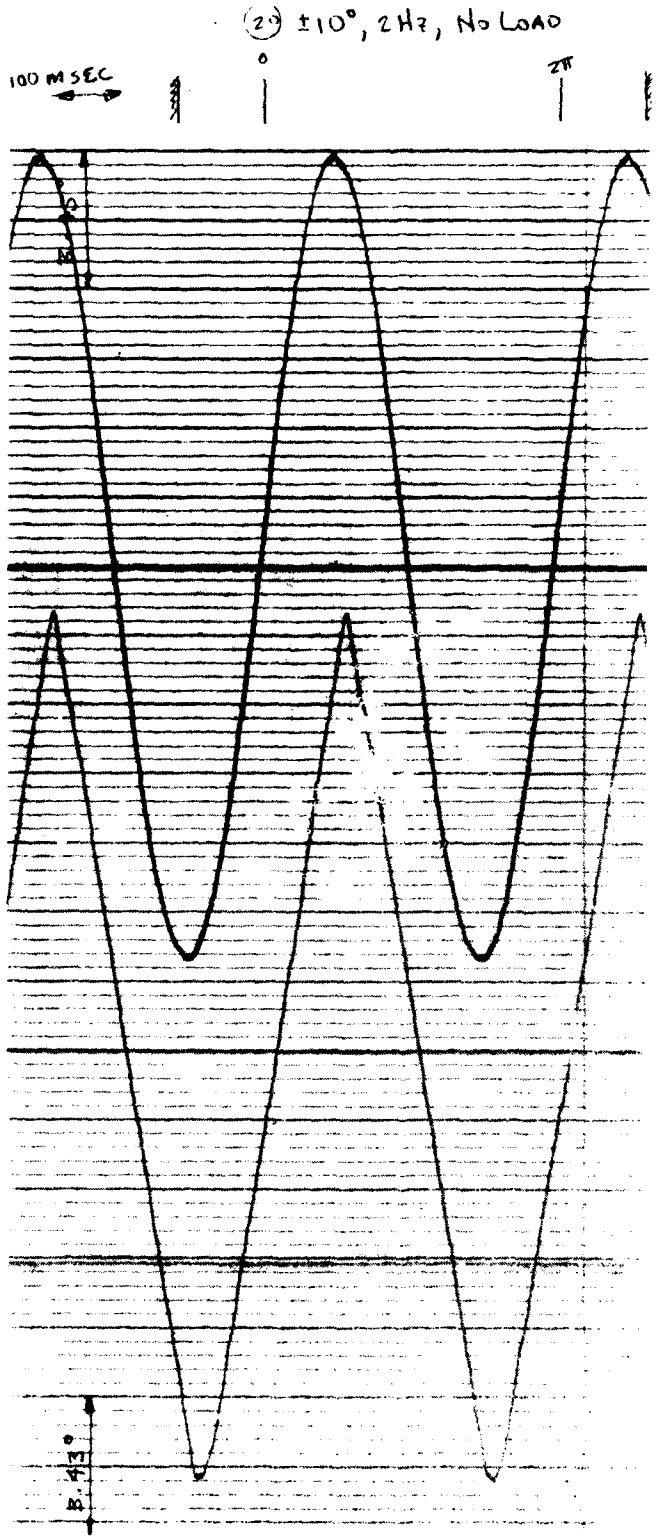

Figure 84. Test 20, ±10° Sine, 2 Hz, No Load

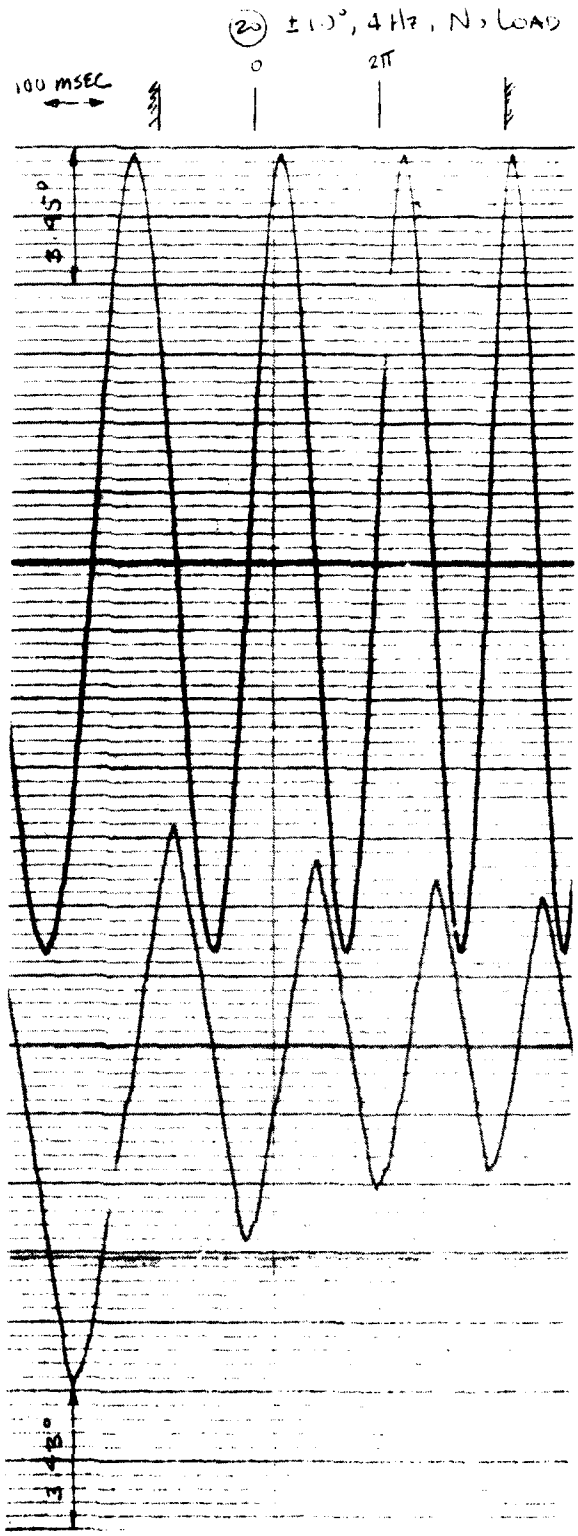

Figure 85. Test 20, ±10° Sine, 4 Hz, No Load

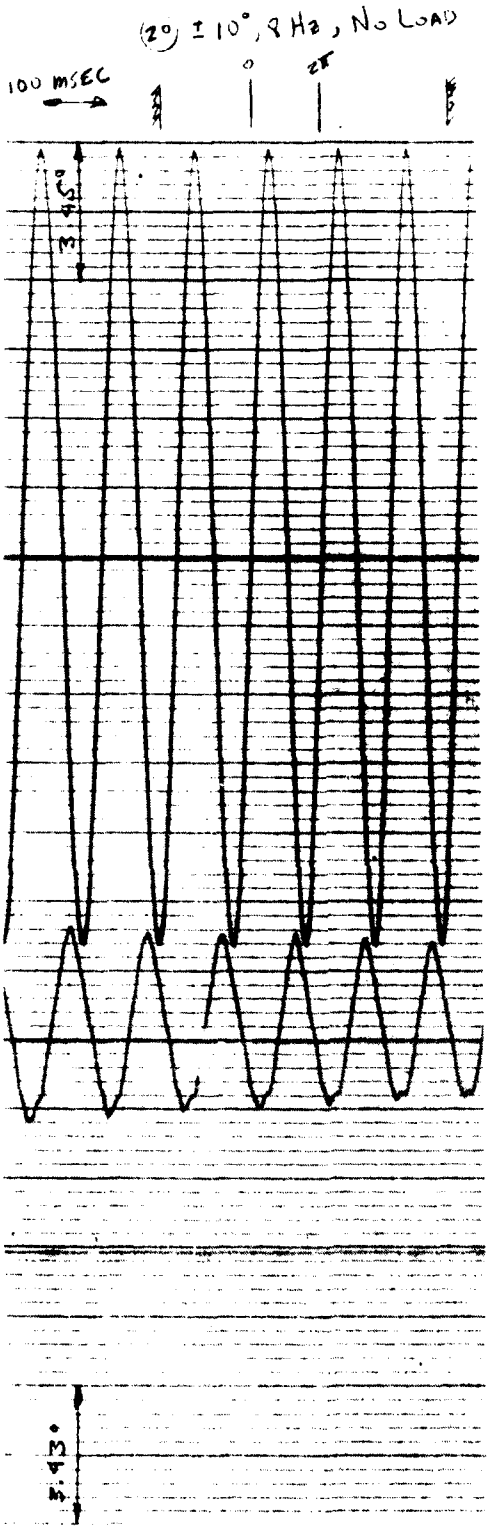

Figure 86. Test 20, ±10° Sine, 8 Hz, No Load

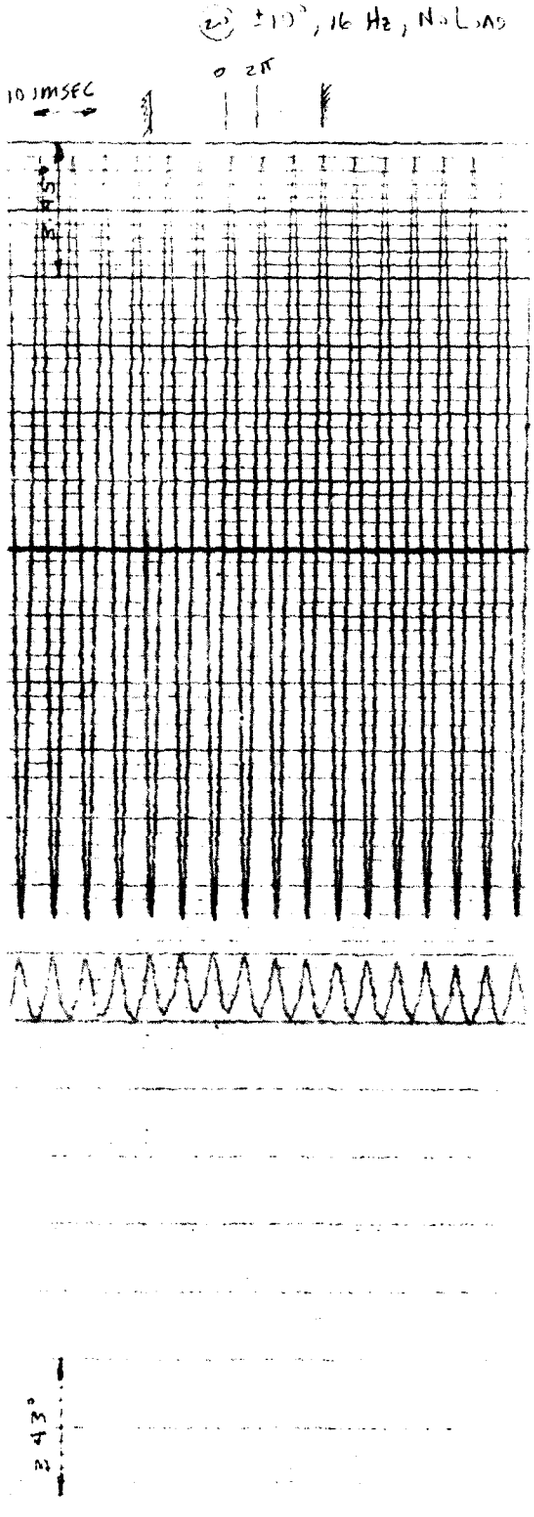

Figure 87. Test 20, ±10° Sine, 16 Hz, No Load

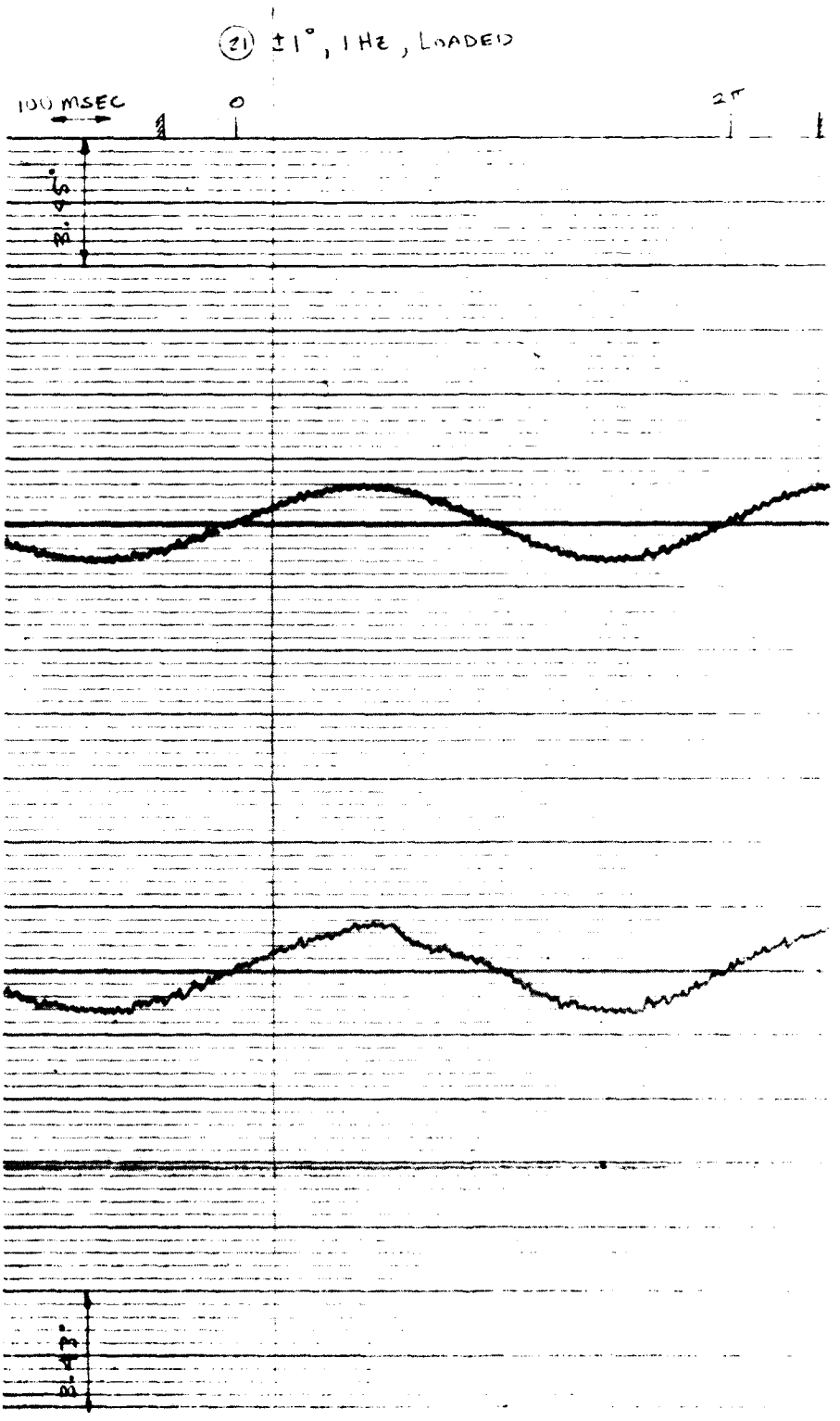

Figure 88. Test 21, ±1° Sine, 1 Hz, Loaded

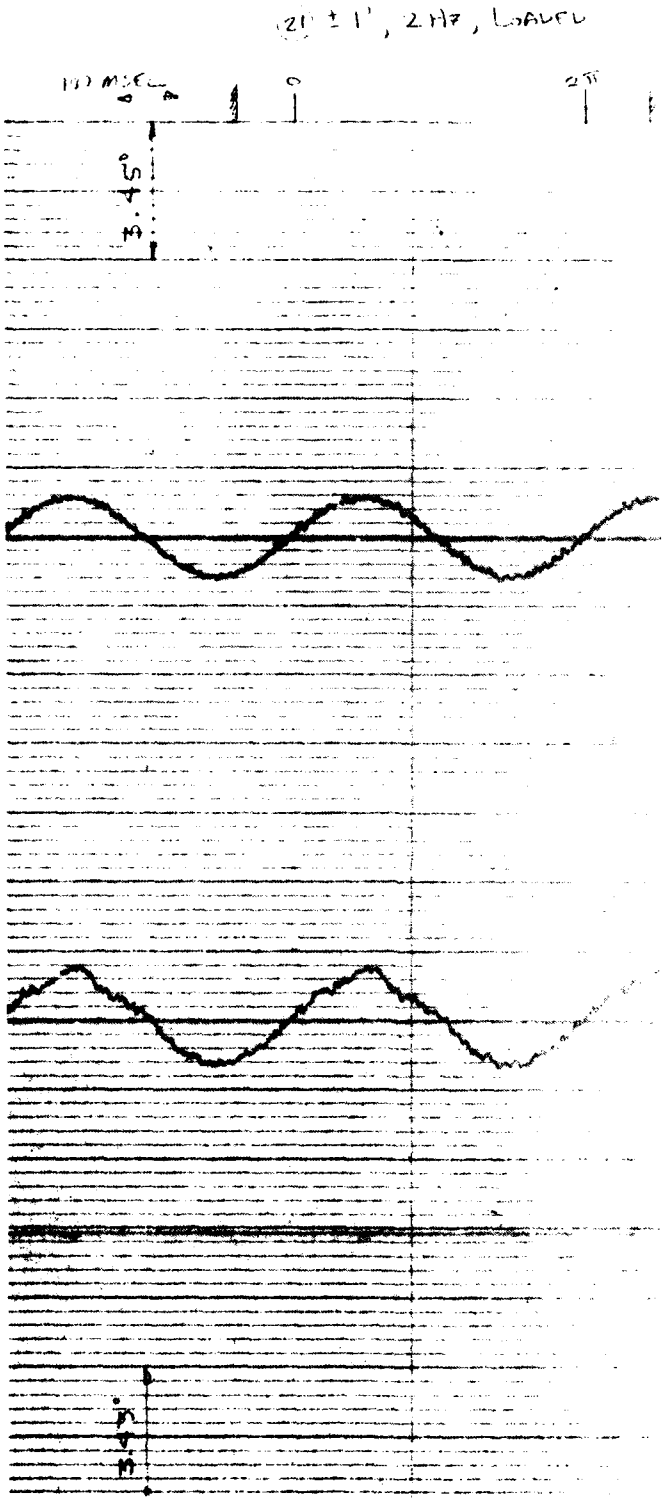

Figure 89. Test 21, ±1° Sine, 2 Hz, Loaded

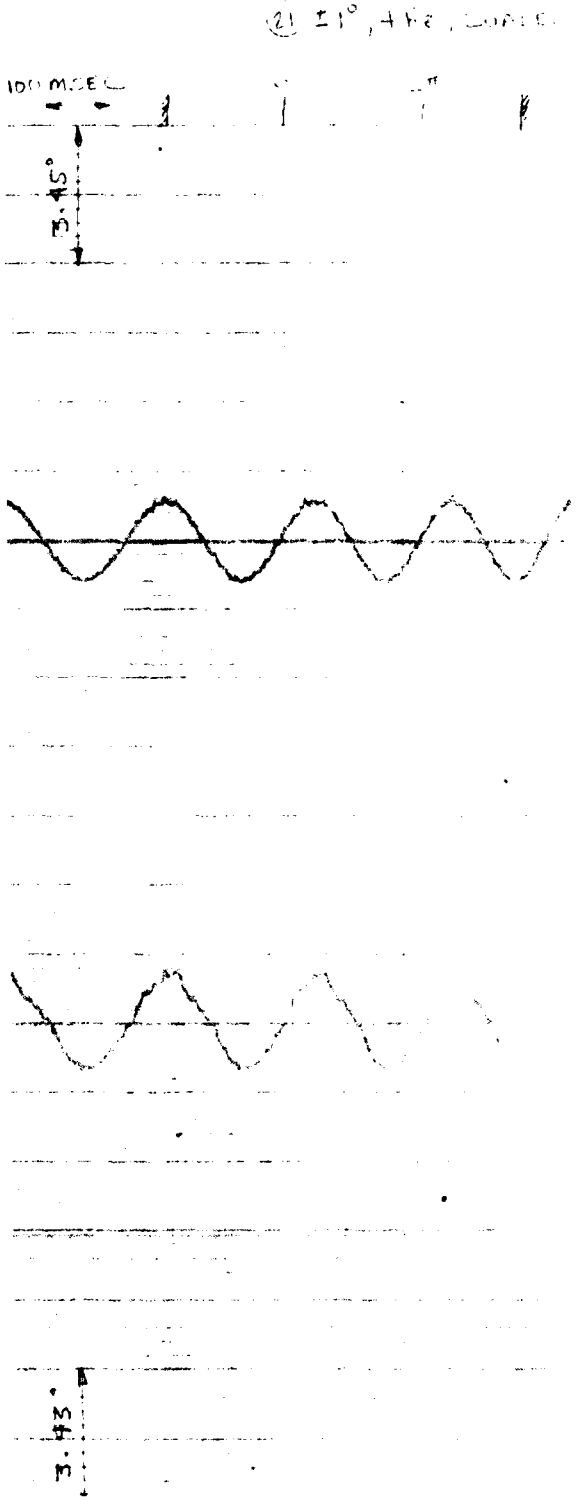

Figure 90. Test 21, ±1° Sine, 4 Hz, Loaded

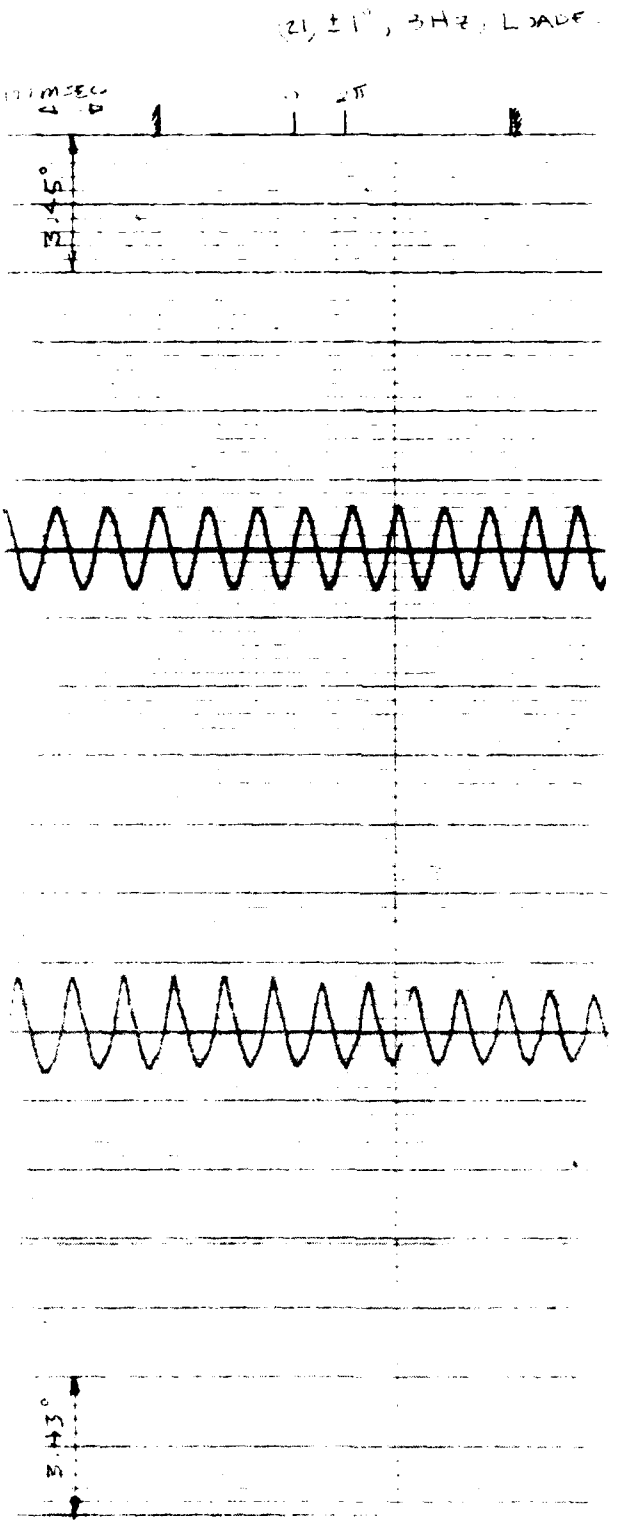

Figure 91. Test 21, ±1° Sine, 8 Hz, Loaded

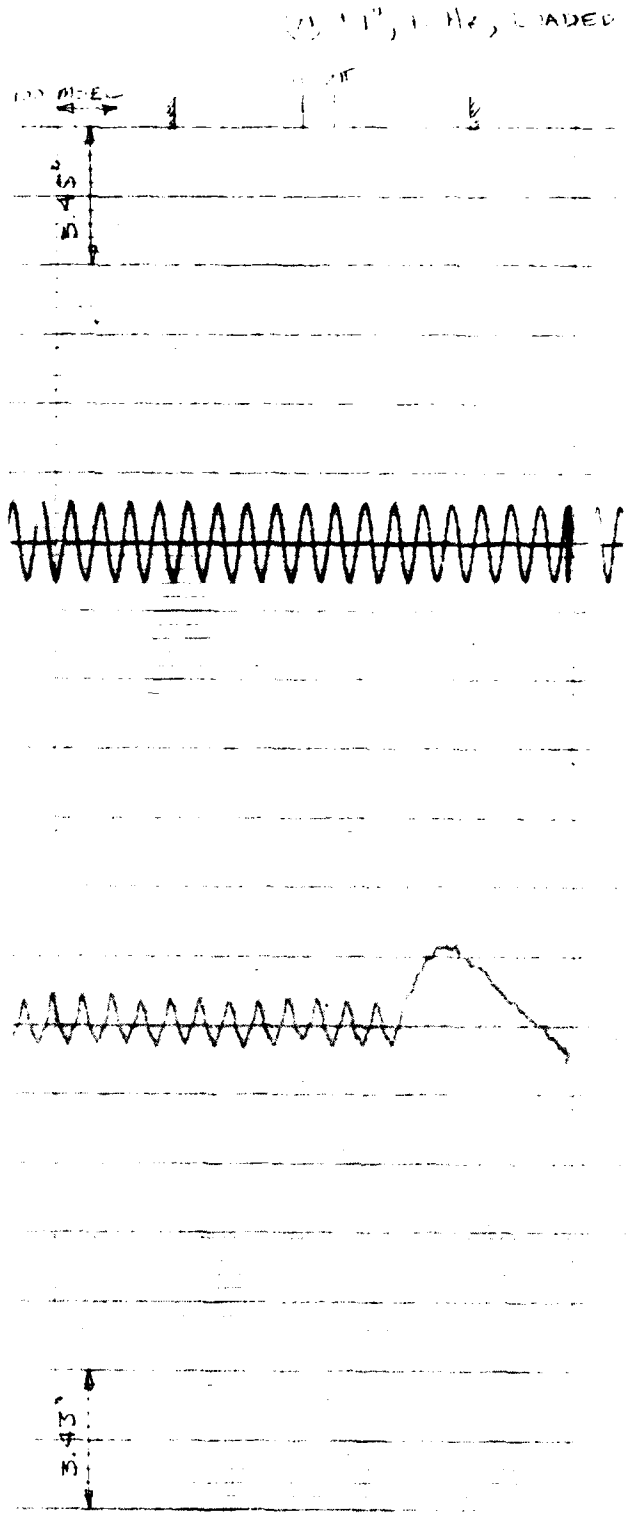

Figure 92. Test 21, ±1° Sine, 16 Hz, Loaded

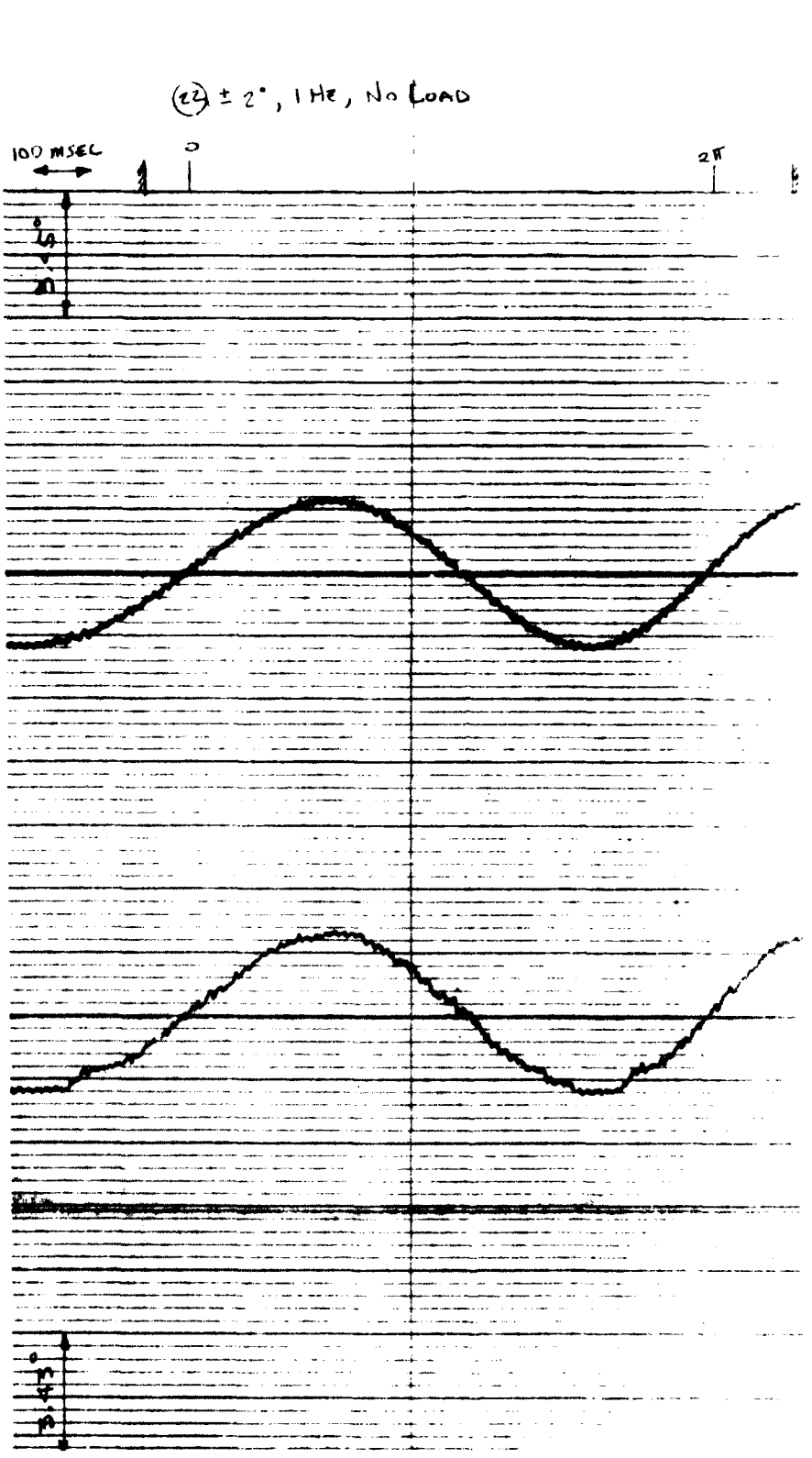

Figure 93. Test 22, ±2° Sine, 1 Hz, Loaded

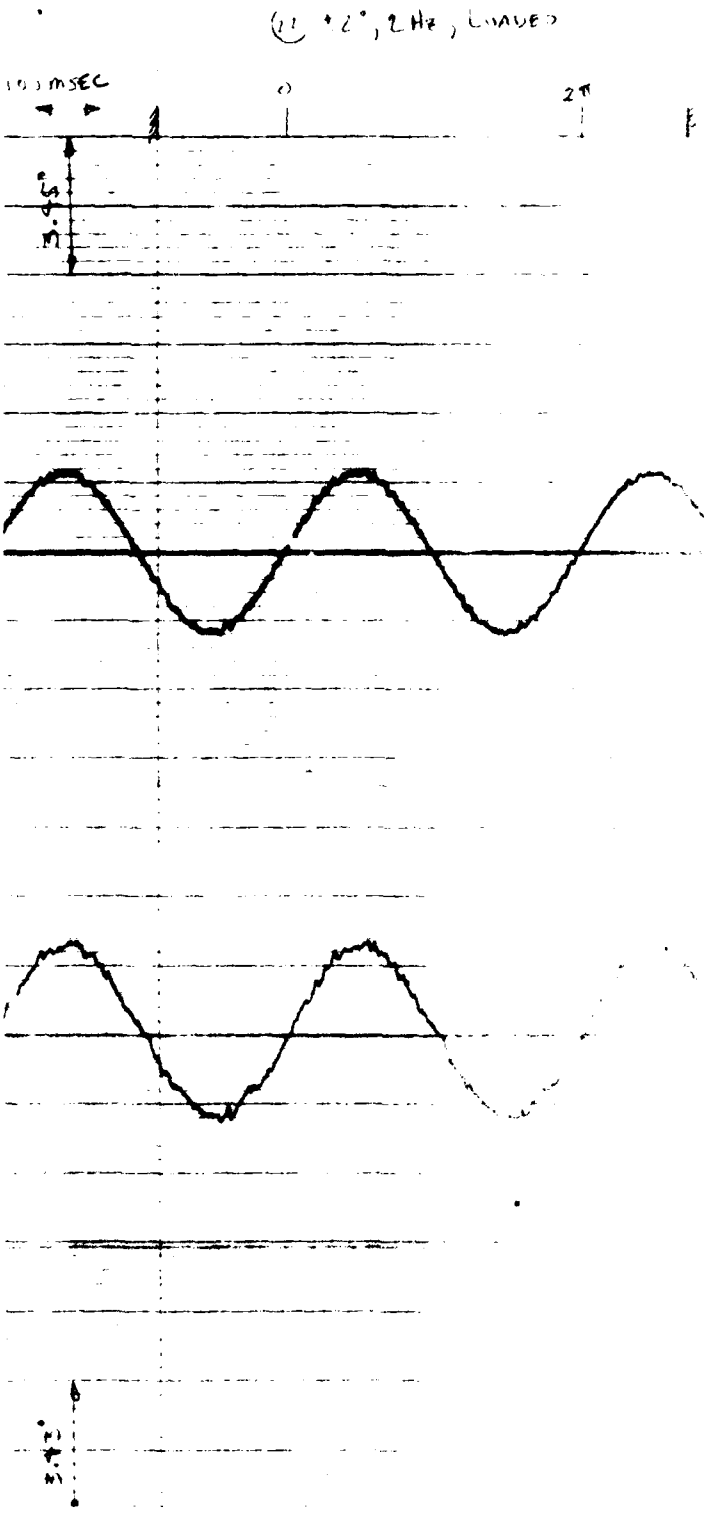

Figure 94. Test 22, ±2° Sine, 2 Hz, Loaded

(22) ±2°, 4 HZ, LOADED

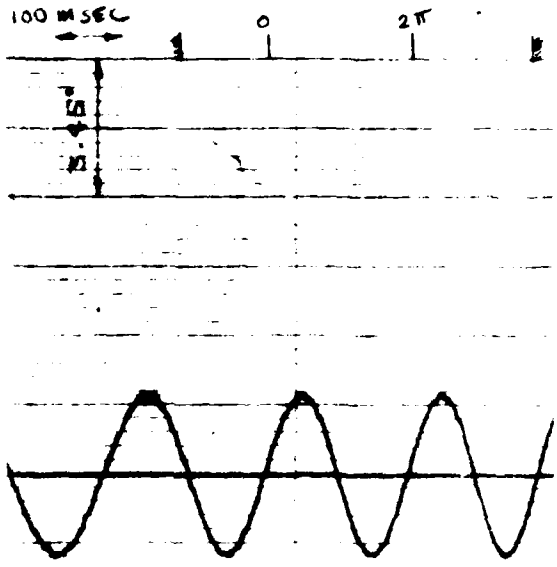

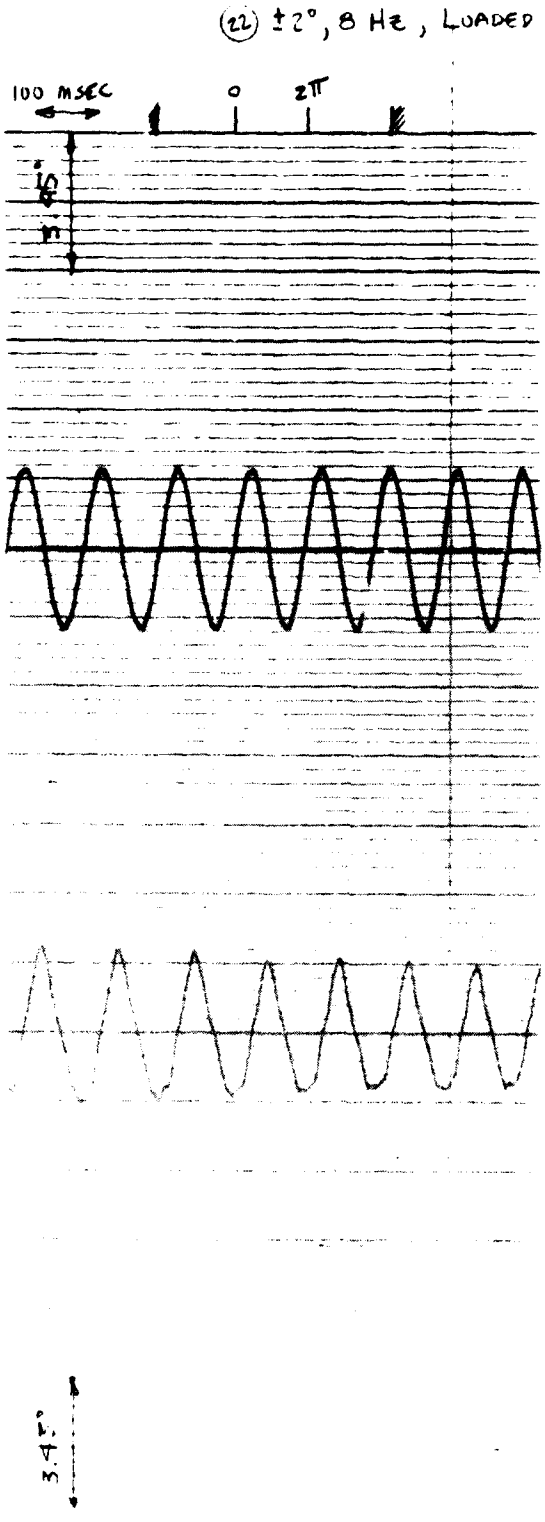

Figure 9. Test 22, ±2° Sine, 8 Hz, Loaded

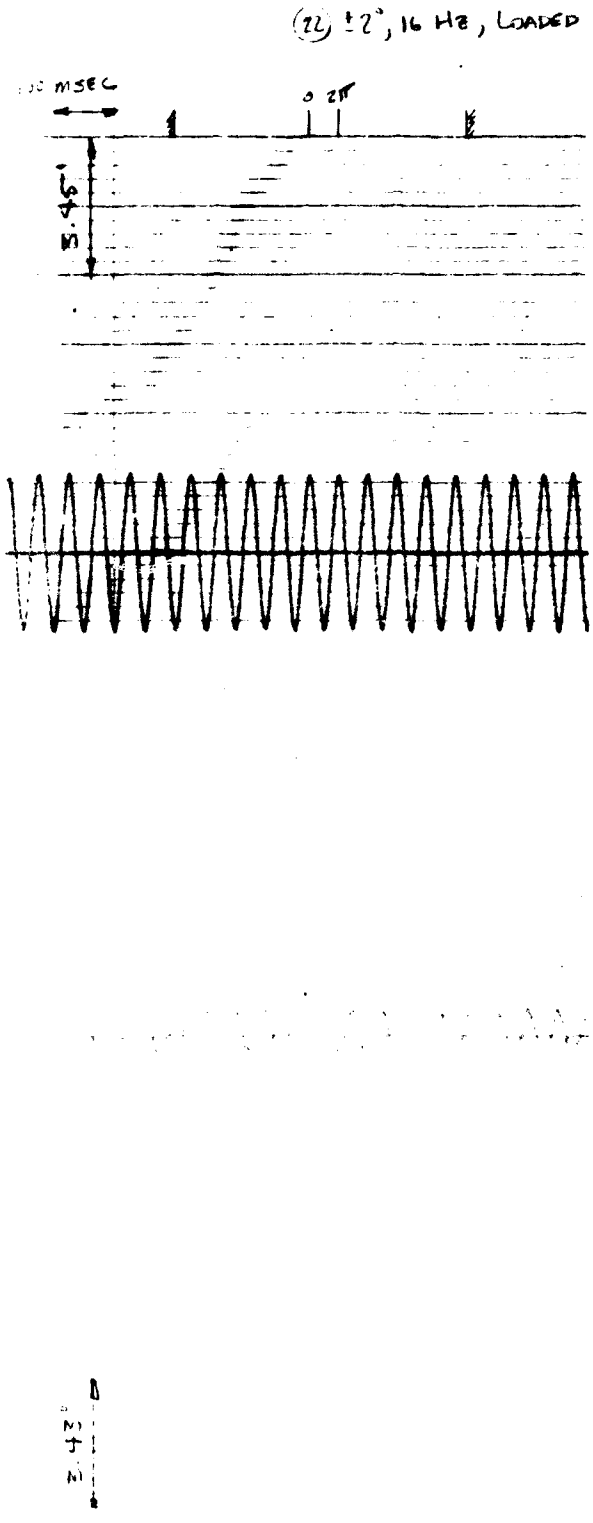

Figure 97. Test 22, ±2° Sine, 16 Hz, Loaded

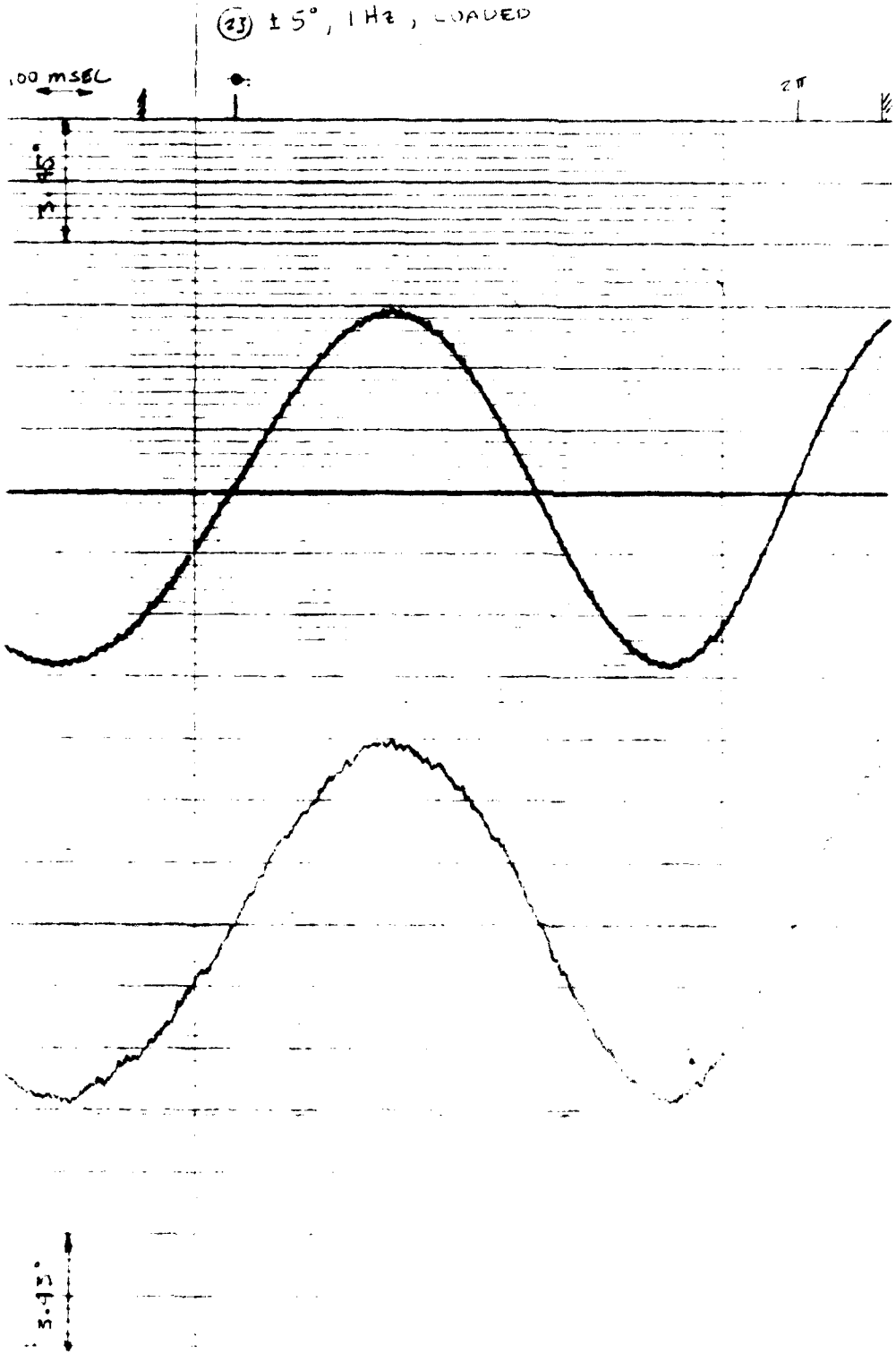

Figure 98. Test 23, ±5° Sine, 1 Hz, Loaded

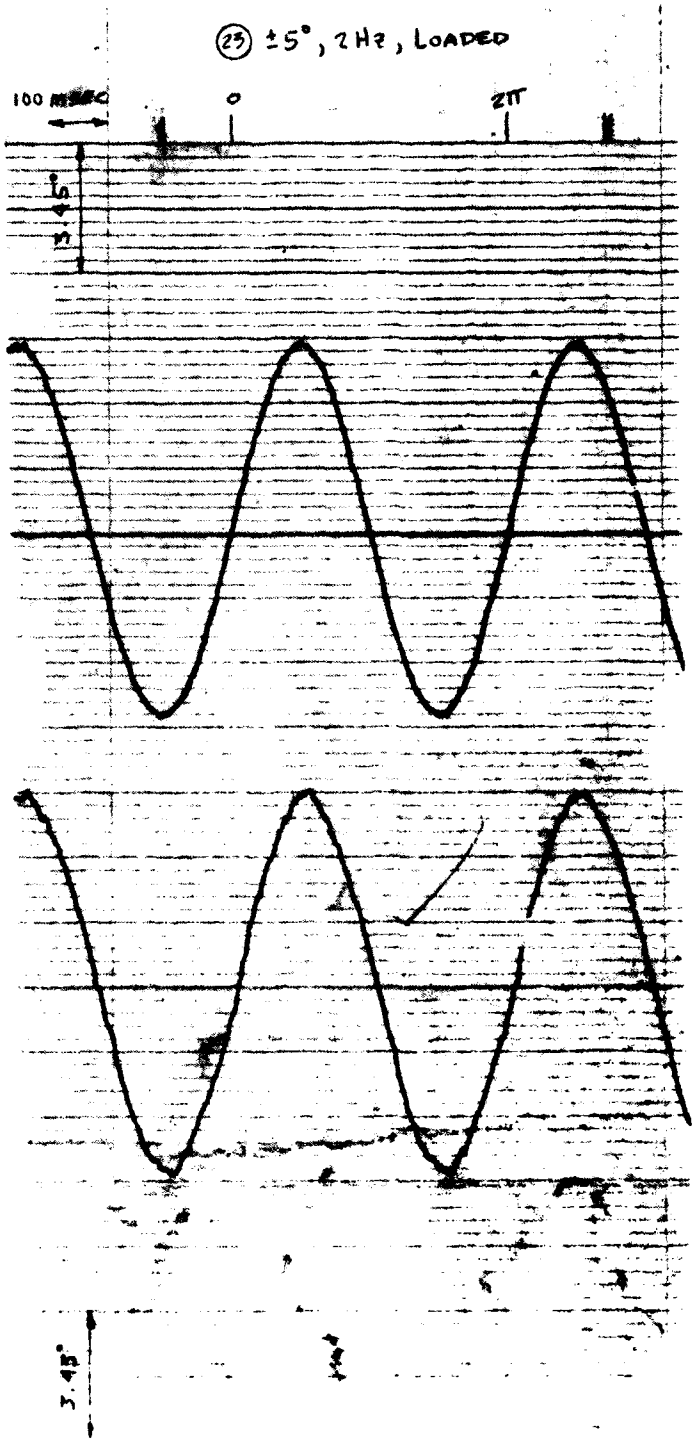
(23) ±5°, 2Hz, LOADED
100 MSEC
0
2π
3.45°
3.45°

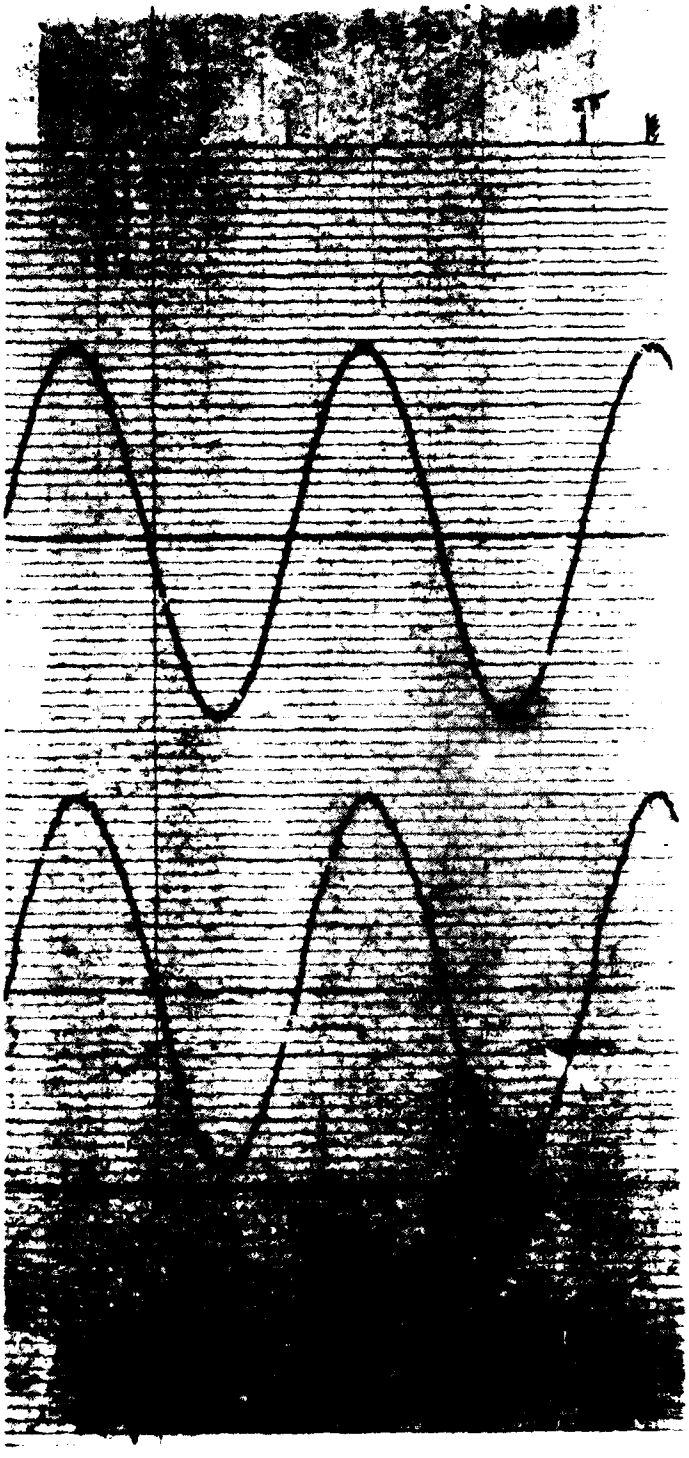

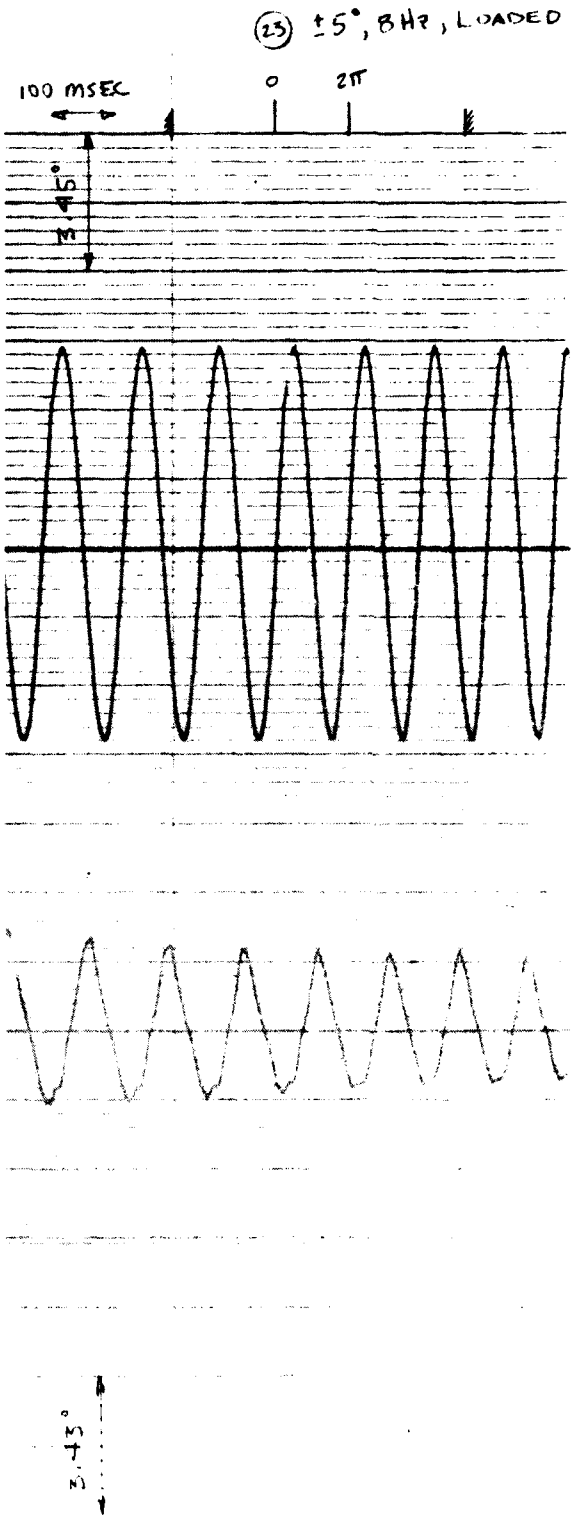

Figure 161. Test 23, ±5° Sine, 8 Hz, Loaded

(23) ±5°, 16 Hz, LOADED

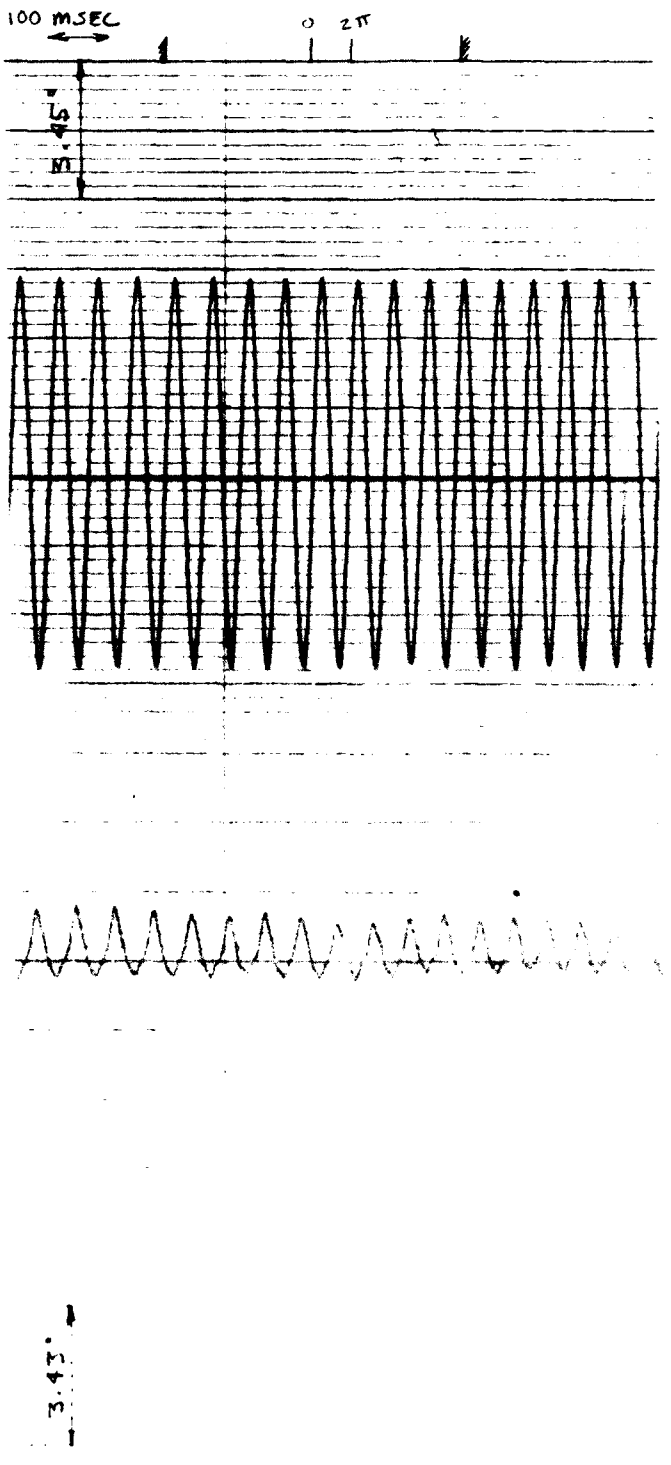

Figure 1. . Test 23, ±5° sine, 16 Hz, loaded

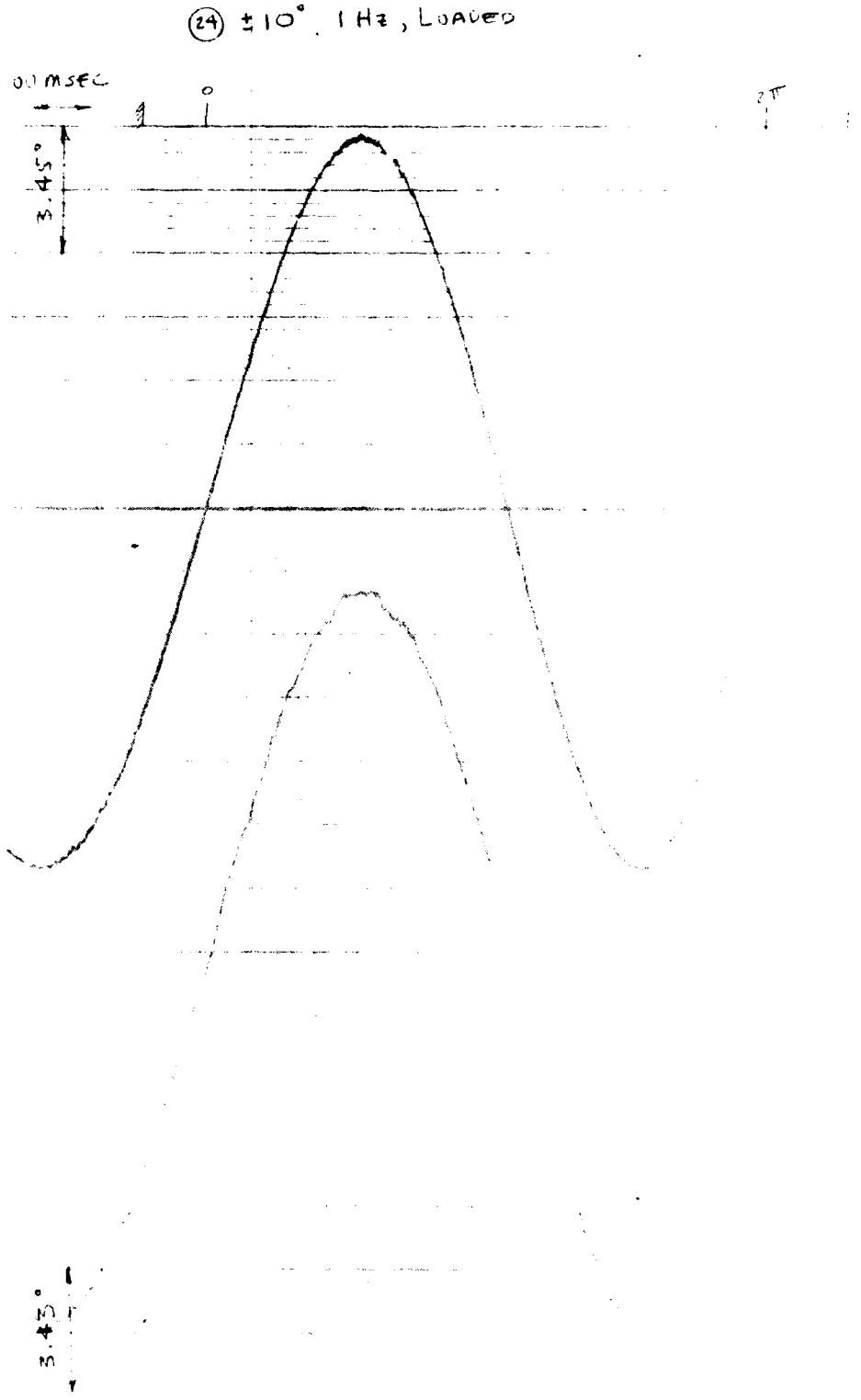

Figure 3-6. Test 24, ±10°, 1 Hz, Loaded

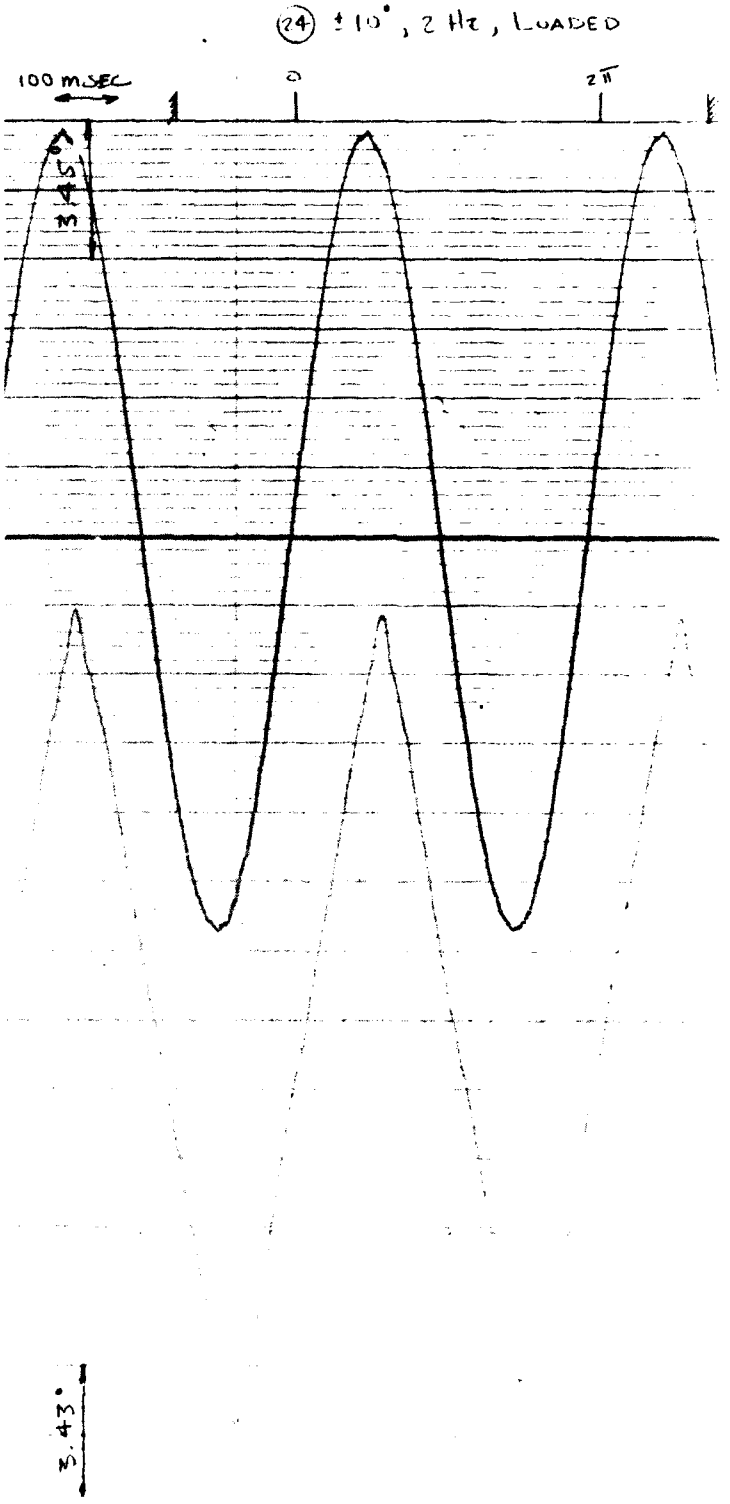

Figure 104. Test 24, ±10° Sine, 2 Hz, Loaded

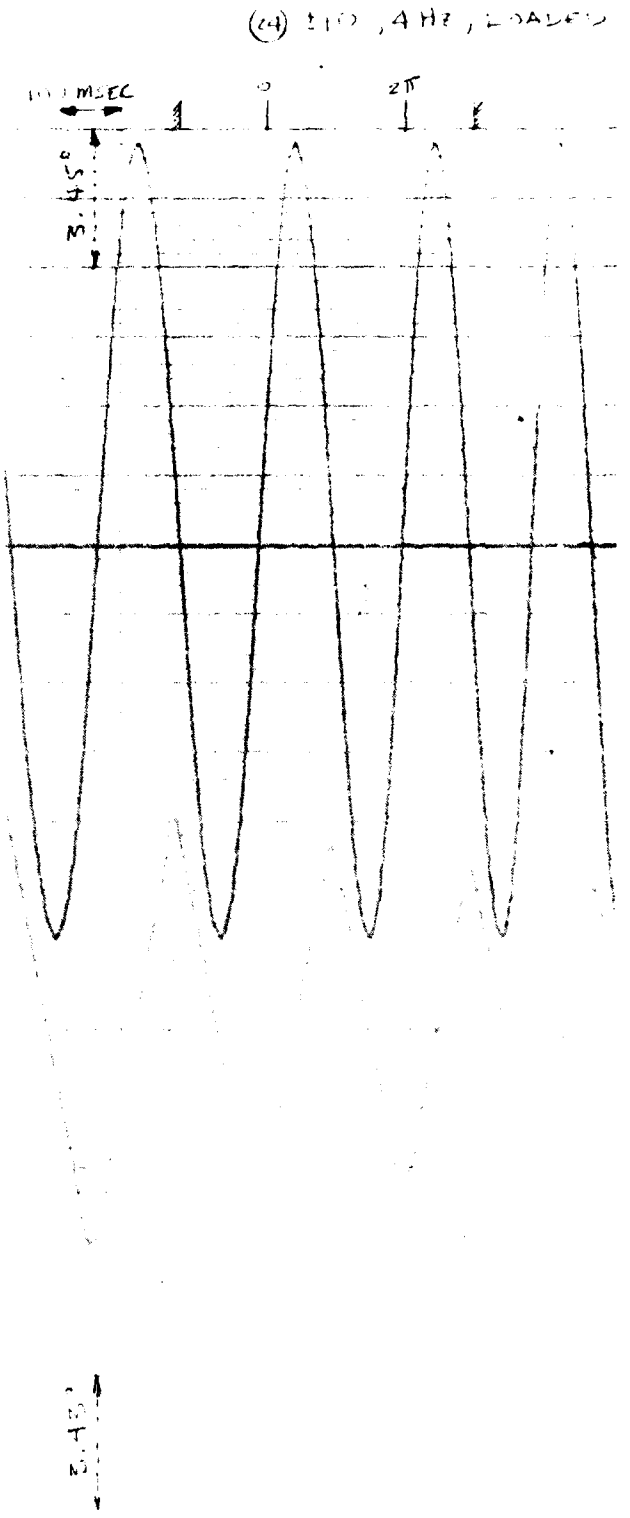

Figure 105. Test 24, ±10° Sine, 4 Hz, Loaded

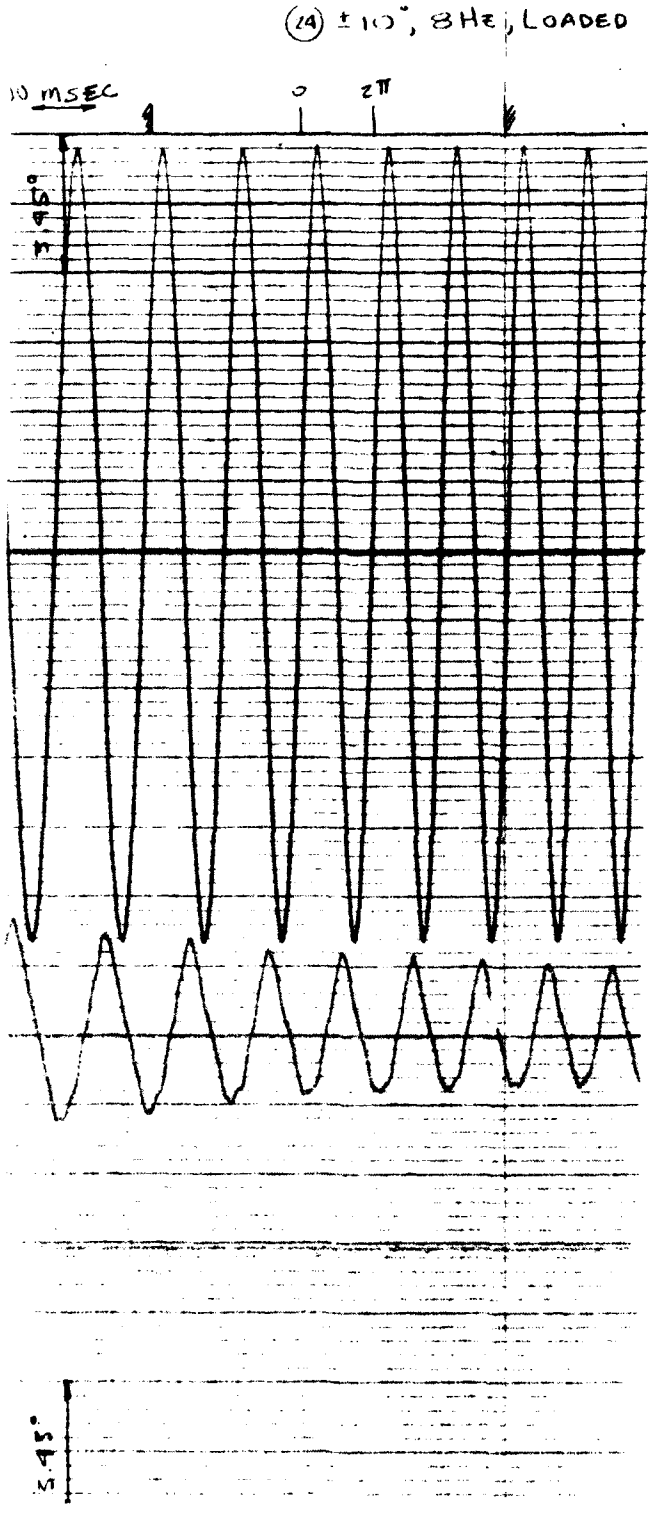

Figure 106. Test 24, ±10° Sine, 8 Hz, Loaded

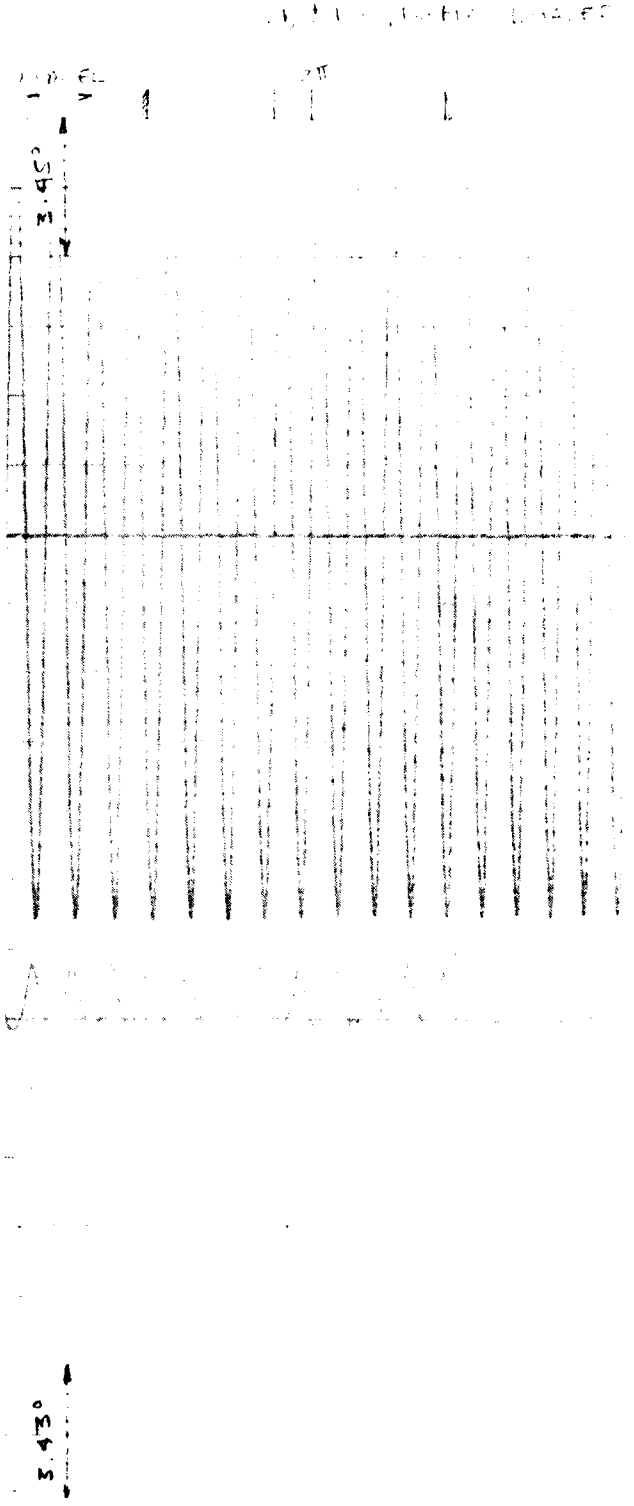

Figure 107. Test 24, ±10° Sine, 16 Hz, Loaded

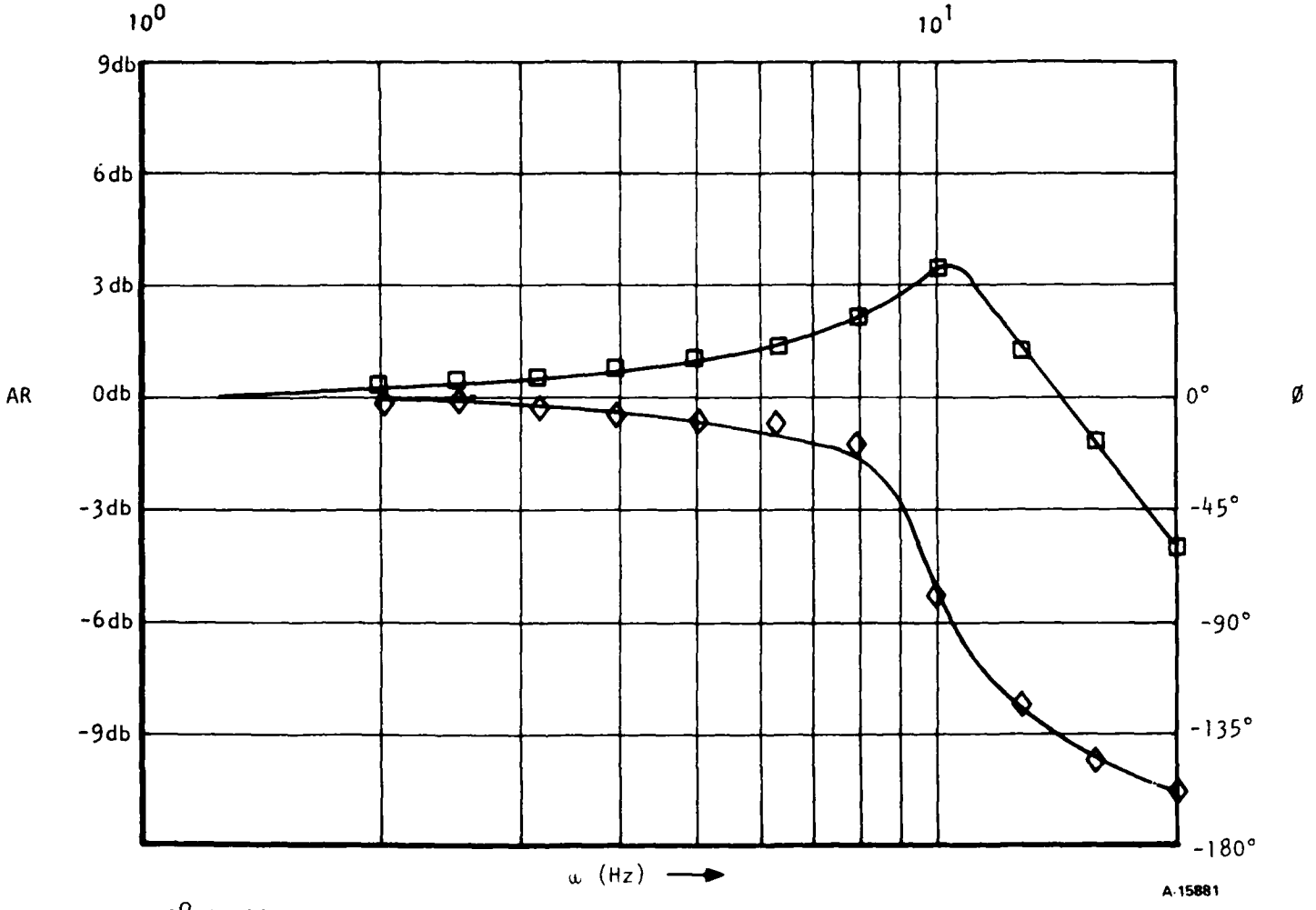

Figure 108. Test 25, Frequency Response, ±1°, 2.55 in.-lb-sec^2

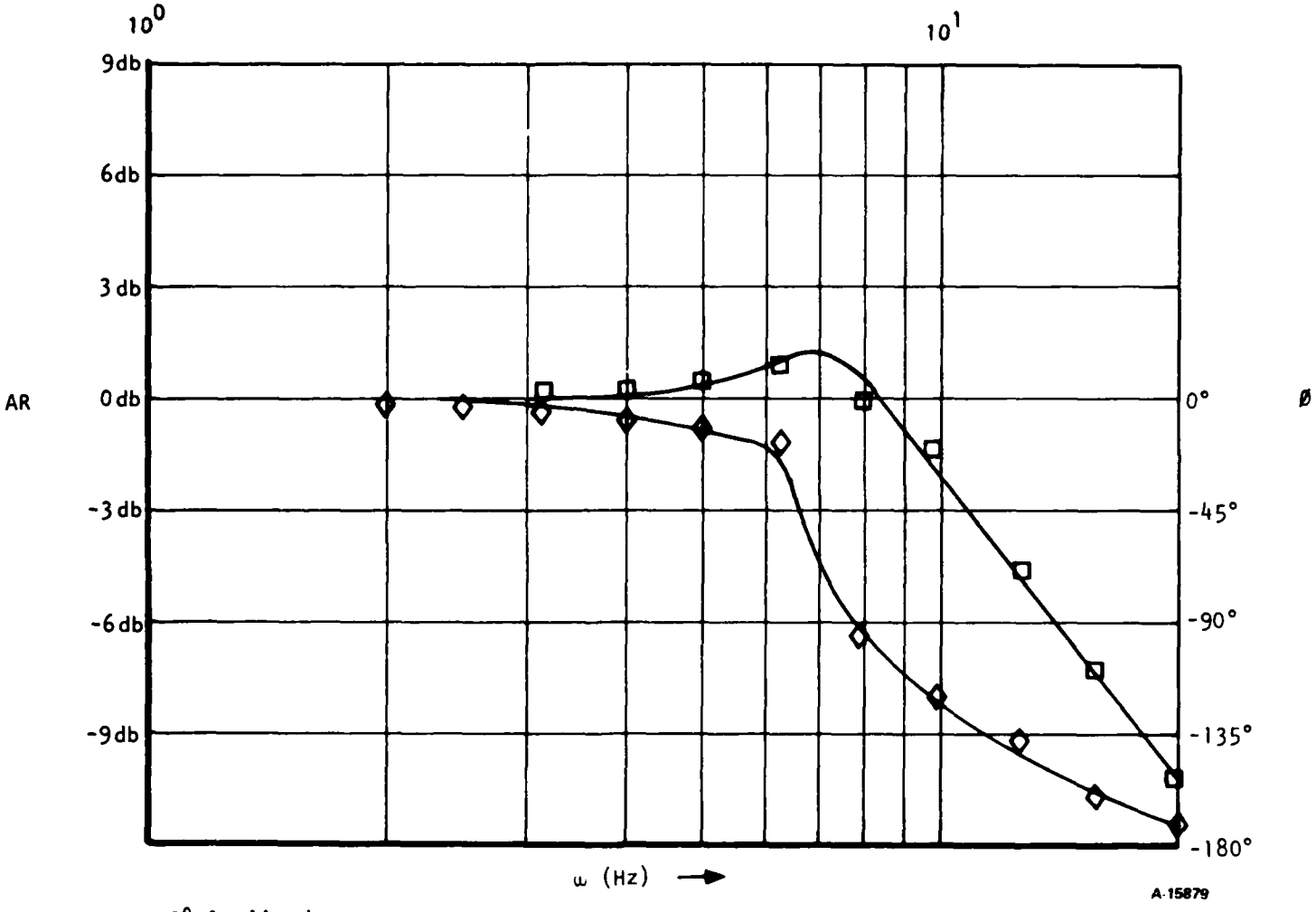

$\pm 2^0$ Amplitude

2.55 in-lb-sec^2

Figure 109. Test 26, Frequency Response, $\pm 2°$, 2.55 in.-lb-sec^2

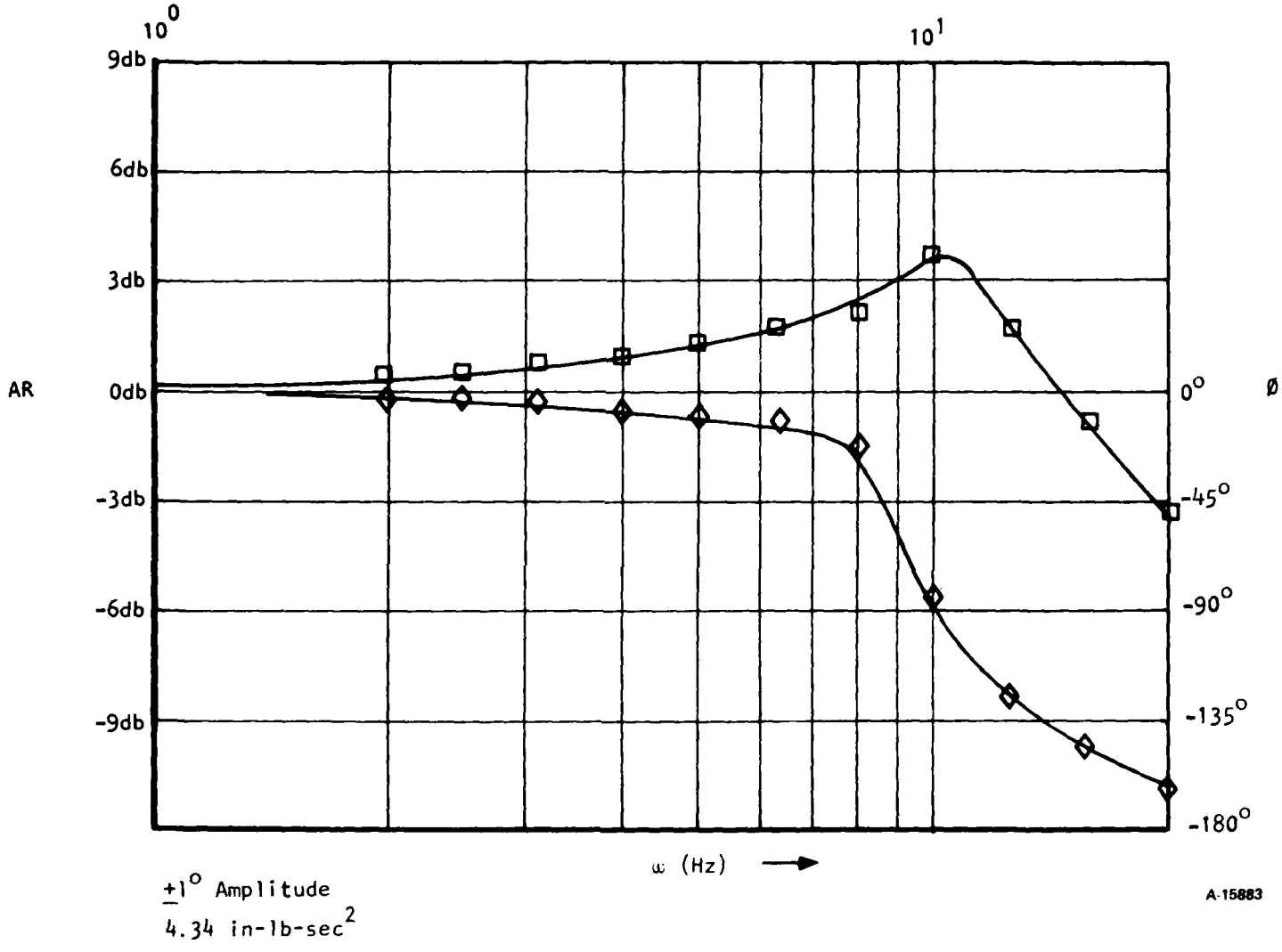

Figure 110. Test 27, Frequency Response, ±1°, 4.34 in.-lb-sec^2

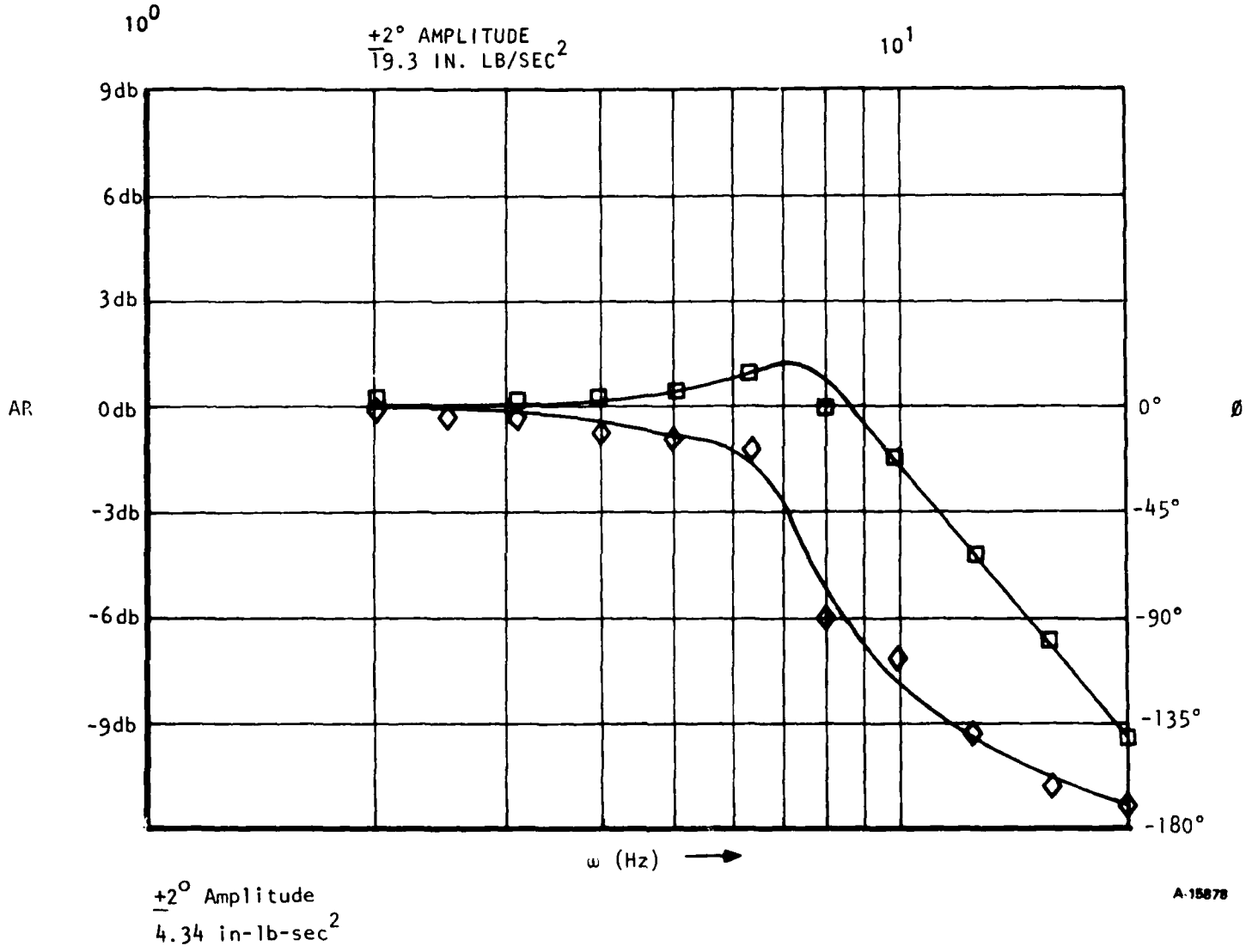

Figure 111. Test 28, Frequency Response, +2°, 4.34 in.-lb-sec^2

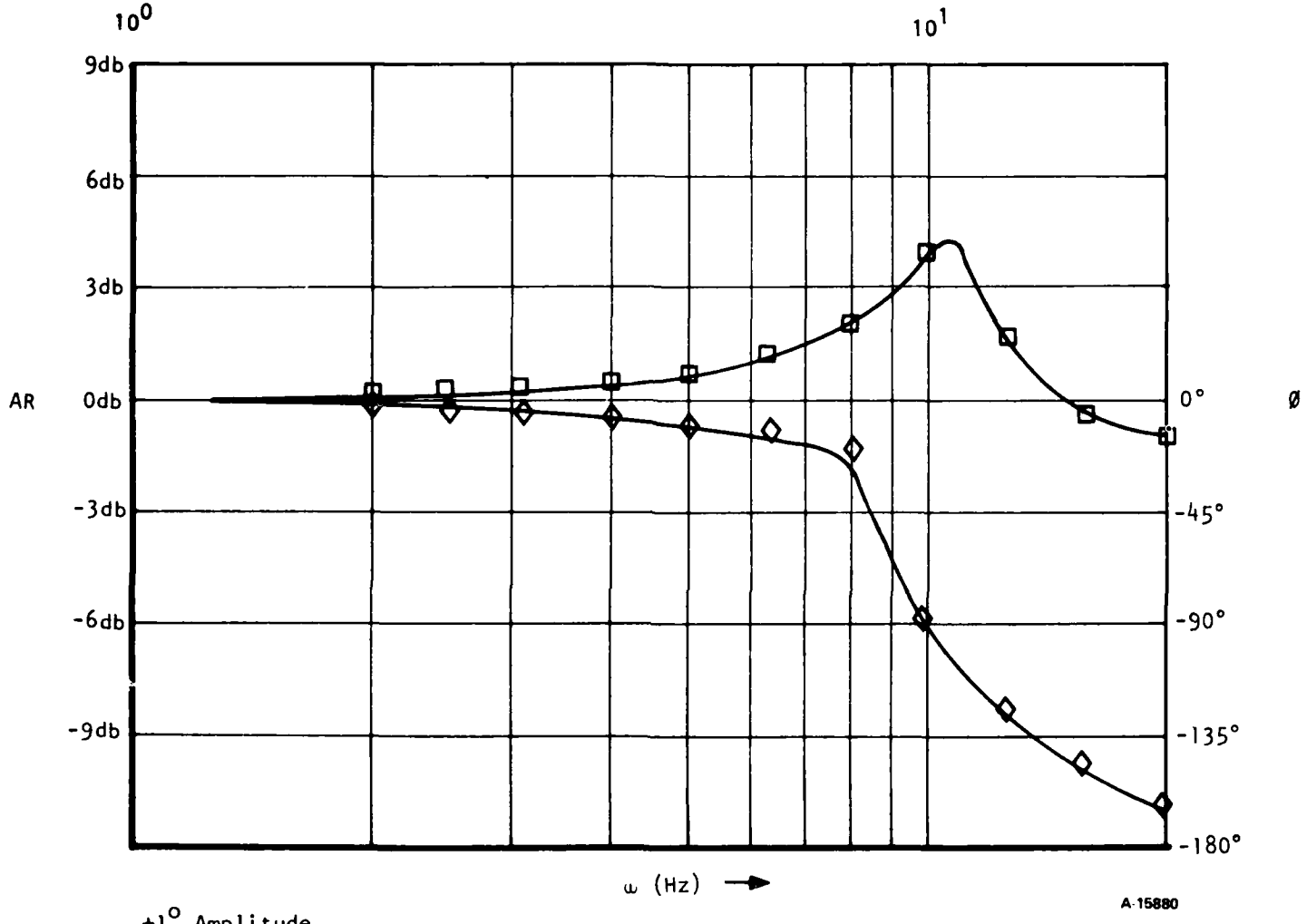

Figure 112. Test 29, Frequency Response, ±1°, 8.04 in.-lb-sec^2

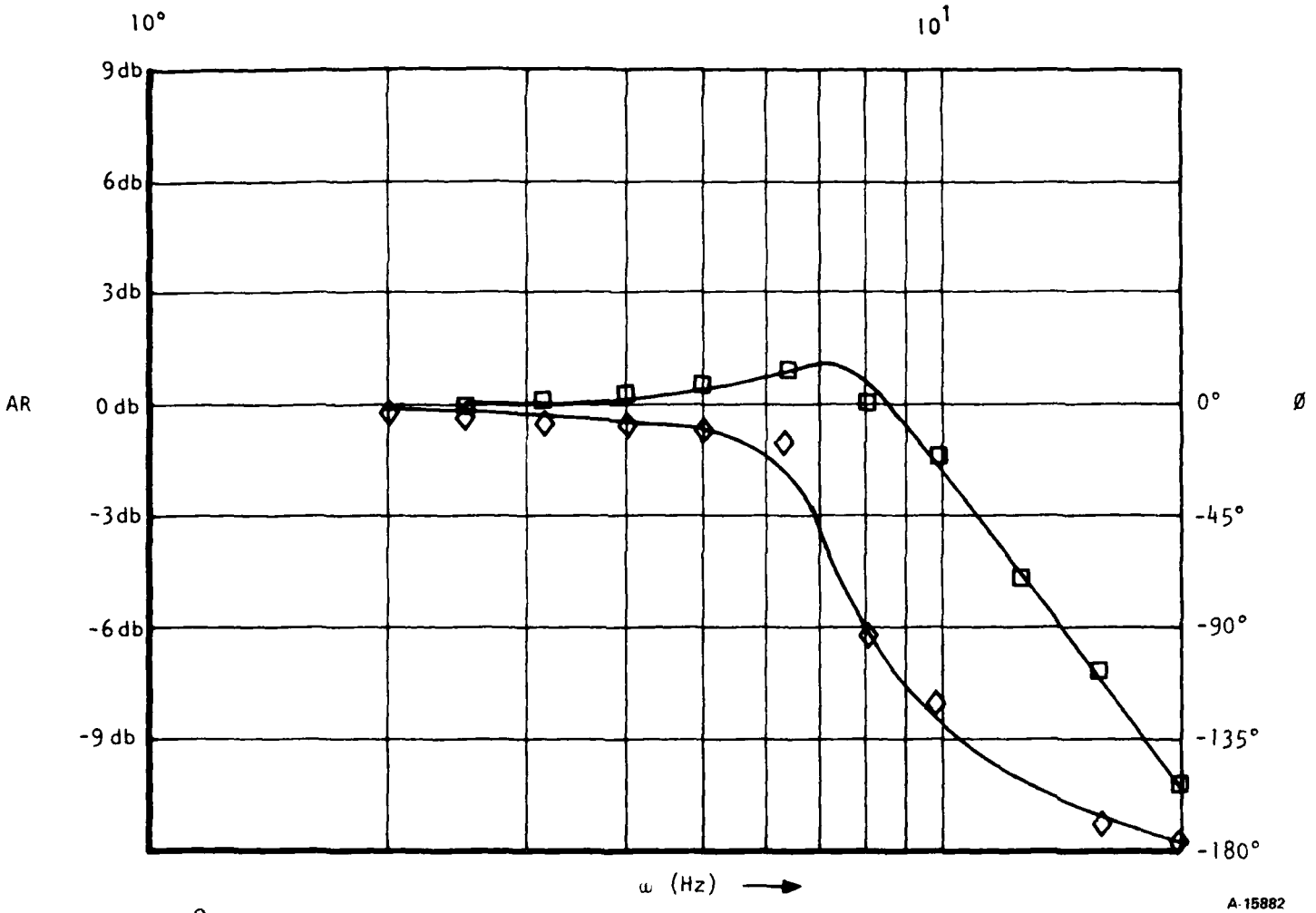

±2° Amplitude
8.04 in-lb-sec²

Figure 113. Test 30, Frequency Response, ±2°, 8.04 in.-lb-sec²

*U.S.Government Printing Office: 1982 — 559-005/4057

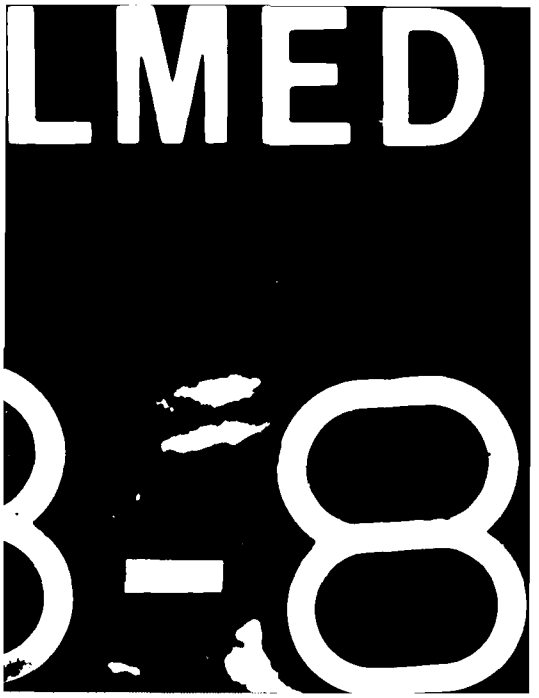
LMED
8-8